Université catholique de Louvain
Faculté d'Ingénierie Biologique, Agronomique et Environnementale
Earth and Life Institute – Environmental Sciences

Dynamic modelling of nitrification in vertical flow constructed wetlands

Ania MORVANNOU

Thèse présentée en vue de l'obtention
du grade de docteur en sciences agronomiques
et ingénierie biologique

Contents

LIST OF FIGURES I

LIST OF TABLES V

LIST OF ACRONYMS VII

LIST OF SYMBOLS IX

CHAPTER 1 1
BACKGROUND, LITERATURE REVIEW AND STUDY OBJECTIVES 1

1.1. THE TWO-STAGE VF CONSTRUCTED WETLANDS, AN ATTRACTIVE TECHNOLOGY 3

1.2. VFCW: BASIC PRINCIPLES AND TECHNICAL ASPECTS 5

1.2.1. First treatment stage 7

1.2.2. Plant effects 8

1.2.3. Individual processes occurring in a VFCW 9

1.2.4. Biological and chemical processes 10

1.2.4.i. Endogenous respiration 10

1.2.4.ii. Organic matter removal 10

1.2.4.iii. Nitrogen removal 11

1.2.5. VFCW aeration: transport, consumption and oxygen renewal 13

1.2.5.i. Oxygen transfers toward the biomass 15

1.2.5.ii. Gas content variation within the VFCW 15

1.2.6. Clogging 16

1.3. VFCW MODELLING 18

1.3.1. Limitations of the CW modelling 18

1.3.2. Dynamic VFCW modelling 18

1.3.3. Model selection 20

1.4. IMPROVING EXISTING MODELS OF VFCW WITH IN-SITU AND EX-SITU EXPERIMENTAL INVESTIGATIONS 21

1.4.1. Problem statement 21
1.4.2. Hydraulic model: methods for estimating the hydraulic parameters 22
1.4.3. Biological model 24
1.4.3.i. Need for calibration of the parameters 24
1.4.3.ii. Ex-situ experiences with respirometry (biodegradability of wastewater, parameters determination) 25

1.5. OBJECTIVES OF THE RESEARCH 30

1.6. OUTLINE OF THE THESIS 31

CHAPTER 2 33
ON THE CHARACTERIZATION OF THE HYDRAULIC PROPERTIES OF THE FILTERING MATERIAL OF A VERTICAL FLOW CONSTRUCTED WETLAND 33

2.1. INTRODUCTION 34

2.2. MATERIALS AND METHODS 34
2.2.1. The VFCW studied 34
2.2.2. In-situ monitoring of the hydraulic behavior of the VFCW 35
2.2.3. Hydraulic parameters of the VFCW materials 36
2.2.3.i. Model and procedure 36
2.2.3.ii. Laboratory scale experiments 37
2.2.3.iii. Inverse modelling using in-situ measurements 40
2.2.3.iv. A global set of parameters 40
2.2.4. Model validation 41

2.3. RESULTS AND DISCUSSION 42
2.3.1. Parameter optimization 42
2.3.1.i. Laboratory experiments 42
2.3.1.ii. In-situ measurements 46
2.3.1.iii. Parameter integration 48
2.3.2. Comparison of the different methods 49

2.4. CONCLUSION 53

CHAPTER 3 55

IMAGING OF VERTICAL FLOW CONSTRUCTED WETLAND USING ELECTRICAL RESISTIVITY TOMOGRAPHY AND TIME DOMAIN REFLECTOMETRY **55**

3.1. INTRODUCTION 56

3.2. MATERIALS AND METHODS 58

3.2.1. Evieu vertical flow constructed wetland 58

3.2.2. TDR calibration procedure 58

3.2.3. The experimental setup 60

3.2.4. ERT and TDR data processing 61

3.2.5. Direct mapping 63

3.3. RESULTS AND DISCUSSION 63

3.3.1. TDR calibration 63

3.3.2. The feeding period 66

3.3.2.i. Water front infiltration 66

3.3.2.ii. The dynamics of the filter clogging 68

3.3.2.iii. Influent distribution 69

3.3.3. The rest period 70

3.3.4. Direct mapping 71

3.4. CONCLUSIONS 72

CHAPTER 4 **73**

A - MEASURING THE NITRIFICATION RATE **73**

4A.1. THE SELF-HEATING TEST (CALORIMETRY PRINCIPLES) **ERREUR ! SIGNET NON DEFINI.**

4A.2. MEASURING CHEMICAL FORMS 75

4A.2.1. Acid-base titration 75

4A.2.2. Monitoring nitrate 76

4A.3. RESPIROMETRY 77

4A.3.1. Respirometry for saturated conditions (liquid respirometry) 77

4A.3.2. Respirometry for unsaturated conditions (solid respirometry) 77

CHAPTER 4 79
B - SOLID RESPIROMETRY TO CHARACTERIZE THE NITRIFICATION KINETIC: A BETTER INSIGHT FOR MODELLING NITROGEN CONVERSION IN VFCW 79

4B.1. INTRODUCTION 80

4B.2. MATERIALS AND METHODS 80

4B.2.1. The solid respirometer 80
4B.2.1.i. Equipment and operating conditions 80
4B.2.1.ii. Sensitivity of the method 82
4B.2.1.iii. Respirometric index 82

4B.2.2. Determining of the nitrification rate 84
4B.2.2.i. Liquid addition, percolate release, and nitrification index 84
4B.2.2.ii. Calculating nitrification rates from DRI_{max},$CO(t_F)$ 85
4B.2.2.iii. Experimental conditions tested to adjust liquid injection 86
4B.2.2.iv. Other conventional protocols for comparing solid respirometry results 88

4B.2.3. Determining maximum nitrification rate and concentration of autotrophic biomass developed in a VFCW plant 88
4B.2.3.i. Sampling and preparation 88
4B.2.3.ii. Determining the maximum nitrification rate ($R_{S,max}$) with solid respirometry 89
4B.2.3.iii. Calculating the autotrophic concentration (C_{XA}) by means of nitrogen mass balance 89
4B.2.3.iv. Calculating the maximum autotrophic growth rate ($\mu_{A,\,max}$)90

4B.3. RESULTS AND DISCUSSION 90

4B.3.1. Impact of injecting liquid and consequences on measuring nitrification 90
4B.3.1.i. Impact of the injected volume and the concentration of nitrogen 90
4B.3.1.ii. Impact of adding "ammonium-free" water, and subsequent water containing ammonium 92
4B.3.1.iii. Impact of adding only water containing ammonium (no previous ammonium-free water) 93
4B.3.1.iv. Influence of the injected nitrogen mass 94

4B.3.2. Evaluation of the proposed method 95
4B.3.2.i. Comparison with a conventional method 95
4B.3.2.ii. Comparing existing literature values 96

4B.3.3. Determining the concentration and the maximum growth rate of autotrophic biomass 97

4B.4. CONCLUSIONS 98

CHAPTER 5 101
NITROGEN REMOVAL MODELLING IN THE FIRST STAGE OF A FRENCH-TYPE VFCW WITH CW2D: ABILITY AND LIMITS* 101

5.1. INTRODUCTION 102

5.2. MATERIAL AND METHODS 102

5.2.1. The VFCW plant 102

5.2.2. Strategy of sampling and analysis 103

5.2.2.i. Offline analysis 104

5.2.2.ii. Online recording 105

5.2.3. Conceptual dynamic model CW2D and simulations of the VFCW behavior 106

5.2.4. Calibration strategy and simulations 108

5.2.4.i. Input data 109

5.2.4.ii. Initial and boundary conditions 109

5.2.4.iii. Simulations 110

5.3. RESULTS AND DISCUSSION 113

5.3.1. Input data 113

5.3.1.i. Individual concentrations 113

5.3.1.ii. Calibrated parameters values 115

5.3.2. Comparison between simulated and measured data with calibrated parameters 117

5.3.2.i. Online monitoring (COD, nitrogen forms) 117

5.3.2.ii. In-situ monitoring (off-line) 122

5.3.3. Discussion 125

5.3.3.i. Fate of nitrogen during feeding and feeding+rest periods 125

5.3.3.ii. Additional simulation consecutive to a previous simulation period 127

5.3.3.iii. Improving quality of modelling: additional measurements, modification of model 129

5.4. CONCLUSION 131

CHAPTER 6 133
CONCLUSIONS AND PERSPECTIVES 133

APPENDICES 137
AVAILABLE MODELS FOR VFCW MODELLING 139
TABLES FROM THE CW2D MODEL 145
RESPIROMETRIC METHODS FOR THE CARBON OXIDATION 149
RESPIROMETRIC TECHNIQUES APPLIED TO STUDIES OF THE COMPOST STABILITY, LIQUID SLUDGE FOR COMPOSTING AND WASTEWATER FROM VFCW 155
CHARACTERISTICS OF THE DIFFERENT DEVICES AVAILABLE 159

REFERENCES 163

PUBLICATIONS AND CONFERENCES 184

List of Figures

Figure 1.1: A typical treatment plant with a two-stage VFCW configuration (Source: Boutin *et al.*, 2000). 4

Figure 1.2: Particle size profiles (Source: Molle *et al.*, 2005). 4

Figure 1.3: Scheme of a VFCW (Molle *et al.*, 2005) 6

Figure 2.1: Set-up of the *in-situ* experiment: (left) Top view of the VFCW with the six vertical trenches for the TDR probes. (right) Longitudinal section of the VFCW with the 24 TDR probes inserted within the four layers of the VFCW 36

Figure 2.2: Set-up of the evaporation experiment 39

Figure 2.3: Water retention curves determined during the sand box and pressure chamber experiments 43

Figure 2.4: Water contents and their uncertainties from TDR probe calibration at various VFCW depths (vertical trench 2) before and during the monitoring campaign 46

Figure 2.5: Hydraulic parameter estimates and confidence intervals (95 %) from the *in-situ* data inversion for the four layers and all vertical trenches (Eq. 2.1 and 2.2, HYDRUS software) 47

Figure 2.6: Measured and simulated water content evolution in the VFCW at different depths during the monitoring campaign (Simulation performed with hydraulic parameters from *in-situ* water content data inversion) 49

Figure 2.8: K_s values for the four layers through the various optimizations 50

Figure 3.1: Experimental setup for water flow monitoring of a VFCW 60

Figure 3.2: Daily rainfall and average temperature in the sludge during the experiment 62

Figure 3.3: Reflection coefficient of TDR signal versus apparent distance for probes inserted in sludge and water (left). Material specific calibration curve of water contents versus dielectric constants (right). Dashed lines represent 95 % confidence intervals 63

Figure 3.4: Schemes of a TDR probe without coating (left) and a TDR with coating (right) with half of center-to-center spacing of rods without and with coating (s_0 and s_1, respectively) and the radius of rods without and with coating (r_0 and r_1, respectively) 65

Figure 3.5: Evolution of water content during the experiment at vertical trench 4. Shaded area corresponds to confidence intervals _____ 66
Figure 3.6: (left) Water content versus depth at different times after a load. (right) Water content versus time at different depths after a load _____ 67
Figure 3.7: (top) Reference cross-section resistivity image (in log scale), (bottom) water content versus electrical resistivity at TDR positions for all time-lapse measurements _____ 68
Figure 3.8: (left) Resistivity ratio tomograms at three selected time lapses during the feeding period. (right) Distribution of change ratio values ____ 69
Figure 3.9: (left) Resistivity ratio tomograms at three selected time lapses during the rest period. (right) Distribution of change ratio values _____ 70
Figure 3.10: (left) Calibration relationship between electrical resistivity and water content for the gravel layer estimated using the calibration set. (right) Measured water content versus estimated water content obtained by applying the calibration relationship on the validation dataset _____ 71

Figure 4A.1: Example of a device combining respirometry and titrimetry measurement for activated sludge study (Source: Gernaey *et al.*, 2001) __ 76

Figure 4B.1: Solid respirometer device _____ 81
Figure 4B.2: Examples of *DRI(t)* and *CO(t)* results for carbon degradation in three organic wastes (colonized sand and gravel, sludge) _____ 83
Figure 4B.3: Respirogram obtained after addition of ammonia for the nitrification study _____ 84
Figure 4B.4: *CO* (left) and *DRImax* (right) measured for different batches loaded with different nitrogen load_____ 91
Figure 4B.5: NH_4-N, NO_3-N and equivalent *CO* measured (mgN) for the successive addition of water with or without ammonium _____ 92
Figure 4B.6: (a) Mass of NH_4-N (injected and released), NO_3-N (released), nitrified nitrogen (mg N) and (b) *CO* measured for the successive addition of water with ammonium _____ 93
Figure 4B.7: $R_{S,\,max}$ and $R_{S,liq}$ measured at different injected nitrogen mass for a colonized gravel sample_____ 94

Figure 5.1: Scheme of the studied VFCW, locations of measurements and sampling points (not on scale) _____ 103
Figure 5.2: Scheme of VFCW layers phases, compounds and processes predicted by CW2D (Adapted from Langergraber and Simunek, 2005) _ 108
Figure 5.3: Various stages to calibrate CW2D (Adapted from Delrue *et al.*, 2010)_____ 108

Figure 5.4: COD fractions of raw wastewater of Evieu samples and literature data (from Pasztor *et al.*, 2009) 114

Table 5.6: Parameters values (biological) modified in order to simulate the measured values (20 °C) 116

Figure 5.5: Simulated and measured dissolved COD concentrations in the effluent for 3.5 day-period of the FP 118

Figure 5.6: (a) CR concentrations simulated in the four layers during both feeding and rest periods. (b) CI concentrations simulated in the four layers during both feeding and rest periods 119

Figure 5.7: Simulated and measured average concentrations for NH_4-N (a) and NO_3-N (b) in the effluent for 3.5 day-period of feeding 120

Figure 5.8: Simulated and measured instantaneous concentrations for NH_4-N (a) and NO_3-N (b) in the effluent for 3.5 day-period of feeding 121

Figure 5.9: Calculated (continuous curve) and measured (spots) oxygen contents at different depths of the VFCW for the two measurement points (red: layer 1; blue: layer 2; green: layer 3; black: layer 4) 122

Figure 5.10: Simulated XH (a) and XAN (b) concentrations at different depths and times after the monitoring campaign beginning (FP = feeding period, RP = rest period) 124

Figure 5.11: Nitrogen fluxes (gN) calculated for feeding (a) and feeding+rest (b) periods 126

Figure 5.12: Simulated NH_4-N (a) and NO_3-N (b) concentrations for additional simulation ("fictive" feeding period) consecutive to the previously simulation period 128

Figure 5.13: Calculated (continuous curve) and measured (spots) oxygen contents at different depths of the VFCW for the two measurement points for the second simulation (red: layer 1; blue: layer 2; green: layer 3; black: layer 4) 129

Figure V.1: Respirometric device used by Berthe *et al.* (2007) after modifications of the Tremier *et al.* (2005) device 160

List of Tables

Table 1.1: Influent characteristics of wastewater for small communities (< 2000 PE) (Average values; standard deviations (SD); and minimum and maximum values of the 90 % confidence interval. Between 2000 and 10000 measurements were used according to the estimated parameter. Source: Mercoiret *et al.*, 2010) 2

Table 1.2: Effluent threshold for wastewater treatment plants (Source: French decree from 22 June 2007). 2

Table 1.3: VFCW characteristics (Source: Boutin *et al.* 2007) 7

Table 1.4: Conventional design loads for the first treatment stage for the dry weather flow (Source: Molle *et al.*, 2008) 7

Table 1.5: Thresholds for hydraulic loads for vertical flow reed beds (French configuration) (Source: Molle *et al.*, 2006) 7

Table 1.6: Models existing for VFCW modelling (details presented in Appendix I) 19

Table 1.7: Main operating conditions for respirometric methods used for compost, activated sludge and wastewater from VFCW 28

Table 2.1: Hydraulic parameter assessment strategy 37

Table 2.2: Saturated conductivity and volatile matter content for different layers of the studied VFCW 42

Table 2.5: Parameter values and confidence intervals (95 %) of the hydraulic properties of the VFCW as obtained from the combination of the results of direct laboratory, inverse laboratory and *in-situ* inverse procedures. 48

Table 4B.1: Strategy to adjust, evaluate and apply the solid respirometric method 86

Table 4B.2: Comparison of $R_{V,\,max}$ to literature values [mg $O_2/L_{sample}/h$] 96

Table 4B.3: Maximum nitrification rate ($R_{v,max}$), concentration (C_{XA}), fraction released by treated effluent and maximum growth rate ($\mu_{A,max}$) for the autotrophic biomass 97

Table 5.1: Analyses carried out on raw wastewater and VFCW effluent samples 103

Table 5.2: Initial conditions for simulations 110

Table 5.3: Average concentrations and standard deviations ($mg.L^{-1}$) of the components contained in the raw wastewater applied to the VFCW for the 3.5 feeding days (28 samples) 113
Table 5.4: Oxygen re-aeration rate modified compared to CW2D initial value 115
Table 5.5: Parameters values (adsorption) modified in order to simulate the measured values 116

Table II.2: Reaction rates in CW2D 146
Table II.3: Kinetic parameters in CW2D (Henze *et al.*, 1995) 147

List of Acronyms

ASM	Activated Sludge Model
BCOD	biodegradable COD fraction [mgCOD/L]
BOD	biological oxygen demand (for 5 days) [mgO_2/L]
CHSCM	Constant Head Soil Core Method
CI	inerte soluble organic matter [mgCOD/L]
COD	Chemical Oxygen Demand [mgO_2/L]
COD_{cf}	Chemical Oxygen Demand after a coagulation/filtration step [mgO_2/L]
CR	rapidly biodegradable organic matter [mgCOD/L]
CS	slowly biodegradable organic matter [mgCOD/L]
CV	Coefficient of Variation [-]
CW	Constructed Wetland
DERU	european domestic wastewater directive (21 May 1991)
DM	Dry Matter content (%)
DRI	Dynamic Respiration Index [mg O_2/kg DM/h])
DRI_{max}	Maximum Dynamic Respiration Index [mg O_2/kg DM/h])
ERT	Electrical Resistivity Tomography
FAS	Free Air Space [%]
FP	Feeding Period
HFCW	Horizontal Flow Constructed Wetland
KN	Kjeldahl Nitrogen
MAE	Mean Absolute Error [mg/L]
MARE	Mean Absolute Relative Error [%]
OD_{12}/OD_{20}	Oxygen Demand in 12/20 hours [mgO_2/gVS]
OUR	Oxygen Uptake Rate [$mgO_2/gVS/h$]
PE	People Equivalent
RETC	RETention Curve (software)
RP	Rest Period
SD	Standard Deviation
SF(CW)	Surface Flow (Constructed Wetland)

SOUR	Specific Oxygen Uptake Rate [mgO_2/gVS/h]
SRT	Sludge Retention Time
SSF(CW)	Subsurface Flow (Constructed Wetland)
TDR	Time Domain Reflectometry
TOD	Total Oxygen Demand [mgO_2]
TSS	Total Suspended Solids [mg/L]
UC	Uniformity Coefficient (d_{60}/d_{10}) [-]
VFCW	Vertical Flow Constructed Wetland
VM	Volatile Matter content [%DM]
VS	Total Volatile Solids [kg]
XA	autotrophic biomasses [mgCOD/L]
XANb/XANs	autotrophic *Nitrobacter/Nitrosomonas* biomass [mgCOD/L]
XH	heterotrophic biomass [mgCOD/L]
Xi	inerte particular organic matter [mgCOD/L]

List of Symbols

α	Fitting scale parameter [1/cm]
Alpha	First-order rate coefficient for one-site non-equilibrium adsorption; Mass transfer coefficient for solute exchange between mobile and immobile liquid regions [1/d]
AT_4	Cumulative oxygen uptake recorded during 96 h (four days) [gO_2/kgDM]
b_A	Rate constant for autotrophic biomass lysis [1/d]
C_{IP}	Concentration in inorganic phosphorus [mg P/L]
C_{NH4}	Concentration in ammonium [mg N/L]
C_{O2}	Concentration of oxygen [mg O_2/L]
$CO(t_F)$	Total consumed oxygen mass during the period t_F [mg O_2/kg DM]
c_{XANb}	Concentration of the nitrifying bacteria *Nitrobacter* in the liquid phase [mg $COD_{biomass}$/kg DM]
c_{XANs}	Concentration of the nitrifying bacteria *Nitrosomonas* in the liquid phase [mg $COD_{biomass}$/kg DM]
d_{10}	Particle diameter at cumulative 10% from fine particle side of the cumulative particle size distribution [mm]
h	Actual pressure head [cm]
$K_{ANs,IP}$	Saturation/inhibition coefficient for inorganic phosphorus [mg P/L]
$K_{ANs,NH4}$	Saturation/inhibition coefficient for nitrogen [mg NH_4-N/L]
$K_{ANs,O2}$	Saturation/inhibition coefficient for oxygen [mg O_2/L]
K_{app}	Apparent dielectric constant [-]
Kd	Adsorption isotherm coefficient [dm_{water}^3/kg_{solid}]
K_La	Oxygen re-aeration rate [1/d]
K_s	Saturated hydraulic conductivity [cm/s]
$K(\theta)$	Actual hydraulic conductivity dependent on

	the actual water content θ [cm/s]
λ	Mualem pore connectivity parameter [-]
$\mu_{A,max}$	Maximum aerobic growth rate coefficient for autotrophic biomass [1/h]
μ_{ANb}	Maximum aerobic growth rate of the nitrifying bacteria *Nitrobacter* [1/h]
μ_{ANs}	Maximum aerobic growth rate of the nitrifying bacteria *Nitrosomonas* [1/h]
n	Shape parameter [-]
ρ	Concentration of dry matter needed to assess $R_{V,max}$ once samples from VFCW were get rid off of dead leaves, roots [g DM/L_{sample}]
rO_2	Oxygen uptake rate [$mmolO_2/kgDM/h$]
$R_{s,\ max}$	Maximum nitrification rate [mg O_2/kg DM/h]
$R_{V,max}$	Maximum volumetric nitrification rate [mg $O_2/L_{sample}/h$]
S_e	Effective fluid saturation [-]
θ(h)	Actual water content dependent on h [$cm_{water}^3/cm_{media}^3$]
θ_r	Residual volumetric water content [$cm_{water}^3/cm_{media}^3$]
θ_s	Saturated volumetric water content [$cm_{water}^3/cm_{media}^3$]
θ_{s_gravel}	Saturated volumetric water content for gravel sample [$cm_{water}^3/cm_{media}^3$]
θ_{s_sludge}	Saturated volumetric water content for sludge sample [$cm_{water}^3/cm_{media}^3$]
Y_{AN}	Cellular yield coefficient [g $COD_{biomass}/gNH_4$-N $_{nitrified}$]

Chapter 1

Background, literature review and study objectives

Excessive use and pollution of freshwater resources are nowadays global environmental issues that exert pressure on the sustainability of global ecosystems. Water issues therefore rank very high at the global political environmental agenda. Water issues can be a source of serious geopolitical conflicts, but can also be an opportunity for developing management and policies that convert to sustainable development. In any case, technologies that allow protecting global freshwater resources at a reasonable cost, while preserving the ecosystems are very much needed. This study takes place in this global context and focuses on low cost waste water treatment technologies as a way to protect global freshwater ecosystems.

Waste water treatment is indeed a central issue in the water resources domain (Asano, 1991). Present global population levels are at the origin of a pressure of waste water on freshwater systems that must be reduced to maintain freshwater ecosystem functioning. Among the various sources of water contamination, eutrophication is one of the major issues of water quality degradation. Eutrophication is an aquatic ecosystem process that develops when the water body receives too much nutrients that can be easily assimilated by aquatic vegetation. Main nutrients causing this phenomenon are phosphorus and nitrogen (ammonium, nitrate and nitrite). Such nutrients released in excessive amounts in water bodies cause aquatic vegetation over-proliferation, especially exponential growth of algae. High levels of organic matter combined with decomposing algae reduce the available oxygen status of the water body. Furthermore, some types of algae, like red tide, produce a deadly neurotoxin hazardous or even fatal to both marine life and humans. As a result, eutrophication destroys fisheries, habitats, ecosystems, and causes the death of marine life living in or dependent on this water body, and finally results in overall water quality degradation. Wastewater from agricultural, domestic or animal origins that are rich in these nutrients must therefore be appropriately treated to reduce this eutrophication problem.
As an example, Table 1.1 presents the average pollutant concentrations in wastewater at a treatment plant entrance for small communities (< 2000 people equivalent (PE)). Different water policy can be developed, imposing different effluent thresholds such as the European domestic wastewater directive (DERU, 21 May 1991) which envisages a good ecological level of

the water after treatment. In France, the ministerial decree from 22 June 2007 gives the effluent threshold values that a treatment plant with a capacity between 200 and 2000 PE must achieve (Table 1.2).

Table 1.1: Influent characteristics of wastewater for small communities (< 2000 PE) (Average values; standard deviations (SD); and minimum and maximum values of the 90 % confidence interval. Between 2000 and 10000 measurements were used according to the estimated parameter. Source: Mercoiret *et al.*, 2010)

COD ($mg.L^{-1}$)	BOD_5 ($mg.L^{-1}$)	TSS ($mg.L^{-1}$)	KN ($mg.L^{-1}$)	NH_4-N ($mg.L^{-1}$)	P_{total} ($mg.L^{-1}$)
646	265	288	67	54.9	9.4
SD = 395	SD = 171	SD = 226	SD = 35	SD = 27.0	SD = 5.3
Min = 122	Min = 39	Min = 53	Min = 14	Min = 12.0	Min = 2.0
Max = 1341	Max = 570	Max = 696	Max = 123	Max = 98.3	Max = 18.4

COD: chemical oxygen demand; BOD: biological oxygen demand (for 5 days); TSS: total suspended solids; KN: Kjeldahl nitrogen.

Table 1.2: Effluent threshold for wastewater treatment plants (Source: French decree from 22 June 2007).

Parameter	Maximum concentration in discharged effluent	Minimum removal efficiency
COD	125 $mg.L^{-1}$	75 %
BOD_5	25 $mg.L^{-1}$	70 %
TSS	35 $mg.L^{-1}$	90 %
KN	15 $mg.L^{-1}$	70 %

Particularly due to its role in eutrophication, and potential toxicity to aquatic species, nitrogen is a nutrient of primary concern in the wastewater treatment process. Nitrogen is one of the most common contaminants in groundwater (Heaton, 1986), and high concentrations of nitrate nitrogen have long been recognized as a health hazard in drinking water (Magee, 1982). In wastewater, ammonium is typically the principal form of nitrogen. Present in wastewater by the ammonification of urea and organic nitrogen, ammonium is a strong oxygen consumer: 4.3 g of oxygen are necessary to nitrify one gram of ammonium nitrogen. The presence of ammonium nitrogen therefore promotes eutrophication. In addition, ammonium nitrogen is toxic to aquatic life at certain concentrations in relation to water temperature, salinity and pH (Thurston *et al.*, 1981). Thus nitrification is the minimal nitrogen treatment step that has to be done in a wastewater treatment process. When it is necessary to remove the total nitrogen (eutrophication), it is advisable to

recreate favourable conditions for the denitrification: an anoxic environment sufficiently rich in dissolved carbon easily assimilated by microorganisms.

For small and medium size communities (50 – 5000 PE), wastewater treatment by constructed wetland (CW) plants has become an important treatment alternative in France. Currently, two main CW types exist to treat domestic wastewater: surface flow (SF) and subsurface flow (SSF) CWs (Kadlec and Knight 1996; Kadlec, 2000). SF CWs are systems with a free water depth and dense vegetation. Typical water depths are of 0.4 m. SSF do not have free water. Compared to the previous systems, the contact surface between water, microorganisms and the media is more important in SSF CW systems, allowing reducing the surface area necessary for their installation (Haberl *et al.,* 2003; Kadlec, 2008) and increasing the treatment efficiency. Generally, to prevent clogging of the porous media, the use of traditional SSF CW is limited to pretreated wastewater, containing less particulate matter content. SSF CWs are divided into horizontal flow (HFCW) and vertical flow (VFCW) systems depending on the water flow direction through the porous media as well as the biological conditions. HFCW are saturated (anoxic) while VFCW are unsaturated (aerobic). These latter will be the subject of this study.

1.1. The two-stage VF constructed wetlands, an attractive technology

Wastewater treatment based on CWs is an attractive technology for small communities (< 2000 PE) and is becoming more and more applied for medium size communities (< 5000 PE). As natural treatment systems, CWs require a large specific area compared to intensive technical solutions such as wastewater treatment by activated sludge, but lower than waste stabilization ponds. The simplicity of operation, its low cost and the reliability of treatment efficiency are often compatible with the limited resources that can be dedicated to wastewater treatment in these communities (Kadlec *et al.*, 2000). They provide also other additional benefits, including the acceptance of the fluctuation of the pollutant loads and fluxes and opportunities for treated water recycling and reuse (Haberl *et al.*, 2003). CW design is based on an acceptable organic load, often expressed as a filter surface unity per people equivalent. Current recommendations suggest two treatment stages, with three units in parallel on the first stage and two for the second, as shown on the Figure 1.1. Work experience shows that the two stage French VFCWs allow to reach high level of organic matter treatment in terms of biological oxygen demand (BOD), chemical oxygen demand (COD) and total suspended solids (TSS)),

and a quite complete nitrification of the Kjeldahl nitrogen (KN) load (Molle *et al.*, 2005). In addition, when the altitude difference between the inlet and the outlet is sufficient, the system can work without provision of energy.

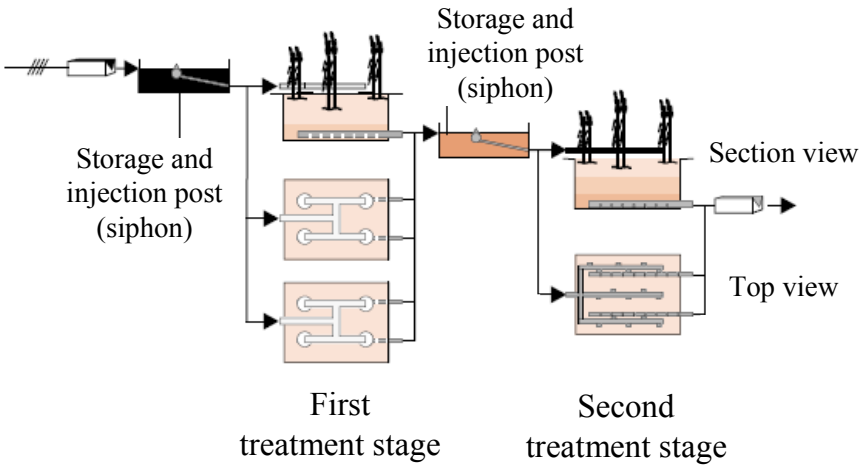


Figure 1.1: A typical treatment plant with a two-stage VFCW configuration (Source: Boutin *et al.*, 2000).

The individual processes that occur in the filter are a mechanical filtration and a biological aerobic degradation by microorganisms that develop on granular materials. Figure 1.2 presents the material particle size profiles used for each stage. The first is filled with a material with coarser particle size than for the second stage, according to treatments carried out on each of the stages.

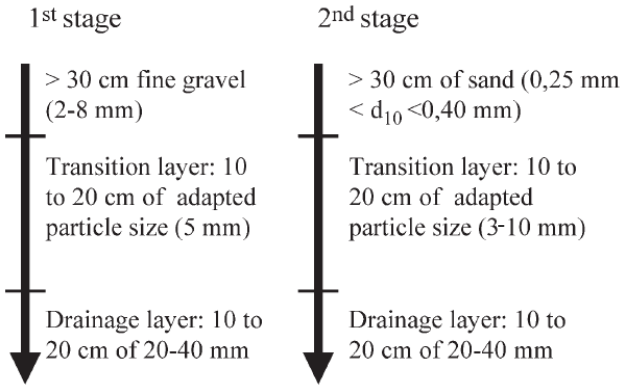


Figure 1.2: Particle size profiles (Source: Molle *et al.*, 2005).

TSS retained on the deposit surface are subject to mineralization (around 60 %) leading to an increase in the sludge content stored on filters of the first stage, with around 1.5 cm of sludge development per year (Molle *et al.*, 2005). For not exceeding a 20 cm of sludge deposit, that would limit infiltration and oxygen renewal, the deposits are withdrawn after 10 to 15 years of operation. A rest period is necessary before sludge extraction in order to diminish pathogen content. In such cases, the sludge can be directly used on agricultural field as no metals are present in the sludge (which can be the case if the network collects wastewater from an industrial activity).

When the treatment objective implies a nitrate removal of the effluent, it is necessary to include a horizontal flow constructed wetland (HFCW) in the treatment chain. If implemented after the first stage instead of the second stage VFCW, Molle *et al.* (2008) showed that complete nitrogen removal cannot be maintained in cold season because of a lack of nitrification. If HFCW was implemented as a third stage, nitrification will be more complete, but denitrification rates will decrease due to a lack of carbon. As a consequence, the design of CW plants aiming at treating total nitrogen throughout the year is based on three stages SSF CW systems with a horizontal flow one between the vertical flow stage and a recirculation from the outlet to the inlet of the horizontal stage. This design increases the footprint of the plant as well as its cost (in France, HFCW is generally designed on the basis of 2 $m^2.PE^{-1}$).

The operational objective in which this PhD study has been performed is consequently to improve nitrification on the first stage of the VFCW in order to develop, in future, total nitrogen removal CW plants using only two stages of treatment without recirculation. The reduction of the total footprint and cost of CW systems is also a big economical stake for its development. Before thinking to use specific material like zeolites, which will increase the construction cost, the first step is to better understand the nitrogen dynamics in the first stage of VFCW, fed with raw wastewater. This PhD work focuses on this part of CW treatment systems and adopts a modelling approach to study nitrogen dynamics on the VFCW.

1.2. VFCW: basic principles and technical aspects

Among the different CW systems treating domestic wastewater, the two-stage VFCW is the most developed system in France. The main process originality is the direct feeding of the VFCW with raw wastewater on the first stage (Molle *et al.*, 2005). No primary settling is necessary to cope with the TSS issue, allowing therefore an easier sludge management in

comparison with technologies with primary sludge production. This system was developed by Cemagref more than twenty years ago (Liénard, 1987) and in 2004 more than 400 VFCWs were operational. The annual rate of new constructions was valued at more than 100 plants in 2003 (Molle *et al.*, 2005). Nowadays we estimate that more than 2000 communities have been equipped with this treatment system. VFCWs are largely popular when nitrification and other strictly aerobic processes are required (Langergraber and Haberl, 2001; Kayser and Kunst, 2005).

Separated and sealed filters are filled with materials of different size particles (gravel for first VF, sand for the second VF, see Figure 1.2) according to the quality of the wastewater that has to be treated and the treatment stage (Figure 1.3). They are planted with *Phragmites australis*. The raw wastewater (= influent) is spread intermittently by batches (after a temporary storage of wastewater) on the filter surface with a specific areal flow rate, by gravity (siphons) or by pumps. This batch feeding covers the entire filter surface and provides a good water distribution of the influent onto the filter surface. Moreover, it improves the TSS distribution and oxygen renewal (Forquet *et al.*, 2009a).

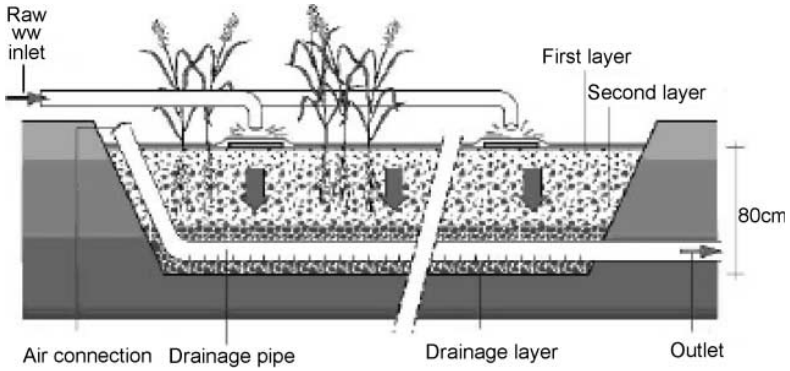


Figure 1.3: Scheme of a VFCW (Molle *et al.*, 2005)

Each filter is fed for three to four days, alternately with the others. Therefore each primary stage unit receives the complete organic load during the feeding period. Water flowing vertically through the filter, is subjected to physical, chemical and biological treatments. The treated effluent is then drained (draining layer), collected by a drainage system and is channeled towards the second treatment stage. After this period, a rest period is required with a length twice longer than the feeding period for the first stage. This alternation of periods are fundamental for regulating the growth of the biomass that develops on the media, for restoring oxygen budget within the filter, and to promote deposit mineralization in order to reduce clogging risks (Liénard *et al.*, 1990).

Table 1.3 summarizes the specific characteristics to manage VFCW plants.

Table 1.3: VFCW characteristics (Source: Boutin *et al.* 2007)

Wastewater	Condition	Degradation	Alternation	Feeding	Design	Depth	Slope
Raw	Aerobic	- Carbon - Full nitrification	Necessary	Batches	2-2.5 $m^2.PE^{-1}$	60 cm	Useful

1.2.1. First treatment stage

The design of the filter is based on acceptable areal loads onto the filter in operation. Table 1.4 presents the classical design loads for the first stage filters during dry weather flow.

Table 1.4: Conventional design loads for the first treatment stage for the dry weather flow (Source: Molle *et al.*, 2008)

	Hydraulic load ($m.d^{-1}$)	COD ($g.m^{-2}.d^{-1}$)	TSS ($g.m^{-2}.d^{-1}$)	KN ($g.m^{-2}.d^{-1}$)
Design loads on the 1st stage filter in operation	0.38	300	150	25-30

These acceptable loads lead to a surface area of about 1.2 $m^2.PE^{-1}$ for the three filters of the first stage. A national survey carried out by Molle *et al.* (2005) evaluated treatment performances. For the first stage of treatment, removal rate are about 80 % for COD, 92 % for TSS, but KN removal or conversion to NO_3-N remains limited (60 %, Molle *et al.*, 2008). VFCW are also known to be able to accept load variations. Thresholds for hydraulic loads are presented in Table 1.5.

Table 1.5: Thresholds for hydraulic loads for vertical flow reed beds (French configuration) (Source: Molle *et al.*, 2006)

Deposit layer (cm)	0-10		0-25	
Hydraulic load	Once a week	Once a month	Once a week	Once a month
$m.d^{-1}$	1.80	3.50	0.90	1.80
$m.h^{-1}$	0.25		0.11	

1.2.2. Plant effects

Various plant species can be used for VFCWs, but generally macrophytes and particularly reeds (*Phragmites australis*) are preferred due to their resistance to environmental conditions (long flooding periods of the filter surface, dry periods, high organic matter contents) and the fast growth of their roots and rhizomes (Brix, 1987).

Generally it is assumed that nutrient uptake by the vegetation growth plays a minor role in the wastewater treatment by VFCW. According Langergraber (2005), for a domestic wastewater treatment plant, removal potential of the nitrogen and phosphorus loads by macrophytes is around 1.9 % of the received load. Therefore, the direct role of plants in nutrient assimilation is negligible. On the other side, macrophytes have generally the faculty to transfer oxygen formed by photosynthesis through roots and rhizomes, generating aerobic zones around the roots. The oxygen excess is released by small roots and quickly consumed by the oxygen local demand. The oxygenation during the winter period is very low. Brix (1997) considers that a release of 0.02 $gO_2.m^{-2}.d^{-1}$ for *Phragmites australis* in winter. If we compare such oxygen provision to the loads applied (300 $gCOD.m^{-2}.d^{-1}$ and 25-30 $gKN.m^{-2}.d^{-1}$), it is obvious that the oxygen provision by macrophytes is negligible. In addition, oxygen convection and diffusion is a major issue (see section 1.2.5.).

Macrophytes play therefore mainly a physical role (Grison, 1999) in SSF systems:

- By the stalk growth particularly, they reduce clogging risks. Water can thus pass through the various filter layers;
- The root development increases the surface attachment for the microorganisms' development (Brix, 1997). They contribute also to provide a biodegradation of the organic part of the TSS and they release in the system some organic compounds with small weight, that can be easily degraded biologically;
- The foliar cover seems to be a thermal insulator for cold seasons with an impact on treatment capacity (Jenssen *et al.*, 1994).

In the French system, the mechanical role of plants is by far the most important. The sludge deposit forms a layer that reduce both hydraulic and oxygen transfer capabilities. The stems that pierce this sludge layer increase the infiltration rate (Molle *et al.*, 2006) and oxygen transfers through the surface, once ponding is over.

1.2.3. Individual processes occurring in a VFCW

VFCWs are artificial physical-chemical and biological reactors, in which the biomass grows attached to the mineral media. Biomass is the main constituent responsible for the pollutant degradation but, if not controlled, it can influence the water flow and gaseous transfer and clog the filter. Indeed, biofilm, as organic matter accumulation, reduces the material porosity and permeability. To control the biomass, i.e. the biofilm and the accumulated organic matter, rest periods are introduced. Their role is to promote aerobic mineralization of the biomaterial. However, the biofilm presents many secondary advantages. According Flemming (1993), the biofilm:

- Promotes the transfer of the nutrients of the liquid phase through the system;
- Protects the system against pH and salinity fluctuations, compression forces and drying;
- Preserves genetic information, promotes the gene transfer due to the long retention time of the microorganisms in the system;
- Creates ecological niches, anaerobic zones in aerobic areas for example. With in-situ gas content measurements carried out into a VFCW during one feeding period, Giraldo and Zarate (2001) pointed out that the oxygen content was not fully recovered when a new discharge occurred, leading to local anaerobic activity within the filter.
- Plays a particular role in the specific sorption that will increase retention time of anions and cations. For example organic matter can adsorb ammonium (McNevin *et al.*, 1999). The biofilm plays also a significant role in the adsorption of ammonium as it has been pointed out by Mc Bride and Tanner (2000).

As a consequence phenomena implied in pollutant removal on VFCW systems are diverse (physical, chemical, biological) and depend on various parameters such as water flow and oxygen transfers. According to the wastewater characteristics (solid or dissolved part, easily biodegradable or not, ionic strength, etc.), the influent is subject to various treatment mechanisms:

- **TSS filtration** more or less advanced according to the media pore size distribution and connectivity, the biofilm development and the sludge deposit;
- **Chemical transformations** (sorption, precipitation) according to the mineral characteristics of the media and the properties of the organic matter;

- **Biological conversion** along the filter of the organic matter and nitrogen contained in water, thanks to microorganisms present around the constituting media and reed roots.

Biological mechanisms are briefly described below.

1.2.4. Biological and chemical processes

The quality improvement of the wastewater mainly occurs in the upper part of the filter. Indeed, TSS are mainly retained by the filtering material and generate a deposit layer (sludge deposit) on the filter surface which allows a slower infiltration and therefore a better effluent distribution. Reeds pierce the sludge deposit, allowing the water and air flows entrance (Molle, 2003). These conditions avoid the frequent and regular sludge extraction.

1.2.4.i. Endogenous respiration

Endogenous respiration expresses the oxygen consumption and the carbon dioxide (CO_2) production generated by the own microorganisms metabolism, for maintenance, not for growth. Respiration is thus a quantitative expression of the active biomass present in the system.

1.2.4.ii. Organic matter removal

Generally, organic matter in wastewater is expressed in units of chemical or biological oxygen demand (COD or BOD_5). When it is applied to a VFCW it is exposed either to a full oxidation (mineralization), a conversion into other molecules, or no transformation. According to Henze *et al.* (1987), organic matter in wastewater can be represented by the following chemical composition: $C_{18}H_{19}O_9N$. Organic matter mineralization can be described by the followings equations (El Mossaoui, 2001):

$$C_{18}H_{19}O_9N + 17.5\ O_2 + H^+ \rightarrow 18\ CO_2 + 8\ H_2O + NH_4^+ \quad \text{(without nitrification)} \qquad [Eq.1.1]$$

$$C_{18}H_{19}O_9N + 19.5\ O_2 + H^+ \rightarrow 18\ CO_2 + 9\ H_2O + H^+ + NO_3^- \quad \text{(with nitrification)} \qquad [Eq.1.2]$$

Oxygen consumptions per gram of organic matter are calculated from these equations and are equal to 1.42 and 1.59 $gO_2.gOM^{-1}$, respectively.

The sludge layer influences COD removal which is sensitive to the infiltration rate (Molle, 2003). This removal is subject to higher variations than TSS, particularly with low hydraulic loads in the presence of heterogeneous distribution of the sludge deposit, which can generate heterogeneous water flows into the filter. Nevertheless, even for organic loads higher than those normally accepted and even if there is a wastewater dilution by parasite water, the TSS and COD removals remain acceptable.

1.2.4.iii. Nitrogen removal

In wastewater, ammonium (NH_4^+) and organic forms are typically the principal forms of nitrogen and come principally from human faeces. Kjeldahl Nitrogen (KN) represents the sum of organic nitrogen and ammonium nitrogen available in the influent. Biological treatments (assimilation, nitrification and denitrification) are the main mechanisms for nitrogen removal. Assimilation, necessary for the metabolism of microorganisms, represents a removal of about 25 % of the nitrogen in wastewater (5 % of the amount of BOD_5 eliminated (Choubert *et al.*, 2008)). This fraction is largely superior as compared to the assimilation for maintaining the reed plants (see above). The organic nitrogen is rapidly subject to the ammonification process (transformation through enzymatic hydrolysis into ammonium) by heterotrophic bacteria before being nitrified. Nitrification is the oxidation of ammonium nitrogen into nitrates by autotrophic microorganisms in the presence of oxygen. The simplified nitrification chemical equation is written as:

$$NH_4^+ + 2O_2 \rightarrow 2H^+ + H_2O + NO_3^- \qquad \text{[Eq. 1.3]}$$

This reaction proceeds in two successive steps (WPCF, 1983):

- The **nitritation**, oxidation of ammonium ions into nitrite carried out by nitrous bacteria (*Nitrosomonas*);

$$NH_4^+ + 3/2\ O_2 + H_2O \rightarrow NO_2^- + 2\ H^+ \qquad \text{[Eq. 1.4]}$$

- The **nitratation**, oxidation of nitrite into nitrate carried out by nitric bacteria (*Nitrobacter*).

$$NO_2^- + ½\ O_2 \rightarrow NO_3^- \qquad \text{[Eq. 1.5]}$$

Nitrification process is summed up by Burvingt and Heduit (1987) as follows (with the chemical formula of the biomass = $C_5H_7O_2N$):

NH_4-N + 1.83 O_2 + 1.98 HCO_3^- → 0.02 $C_5H_7O_2N$ + 1.04 H_2O + 0.98 NO_3-N + 1.88 H_2CO_3 [Eq. 1.6]

It is necessary to consider biological mechanisms so El Mossaoui (2001) suggested the global equation for nitrification including the nitrifying biomass growth (nitrogen assimilation):

0.129 NH_4-N + 2 O_2 + 0.004 CO_3^- + 0.016 CO_2 → 0.004 $C_5H_7O_2N$ + 0.12 H_2O +0.125 NO_3-N + 0.25 H^+ [Eq. 1.7]

Consequently, the oxidation of 1 g of NH_4-N requires theoretically 4.18 g of oxygen and produces 170 mg of biomass (WPCF, 1983).

It is necessary to promote nitrification because it is a preliminary step for denitrification, which occurs under anoxic conditions and consists in nitrate transformation into gaseous nitrogen in order to complete the nitrogen cycle and finally release a product perfectly harmless. The global equation for denitrification follows:

0.61 $C_{18}H_{19}O_9N$ + 4.5 NO_3^- + 0.39 NH_4^+ + 4.15 H_3O^+ → $C_5H_7O_2N$ + 2.27 N_2 + 5.98 CO_2 + 9.3 H_2O [Eq. 1.8]

For 1 g of nitrified nitrogen there is a production of 1.8 g of biomass.
An alternative solution to denitrification is the reuse of the effluent just after the nitrification step as a fertilizer taking advantage of the high nitrate concentration.

However, while TSS and COD removal appears relatively stationary, the nitrification efficiency on the first stage is variable. Ammonium and particular nitrogen removal rates are more sensitive to feeding conditions. Some important variations are recorded (50 to 95 %) according to hydraulic and organic loads received by VFCWs. Despite nitrification efficiency is not significantly correlated to treatment plant age or its depth, an improvement of the Kjeldahl nitrogen (KN) removal is observed over the years. Moreover seasonal variations of nitrification efficiency are observed. Winter period is the worst period for the biological activity, with a lower sludge deposit mineralization and low temperatures. Nitrification is probably the first process to be affected by these restrictive conditions (Molle *et al.*, 2005). On the other hand, Molle *et al.* (2008) pointed out the difficulty to evaluate the real efficiency of nitrogen removal due to its storage in the system (water, material, plant, and biomass). Assessing nitrogen mass balances is a difficult task because of the ammonium storage during the feeding period and nitrate release after the rest period. As a consequence, due to its high sensitivity to oxygenation and functioning conditions, nitrification appears to be a

significant indicator for improving pollutant removal performances in this system.

In summary, there is a need of oxygen to carry out biodegradation for the three following mechanisms:

- Endogenous respiration of biomass;
- Heterotrophic growth (COD conversion); and
- Autotrophic growth (nitrification).

Pollutant load removal is generally expressed by the total oxygen demand (TOD). This oxygen demand is determined by the concentrations in COD, and ammonium and organic nitrogen in influent and effluent: TOD = COD + 4.57*KN (Henze *et al.*, 1987). 4.57 mg of O_2 are needed to eliminate 1 g of KN by nitrification, and previously, we saw that 4.18 mg of O_2 are used to produce only nitrate (without considering biomass growth). Moreover, generally, more than 81 % (i.e. 3.38 mgO_2) of the oxygen consumed is transformed in nitrate form.

1.2.5. VFCW aeration: transport, consumption and oxygen renewal

A key element in VFCW functioning is the aeration quality of the system allowing an important aerobic biodegradation. VFCWs are not water saturated but fed alternately by batches and regulated by a succession of feeding and rest periods. As a result, there is an important temporal variation of the concentration of the different elements present in the filter gaseous phase. As proposed by Vasel (2003), the aeration of a VFCW is ensured by:

- Oxygen convection within the filter linked to the water flow brought by intermittent feedings;
- Oxygen diffusion from the filter surface and aeration chimneys to the porous space. It is linked to the oxygen concentration gradient between the atmosphere and the filter;
- Supply in the dissolved form in the influent that depends on temperature and pressure, with for instance a maximum concentration of about 10 mg.L^{-1} at 10°C. It is negligible in comparison with the TOD;
- Macrophytes roots, during the oxygen production by photosynthesis. This supply is negligible.

Therefore, air flux within the filter, and consequently the oxygen supply are mainly convective and diffusive types.

Molecular **diffusion** takes place, either through the filter surface between two batches when the surface is not flooded and during rest periods, or by passive aeration systems allowing aeration by the filter bottom (drainage layer connected to the atmosphere by aeration chimneys for example). Three main parameter groups influence the oxygen diffusion (Ménoret, 2001):

- The soil structure which directly determines the porosity and pore connectivity;
- The soil moisture and the clogging stage which influence the porous space size free for the air flow;
- The temperature which hinders the possible exchanges when it is too low.

Air **convection** within the filter is the consequence of the feeding by batches, which is directly related to the water flow within the unsaturated filter. The entering water pushes the gas present in the porous filter and creates at the same time an aspiration effect of atmospheric air when the filter surface desaturates (Forquet *et al.*, 2009a). Nevertheless, the air volume replaced with convection is inferior to the water volume entering in the filter during a batch. Indeed, the creation of local areas with high and low pressures during the water infiltration has been observed. These areas suggest that convective mass transport within the gaseous phase is buffered within the filter.
In addition, many authors carried out gas tracer measurements in order to evaluate the hydraulic behavior in subsurface CW. Schwager and Boller (1997) simulated oxygen transport in sand filters intermittently fed with MOFAT (Kaluarachchi and Parker, 1990), a method for modelling multicomponent organic chemical transport within multiphase flow, without reactive transport. Simulations were used to assess oxygen flux by convection and diffusion in the ten first centimeters of the filter. Results showed that, between two feedings, oxygen mainly enters into the porous media via diffusion. Studies led by Kayser and Kunst (2004) and by Laber (2001) demonstrated indeed that diffusion is the most important phenomenon and convection was overestimated in various previous studies. Nevertheless, Forquet *et al.* (2009b) showed that convection is greatly influenced by hydraulic load and ponding. Petitjean *et al.* (2011) compared the operation of French second stage VFCW with the Austrian VFCW regarding oxygen renewal. Their designs mostly differ by the applied loads. Conclusions showed that in the former set-up oxygen income by convection dominates, while in the latter, diffusion is the main oxygen renewal process.

During a feeding period, the oxygen concentration of the gaseous phase varies globally as follows (Kayser and Kunst, 2004; Ménoret, 2001):

- At equilibrium, the oxygen content represents nearly 21 % of the gaseous phase (oxygen content in atmosphere) at every depths;

- The phase following the feeding is marked by an oxygen content fall, in reference to its consumption during the nutrient biodegradation and the endogenous respiration;
- An oxygen renewal phase follows which has to be sufficient to have aerobic conditions for the rest of the feeding period.

The system re-oxygenation capability is also influenced by the grain size distribution (Langergraber, 2003). Oxygen content varies according to depth. Ménoret (2001) highlighted that water movements have little impact on re-oxygenation in the upper part of the filter (5 to 10 first centimeters of the filter), which is the principal place of biodegradation and transformation (Kayser and Kunst, 2004). Indeed, the first centimeters of the filter are governed by a high diffusion coefficient which allows an efficient oxygenation of the upper part. Yet, no detailed study was carried out so far on the effect of the sludge layer on oxygen renewal for the particular case of French first stage VFCW.

1.2.5.i. Oxygen transfers toward the biomass

The interface between the biofilm and the gaseous phase presents generally a liquid phase (residual moisture). Therefore, according Ménoret (2001), gas transfer towards the biofilm takes place in three steps:

- A fast step of oxygen transfer to the liquid surface;
- The liquid-gas interface crossing; this step can be represented by the molecular diffusion through a liquid thin thickness;
- The oxygen transfer into the liquid mass by diffusion and convection.

1.2.5.ii. Gas content variation within the VFCW

The biomass distribution is directly linked to the spatial distribution of the organic matter which presents some high vertical variations. Consequently, the biomass will mainly be developed in areas with high organic matter and high atmospheric air provisions. These conditions are present close to the filter surface. Oxygen and carbon dioxide contents present thus high spatial variations. Within the filter, many phenomena and forces can generate gaseous fluxes (Altevogt and Celia, 2004):

- Spatial variation of the molar fraction of one gas component;
- Variation of pressure gradients;
- Movements generated by some differences in density of gas components.

During the feeding period, convection is driven by pressure gradients. On the contrary, as the pressure gradients are decreasing during the rest period, it is possible to ignore convective movement during the rest period (Schwager and Boller, 1997). Gas flow is thus mainly due to the creation of concentration gradients. Molecular diffusion generates gas flux towards lower concentrations in all directions.

All these processes depend on the ability of water and oxygen to flow through the porous filter media. As a consequence, the biomass accumulated within the filter media is of great importance. The clogging risk is directly linked to this biomass growth.

1.2.6. Clogging

The VFCW clogging may have various causes and may result in a considerable reduction of the infiltration capability. Clogging limits infiltration rate of the influent and creates temporarily ponding water at the surface. As a consequence, the gaseous phase cannot be renewed easily through the surface and the oxygen content decreases drastically (Langergraber *et al.*, 2003). The main mechanisms which can generate clogging are described below.

- **TSS accumulation (physical clogging)**

According to the TSS quantity and the particle size distribution of the media, a variable storage of particles on the filter surface and in the media porosity is observed. The storage of these particles has an influence on the porosity distribution and consequently generates a more or less significant reduction of filter permeability. The effective hydraulic porosity is affected and clogging processes appear (Langergraber *et al.*, 2003). In the literature few data are available concerning the maximum TSS acceptable load.

- **Organic load and sludge overproduction (biological clogging)**

According to Ménoret (2001), biological clogging is generated by the filling of the media porosity by the biomass and by-products coming from the metabolism of microorganisms. Clogging occurs if the sludge production from the organic load removal is higher than the biomass decay rate (Langergraber *et al.*, 2003).

The difficulty to define a limit is that clogging depends on:

- The TSS and organic loads and their nature (easily biodegradable or not);
- The particle size distribution of the media;
- The feeding and resting strategies.

As VFCW systems are used in different ways (primary, secondary treatment, continuous or batches feeding, with or without rest period) and using different filter media (gravel, sand …) it is difficult to estimate the clogging limits. Moreover, clogging is never well described. In French system, ponding appears during a batch feeding. This is a normal way of functioning. The clogging results in a continuous ponding between batches. But a daily ponding does not mean that the filter is definitively clogged. The appropriate management of the feeding and resting periods can allow recovering acceptable infiltration rates.

Despite the good treatment performances obtained nowadays on VFCW plants and the important optimization progresses concerning the design and the management of these treatment plants, the nitrification efficiency on the first stage still remains incomplete. At Cemagref, ongoing researches are still carried out to increase performances. Due to the interactions between each process and the fact that these systems are season dependent, the study of nitrification by pilot and/or real scale experiment is necessary. Nevertheless Molle *et al.* (2008) highlighted that treatment efficiency may be improved at the cost of a deeper analysis and a better understanding of the biological processes which take place in VFCWs. But, local performances within the VFCWs are ill-known, particularly because of the lack of biological investigations methods (Langergraber, 2003). It is thus essential to study more accurately nitrification processes taking place in these unsaturated systems, and to understand their limits in order to optimize the design procedure. Therefore it is suggested to improve the modelling of VFCWs as way to unravel process understanding.

1.3. VFCW modelling

1.3.1. Limitations of the CW modelling

CWs are engineered systems designed for optimized treatment conditions found in a natural environment using a complex mix of water, material, plants, litter and a large variety of microorganisms (especially bacteria). On the other side, VFCWs are usually fed intermittently in order to provide a good influent distribution, oxygen diffusion and an adequate retention time as well as a limited clogging in the same time. The large number of physical, chemical and biological processes operating simultaneously and influencing each others makes the CWs difficult to understand. Despite the numerous studies carried out to investigate the performances of treatment by CW, the behaviour of these systems is still difficult to understand and to predict. They are often considered as "black boxes". They suffer from a lack of knowledge of the various interactions between soil, vegetation, water and microorganisms. The most widely used approaches and optimizations for VFCW design are based on empirical rules inferred from the experience of the designers. Examples include the use of a specific surface area (Brix and Johansen, 2004), or the use of a simple first-order model derived from the difference of the concentrations in nutrients between the influent and the effluent (Kadlec and Knight, 1996; Rousseau *et al.*, 2004). However, Kadlec (2000) showed already that first-order decay models are inadequate, highlighting the need to consider the variably saturated conditions in the reactive transport models which represents a large complexity in comparison of models used for saturated conditions (Langergraber *et al.*, 2009a).

With numerical models, it may be possible to get a better understanding of biological and chemical transformation and degradation processes which takes place in VFCWs and therefore to improve their design and operating criteria (Langergraber, 2007). Recently some mechanistic models have been developed for VFCWs, allowing including different hydraulic and reactive processes descriptions in the modelling concepts (Rousseau *et al.*, 2004).

1.3.2. Dynamic VFCW modelling

During the last years, an improvement has been carried out in the modelling of processes describing water flow and organic matter transfer within unsaturated VFCWs. Use is made of simulation tools with various complexity levels allowing to better understand processes which take place inside CWs (Langergraber, 2008). The subsurface transport of contaminants

is generally affected by a large number of physical, chemical and biological processes that often are interactive and not linear. Consequently, Simunek *et al.* (2006) advise to simulate these processes using reactive transport codes which integrate the unsaturated water flow and the convective-dispersive transport with biodegradation processes.

Seven mechanistic or process based models have been recently published to describe the reactive transport under variably saturated conditions and that can be used for the VFCW modelling (Langergraber and Simunek, 2005 (HYDRUS/CW2D); McGechan *et al.*, 2005; Freire *et al.*, 2006; Ojeda *et al.*, 2006; Wanko *et al.*, 2006; Giraldi *et al.*, 2010 (FITOVERT)). They have been developed for VFCWs in order to consistently connect the different hydraulic and reactive processes (Table 1.6).

Table 1.6: Models existing for VFCW modelling (see in Appendix I)

References	Domestic wastewater	Water flow		Main species considered	Biological conversion (kinetics)	Reactive transport	Porosity evolution
		Richards equation	Two-phase flow				
Freire *et al.* (2006)					1st order	X	X
Mc Gechan *et al.* (2005)				N	1st order	X	
Wanko *et al.* (2006)	X	X		C	Monod-type	X	
Forquet *et al.* (2009b) Petitjean *et al* (submitted for publication)	X		X	C, N	Monod-type	X	
Ojeda *et al.* (2006)	X		X	C, N	Monod-type	X	
Simunek *et al.* (1999, 2006) Langergraber and Simunek (2005) HYDRUS/CW2D	X	X		C, N, P	Monod-type	X	
Giraldi *et al.* (2010) FITOVERT	X	X		C, N	Monod-type	X	X

- For describing the variably saturated water conditions, the Richards equation was used by Simunek *et al.* (1999, HYDRUS software), Wanko *et al.* (2006) and Giraldi *et al.* (2010, FITOVERT package). Freire *et al.* (2006) and Mc Gechan *et al.* (2005) opted for a more simplified model. An equivalency of several reactors, combining completely stirred reactors and dead zones mimics the fate of water through the different vertical layers of a CW. Ojeda *et al.* (2006) proposed the diphasic air-water flow approach, that was first experimentally studied by Forquet *et al.* (2009b) through laboratory-scale sand columns under clear water simulations, and

upgraded by Petitjean *et al.* (submitted for publication to *Water Research*) who included biological conversion equations (biokinetic model).

- For the solute transport part, Mc Gechan *et al.* (2005) and Freire *et al.* (2006) used mass balances and transfer coefficients between reactors. Reactive transport with interactions between compounds is considered in CW2D (HYDRUS software, Langergraber and Simunek, 2005), Ojeda *et al.* (2006) model, FITOVERT model (Giraldi *et al.*, 2010) and Petitjean *et al.* (submitted for publication to *Water Research*) model. The bio-geochemical CW2D module incorporates all chemical species and degradation kinetics occurring in the wastewater treatment process (Langergraber and Simunek, 2005), and uses a biokinetic approach as in the ASM model (Henze *et al.*, 2000);

- For the fate of NH_4-N, most of the CW models include NH_4-N production by hydrolysis of organic nitrogen, and removing by integration into new cells (heterotrophic growth), and conversion into NO_3-N under aerobic conditions by nitrification that is further converted into N_2 under anoxic conditions by denitrification (Langergraber *et al.*, 2009a). Those models were using a biokinetic ASM-like model (Henze *et al.*, 2000). Additionally, Simunek *et al.* (2006, HYDRUS software) considered a sorption process onto organic matter for ammonium. In the same way, this sorption process was also studied by Mc Bride and Tanner (2000) and Langergraber *et al.* (2009a) (Freundlich isotherm and linear equilibrium, respectively), including a rapid adsorption with immediate equilibrium (Sikora *et al.*, 1995) maintained all along a feeding batch-period (Giraldo and Zarate, 2001).

1.3.3. Model selection

Comparing the complexity of these various models, as well as their level of description of biochemical transformations of carbon and nitrogen solutes, growth/decay of biomass, the HYDRUS/CW2D model appears to be reasonably complex but realistic to simulate VFCW behavior. Its hydraulic software and user friendliness have been tested many times. Nevertheless its use for the optimization of the design and operating conditions of VFCW still requires more realistic predictions (Langergraber, 2007). Moreover, contrary to Mc Gechan *et al.* (2005) and Freire *et al.* (2006) models, HYDRUS/CW2D takes into account the reactive transport of carbon, nitrogen and phosphorus compounds, making it appropriate for water flow modelling, transport of the various dissolved components and biochemical

phenomena taking place within the VFCWs as well. Concerning the nitrogen species, various transformations can occur in the unsaturated zone: nitrification, denitrification and adsorption mechanisms (Langergraber *et al.*, 2009a). Organic nitrogen may be transformed to NH_4-N and NH_4-N or NO_3-N may be assimilated by microorganisms. NH_4-N may be sorbed by organic matter or nitrified to NO_3-N under oxygenated conditions. In the absence of oxygen, NO_3-N may be converted to N_2 through denitrification. A traditional VFCW operated with alternating periods of wetting (application of wastewater) and drying (no application) introduces sequentially anoxic and aerobic periods. Therefore, both aerobic and anoxic processes take place and the nitrification process needs to be understood to be able to optimize VFCW treatment plant design. Giraldo and Zarate (2001) showed that sorption is one of the most important ways for the COD removal. Moreover, previous experiments carried out by Sikora *et al.* (1995) demonstrated rapid initial ammonium adsorption in studies of experimental constructed wetlands with fresh pea gravel. Accordingly, Mc Bride and Tanner (2000) included sorption processes in the model that they used. While FITOVERT does not consider the nitrogen adsorption process, HYDRUS/CW2D does. Many modelling studies carried out with HYDRUS concerned natural soils (Jacques *et al.*, 2005, 2008; Jiang *et al.* 2010) and most of them concerned water flow during rainfall events (Dittmer *et al.* 2005; Zhang *et al.* 2010), but its use for VFCWs is relatively recent (10 years) and consequently this use is little documented (Langergraber and Simunek, 2005; Toscano *et al.*, 2009). In comparison to previous searches, this study aims modelling VFCW receiving raw wastewater, and contrary to the ordinary matrix used, as fine sand, the main filtering is a coarse material (gravel).

1.4. Improving existing models of VFCW with in-situ and ex-situ experimental investigations

1.4.1. Problem statement

Due to model complexity and hence the low parsimonious status, the HYDRUS/CW2D model calibration/parameterization remains a complicated task. The parameter calibration is necessary and particularly important for models simulating the pollutant species behavior into CWs (Giraldi *et al.*, 2009) where literature values for ASM parameters refer to growth of the biomass only in suspension. This calibration will be more accurate if the hydraulic model is previously properly calibrated.

1.4.2. Hydraulic model: methods for estimating the hydraulic parameters

An accurate calibration of the hydraulic model is essential before to test the entire model in order to get reliable simulations of VFCW systems (Langergraber, 2002). The numerical solution of the flow equation in HYDRUS requires detailed knowledge of the partially-saturated hydraulic properties in the porous medium under study. These properties are difficult to estimate because hydraulic functions are both highly non-linear and variable in space. The hydraulic properties of partially-saturated porous media can be assessed by direct and indirect methods that can be applied at laboratory scale, field scale, or both. For example, the constant or falling head method for determining hydraulic conductivity can be applied on soil cores in-lab or in -field using cylinder infiltrometers (Dane and Topp, 2002). However, direct hydraulic characterization requires restrictive initial and boundary conditions that have limited practicability in the field. Although direct laboratory methods are more accurate, the parameters obtained often fail to reflect real field conditions, and there is no common procedure for transposing in-lab hydraulic properties into in-field hydraulic properties (Russo *et al*., 1991; Ritter *et al*., 2003). The differences between laboratory and field assessments are due to several factors, including differences in support volume, measurement scale and structural status (e.g. different macropore compositions), and hysteretic effects (Schuh *et al.,* 1988; Basile *et al.,* 2003). Consequently, *in situ* measurements are considered more appropriate for assessing the hydraulic properties of partially-saturated porous media (Zou *et al*., 2001; Ramos *et al*. 2006), especially in constructed wetlands where the impact of the reeds on the hydraulic characteristics of the filter cannot be easily measured at the laboratory scale.

The indirect methods used often rely on inverse modelling and are particularly suited to *in situ* assessments of hydraulic properties (Beven and Freer 2001; Hopmans *et al.,* 2002; Vrugt *et al.,* 2003; Minasny and Field, 2005; Lambot *et al.*, 2005,Simunek *et al.,* 2006; Durner *et al.,* 2008). Inverse methods offer adaptable experimental procedures and impose less restrictive boundary conditions than direct methods. They can therefore be applied on transient flow experiments (e.g. Kool *et al.,* 1987) and include many indirect measurement variables in the objective function. Moreover, with inverse modelling, both hydraulic conductivity and water retention characteristics are assessed simultaneously from a single flow experiment. In addition, and in contrast to direct methods, inverse modelling can rigorously assess parameter uncertainty (Kool *et al.,* 1987). Furthermore, hydraulic parameters inferred from inverse methods are often more effective at describing transient flow in real flow systems. The down side is that inverse problems are often ill-posed and can suffer from convergence problems (Russo *et al*.,

1991). Nevertheless, as stated in Durner et al. (2008), inverse-based approaches remain widely recommended, and there are numerous examples of successful estimation of soil hydraulic properties using inverse methods (see Kool *et al.,* 1987; Romano, 1993; Lambot *et al.*, 2002; Hopmans *et al.,* 2002; Ritter *et al.*, 2004; Mertens *et al.,* 2005; Verbist *et al.,* 2009, among many others).

The development of methods for assessing the hydraulic properties of partially-saturated porous media is a thriving field of research in the soil hydrology community, but few studies have attempted to characterize the hydraulic properties of particular porous media such as gravel and sands mixed with sludge in VFCW systems. Giraldi and Iannelli (2009) carried out a lab-scale experiment to assess the saturated hydraulic conductivity of the material in a VFCW. They combined these measurements with generic estimates of the shape parameters, and subsequently modeled water content distributions measured with capacitance probes in laboratory columns and in a VFCW pilot plant. Using these methods, they were able to simply and rapidly identify the real layout of vertical systems, and consequently highlight operational failures. Moreover, they managed to assess unsaturated hydraulic parameters for the main layers (gravel layers) of a vertical-flow bed using only water content measurements and saturated hydraulic conductivity. Langergraber (2003) carried out an inverse modelling with the HYDRUS-2D software to assess the hydraulic parameters of sand used as filtering material. He measured pressure potentials and water contents at different depths (each 10 cm in the main layer) as well as the effluent flow rate. The simulations using the fitted parameter set showed a good match to the measured data. Toscano *et al.* (2009) assessed hydraulic parameters using the inverse simulation proposed in HYDRUS-2D software (Simunek *et al*., 1999), with outflow measurements from a pilot-scale VFCW (secondary treatment) used as input data. Although they did not compare their results against laboratory assessments of hydraulic parameters, the flow simulation study resulted in good correlations between measured and simulated effluent flow rates for two successive loads. Similarly, Maier *et al.* (2009) used an inverse method considering a global optimization based on a stochastic search strategy for parameters. Hydraulic calibration was also carried out on the outflow rate measurement of two VFCWs filled mainly with a mixture of expanded clay and sand. They maximized the fit between observed and simulated filter discharges and revealed potential parameter correlations between certain hydraulic parameters. Another experiment performed on a laboratory sand column used both water content and suction measurements to constrain the inversion (Forquet *et al.*, 2009b).

Although several studies have reported assessments of the hydraulic properties of VFCWs, none has compared the performance of different hydraulic assessment methods specifically in the VFCW setting. Furthermore, there are no published reports allowing the evaluation of different assessment procedures for the specific case of the Cemagref-type VFCW, where a sludge layer develops at the filter surface.

1.4.3. Biological model

1.4.3.i. Need for calibration of the parameters

Biological parameters were largely studied for wastewater components in activated sludge but little research has been done on calibration of the parameters for CWs (Henrichs *et al.*, 2007). A large standard bio-kinetic and stoichiometric parameter set is available in literature for the CW2D calibration (Langergraber and Simunek 2005), and most of the values come from the ASM1 model (Henze *et al.*, 1995), except for the nitrification step (Nowak, 1996). This calibration set has been used and adapted for effluent concentration simulation with VFCW but it has to be notified that for low temperatures, predicted effluent COD and NH_4-N concentrations are quite inaccurate mainly because hydrolysis and nitrification processes are overestimated (Langergraber, 2007). Calibration can be the main cause. To get the parameter set, calibration has traditionally been carried out with pilot units through specific and well-controlled experiments under constant operating conditions (Gernaey *et al.*, 2001; Munz *et al.*, 2008). However, values obtained in these conditions are not totally reliable. First of all, it is difficult to carry out the same configuration and to mimic the same functioning for a pilot unit than a full-scale unit. Another reason concerns experiments and calculations often based on constant coefficients. But, many of these parameters vary in time, over long periods, and few parameters change considerably over a limited time period. Factors such as system configuration, operating conditions, dynamics of microbial populations, temperature, pH, etc., affect parameter values of the process. This is particularly true in the French system where the loads (raw wastewater) and the operating conditions (feeding/rest periods) produce high biomass dynamics within the filter.

Moreover, while the parameter values can change over a period of a few days, influent characteristics can significantly change within a few hours, above all for small communities. As influent composition affects considerably the model behavior, the difficulty of the model calibration is magnified (Henrichs *et al.*, 2007).

On the other hand, examining the sensitivity, variability and uncertainty of the ASM model, Jeppsson (1996) noticed that nitrification and denitrification parameters are the most sensitive compared to COD ones. Therefore, in this present study relating specifically to nitrification, the maximum specific growth rate of autotrophic microorganisms is a key parameter on the nitrification process. Its calibration as well as biochemical kinetic calibration is particularly important, since literature values for CW2D parameters refer to growth of the biomass in suspension with a fixed sludge age.

A research concerning the development of experimental methods aiming at assessing the biochemical parameters of ASM models and more precisely nitrification parameters is necessary (Langergraber, 2008). No technique is currently available (Langergraber and Simunek, 2005) and selecting the ideal index for the study of the biological activity from VFCW samples is tough.

1.4.3.ii. Ex-situ experiences with respirometry (biodegradability of wastewater, parameters determination)

Respirometric methods provide real-time monitoring of the oxygen uptake, and consequently the biodegradation intensity and the nitrification rate can be measured (Ginestet *et al.*, 1998). It is a useful investigative technique of biological systems. It has been identified as the best tool to estimate the biochemical dynamics within VFCWs (Giraldi *et al.*, 2010), and consequently to calibrate ASM models used in the CW domain. It is an appropriate means aiming at characterizing the biodegradability of the concerned matrix. During the biological reactions, the oxygen use and the carbon dioxide production is linked to the metabolic activity and to the organic matter degradation (Adani *et al.*, 2006). The respective rate of the reactions depends on substrate characteristics (quantity and type of biodegradable organic matter) and environmental conditions (temperature, aeration and moisture content).

This technique was successfully developed in domains of composting and proposed for control of suspended growth biomass for twenty years (Lasaridi and Stentiford, 1998; Adani *et al.*, 2004; Spanjers *et al.*, 1995; Vanrolleghem *et al.*, 1999; Ziglio *et al.*, 2001). The main goal is the determination of the rate of oxygen consumption (quantity of oxygen consumed by microorganisms by units of volume and time) by an environmental matrix (sludge, organic waste, soil, etc.) under different operating conditions (temperature, with or without substrates, etc.).

Determining the parameters

During respirometric tests, actual conditions are not reproduced but optimal conditions are searched in order to characterize the **maximum** biodegradation kinetics of the biomass present in the matrix. Therefore, respirometric measurements must only depend on intrinsic parameters of the microbial activity such as the biomass content, biodegradable organic matter concentration and environmental conditions (temperature, moisture, etc.). The oxygen provision has also to be as constant and homogeneous as possible to provide favorable conditions to the biodegradation and not affect the kinetics during the measurements (Tremier *et al.*, 2005).

More specifically, regarding the nitrification study and thanks to optimal conditions (availability of oxygen, ammonium and phosphorus not limiting), we can assess the maximum conversion rate of the nitrogen species. Consequently, among the different equations of the nitrification rate (Eq. 1.9 and 1.10, see Appendix II), only the maximum aerobic growth rate of the nitrifying bacteria *Nitrosomonas* and *Nitrobacter*, $\mu_{AN,s}$ [1/h] and μ_{ANb} [1/h], respectively, as well as their concentrations in the liquid phase, c_{XANs} [mg $COD_{biomass}$/kg DM] and c_{XANb} [mg $COD_{biomass}$/kg DM], respectively, have to be determined.

$$\frac{dc_{O_2}}{dt}_{nitritation} = -\frac{4.57 - Y_{AN}}{Y_{AN}} \mu_{ANs} \cdot \frac{c_{O_2}}{K_{ANs,O_2} + c_{O_2}} \cdot \frac{c_{NH_4}}{K_{ANs,NH_4} + c_{NH_4}} \cdot \frac{c_{IP}}{K_{ANs,IP} + c_{IP}} \cdot c_{XANs} \qquad \text{[Eq. 1.9]}$$

$$\frac{dc_{O_2}}{dt}_{nitratation} = -\frac{4.57 - Y_{AN}}{Y_{AN}} \mu_{ANb} \cdot \frac{c_{O_2}}{K_{ANb,O_2} + c_{O_2}} \cdot \frac{c_{NO_2}}{K_{ANb,NO_2} + c_{NO_2}} \cdot f_{N,ANb} c_{XANb} \qquad \text{[Eq. 1.10]}$$

With $$f_{N,ANb} = \frac{c_{NH_4}}{K_{ANb,NH_4} + c_{NH_4}} \frac{c_{IP}}{K_{ANb,IP} + c_{IP}};$$

Y_{AN} [g $COD_{biomass}$/gNH_4-N $_{nitrified}$], the cellular yield coefficient, $K_{ANs,O2}$ [mg O_2/L], the saturation/inhibition coefficient for oxygen, $K_{ANs,NH4}$ [mg NH_4-N/L], the saturation/inhibition coefficient for nitrogen, $K_{ANs,IP}$ [mg P/L], the saturation/inhibition coefficient for inorganic phosphorus, C_{O2} [mg O_2/L], the concentration of oxygen, C_{NH4} [mg N/L], the concentration in ammonium and C_{IP} [mg P/L], the concentration in inorganic phosphorus.

Under no-limiting conditions, Eq. 1.9 and Eq. 1.10 become:

$$\left(\frac{dc_{O_2}}{dt}\right)_{nitritation_MAX} = -\frac{4.57 - Y_{AN}}{Y_{AN}} \cdot \mu_{ANs} \cdot c_{XANs} \qquad \text{[Eq. 1.11]}$$

$$\left(\frac{dc_{O_2}}{dt}\right)_{nitratation_MAX} = -\frac{4.57 - Y_{AN}}{Y_{AN}} \cdot \mu_{ANb} \cdot c_{XANb} \qquad \text{[Eq. 1.12]}$$

While respirometry is widely used for calibrating ASM-like models (Spanjers *et al.* 1998), the application for studies on samples of CW is new and few experiments are available at the moment. A method to carry out some respirometric test for measurement of VFCW biological activity in terms of kinetics of oxygen consumption, in-situ carbon dioxide production and organic matter degradation is developed by Giraldo and Zarate (2001). It is also shown that the degradation rate of dissolved organic matter is dependent on its concentration and oxygen content in the gaseous phase. This technique could be applied to samples collected at different VFCW depths allowing us to assess μ_{AN} and c_{XAN} for each vertical layer. A comparison between measured and simulated data in relation to carbon and nitrogenous matters could thus be done. Consequently, calibration of the CW2D model could be more precise and some model assumptions confirmed or not. But this respirometric method based on semi-static oxygen uptake measurements from wetland samples requires much more efforts for their extended use as standard calibration tool.

Types of respirometric methods

Various methods exist for measuring the biological activity of sludge. In the context of solid organic matter biodegradation, only the concepts concerning carbon oxidation by heterotrophic biomass were presently considered (Tremier *et al.*, 2005). Methods consist in measuring either the oxygen consumption, or the heat produced by these oxidations or, carrying out some chemical analyses (details presented in Appendix III). These methods are validated and largely used to measure the activity of liquid materials (activated sludge), but there is a lack in literature for the measurement of solid materials. Moreover liquid respirometry (saturated media) is not suitable for the study of the unsaturated matrix of VFCW systems because operating conditions do not reproduce processes and constraints linked to the gaseous oxygen (moisture, media particle size, etc.).

We investigated the literature dedicated to the stability of compost (Lasaridi *et al.*, 2000; Paletski and Young, 1995). Despite the fact that a lot of methods (physical, chemical, biological) have been proposed to determine

the biological stability in solid media, there is no general consensus on the use of one common technique. Respirometric tests are known to be the most reliable methods to measure the biological stability (Lasaridi *et al.*, 2000; Paletski and Young, 1995) as they are a direct measurement of the microbial activity (Adani *et al.* 2004).

A large number of indices exist to characterize and describe the stability and the reactivity of sludge and/or compost. According to the various studies, many different operating conditions are recommended (ideal moisture, experiment length, etc.).

Table 1.7 presents the main operating conditions for some methods used for the biological activity of compost, activated sludge as well as wastewater from VFCW. Proposed methodologies differ in many key aspects such as the phase in which the oxygen measurement is carried out, the respirometry type, sample quantity, water content, assay temperature and length (Appendix IV). Moreover, result expression (oxygen uptake rate or cumulative oxygen consumption) and units (based on dry or volatile solids contained into the sample) depend on the method used for index determination (Barrena *et al.*, 2006). Among indexes presented in Table 1.7 the dynamic respiration index (DRI, [$mgO_2.kgVS^{-1}.h^{-1}$]), is determined by measuring the difference of the oxygen concentration between the entrance and the exit of the air flow passed through the solid sample (Adani *et al.,* 2004). The specific oxygen uptake rate (SOUR, [$mgO_2.gVS^{-1}.h^{-1}$]), and the oxygen demand in twenty hours (OD_{20}, [$mgO_2.gVS^{-1}$]) represent the maximum rate of oxygen uptake and the cumulative oxygen demand for the first twenty hours of the test, respectively (Lasaridi and Stentiford, 1998).

Table 1.7: Main operating conditions for respirometric methods used for compost, activated sludge and wastewater from VFCW

	Dynamic	Solid	O_2 phase	Index
Compost				
Adani *et al.* (2004)	X	X	Gaseous	DRI
Scaglia *et al.* (2007)	X		Liquid	$SOUR/OD_{20}/OD_{12}$
Scaglia and Adani (2008)	X	X	Gaseous	DRI
Liquid sludge by composting				
Lasaridi and Stentiford (1998)	X		Liquid	$SOUR/OD_{20}$
Tremier *et al.* (2005)		X	Gaseous	rO_2 [$mmolO_2.kgDM^{-1}.h^{-1}$]
Berthe *et al.* (2007)	X	X	Gaseous	rO_2 [$mmolO_2.kgDM^{-1}.h^{-1}$]
Wastewater from VFCW				
Giraldo and Zarate (2001)		X	Gaseous	kinetics of O_2 consumption, CO_2 production

The main differences of the different tests consist of:

The analyzed phase. Various tests can be used: measurement of gaseous oxygen content or dissolved oxygen concentration, change of the carbon dioxide rate (Barrena *et al.*, 2006). Lasaridi and Stentiford (1998) declared that this latter measurement can not be used to assess a respiration index of compost. Consequently, methods based on the **oxygen uptake** rate are preferred to estimate the potential biodegradability of solid organic waste (Lasaridi and Stentiford, 1998).

The air supply. Respirometric tests based on the oxygen consumption can be divided between static and dynamic methods in relation to the oxygen consumption measurement carried out without (static) or with (dynamic) a continuous aeration of the biomass (Scaglia *et al.*, 2000; Adani *et al.*, 2004). The choice depends also on the studied media activity: for low activity, static respirometry is recommended and dynamic ones for high activity.

- Static methods consist in oxygen consumption measurement into a closed container without continuous supply. They induce a transfer limitation through the biomass and bacterial cells;
- Dynamic methods, that use a continuous supply of oxygen, have the advantage to minimize the effect of the oxygenation limitations, and can be used for high rate of oxygen uptake and large mass of organic matter.

The output results. Different results are usually calculated. A popular method uses the dynamic respiration index (DRI, [$mgO_2.kgVS^{-1}.h^{-1}$]). A method based on BOD was also suggested by Lasaridi and Stentiford (1998) Using two indices, measuring the specific oxygen uptake rate (SOUR, [$mgO_2.gVS^{-1}.h^{-1}$]) and the oxygen demand in twenty hours (OD_{20}, [$mgO_2.gVS^{-1}$]), is more accurate for a large and longer biological stability. The dry specific oxygen uptake rate (DSOUR) for a dry solid sample is calculated by Iannotti *et al.* (1993). The cumulative oxygen uptake recorded during 96 h (four days) (AT_4, [$gO_2.kgDM^{-1}$]) and the DRI are recommended as parameters for the compost stability estimate (European Commission, 2001; Barrena *et al.*, 2009).

Limits of the existing methods

Due to the transfer limitation through the biomass and bacterial cells, dynamic methods are preferred rather than static methods. Moreover, methods measuring the oxygen content in the liquid phase are considered to be biased for unsaturated matrices. Hence, only methods measuring gaseous oxygen content are suitable. Therefore, only three methods presented in

Table 1.7 could be used or adapted to evaluate respiration from VFCW samples (Adani *et al.*, 2004; Scaglia and Adani, 2008; Berthe *et al.*, 2007). However, the methods proposed by Adani *et al.* (2004) and Scaglia and Adani (2008) were not retained here because their device do not use an air recirculation system. This could generate poor mixed conditions and limiting oxygen uptake rates. The most suitable method for assessing the biodegradability of wastewater and determining biological parameters in VFCW systems should therefore resemble to the Berthe *et al.* (2007) device (Appendix V).

1.5. Objectives of the research

The overall objective of the present work is to improve nitrification in a first stage of a VFCW. As it is inconceivable to test many different operating conditions due to the large number of processes involved in these VFCW systems and in view of the complexity of interacting processes in these systems, numerical models are usually used. Therefore, the objective of the present work is to setup and validate a numerical model predicting carbon and nitrogen concentrations in treated water of a VFCW filled with gravel as a way to unravel the hydraulic and biological processes determining the VFCW functioning. One of the key issues will therefore be to determine numerical values of the hydraulic and biological parameters of the VFCW system.

This approach requires special accent on more fundamental processes involved in a VFCW or related to the metrology. Therefore, the scientific objectives consist of the validation of the concepts used in the model, to point out the oversimplification of the concepts, and to propose suitable modifications.
The key research questions are:

- Hydraulic part:
  - How can the hydraulic parameters of a VFCW be assessed?
  - Can the usual tools used for determining the hydraulic parameters of soil matrices be used or adapted for determining the hydraulic parameters of a VFCW?
- Biological part:
  - Can the biological parameters commonly used for modelling the nitrifying biomass activity in activated sludge be used for modeling a VFCW?
  - How can the biological parameters related to the nitrification step of VFCW be assessed?

The operational benefit is to better define the operating limits of a VFCW, particularly in relation to the nitrification step on the first stage of a waste water treatment process. This work will help to optimize the system design in relation to its application domain (water type, collecting network, geographical zone) and to anticipate rules and regulation evolution in relation to the river quality improvement.
The adopted approach to reach these objectives is therefore to implement and to calibrate the HYDRUS/CW2D model (Langergraber and Simunek, 2005), that initially was developed for a VFCW system filled with sand. The challenge is to accurately simulate the domestic wastewater treatment by VFCW with a different matrix. The experimental approach to improve this model is carried out at two scales:

- At the laboratory-scale, biological turn-over parameters are refined thanks to a respirometric device aiming to quantify bacterial activities of nitrogen transformations (nitrification), and hydraulic parameters are determined for the different matrix layers involved in the VFCW system.
- At the treatment plant scale, the first stage of a SSF system is monitored. This monitoring is done for the VFCW plant of Evieu (Ain, France) built in 2003 and treating wastewater of 100 PE. This system is subject to a regular monitoring by the Cemagref since its start-up. Its first stage is subject to a detailed monitoring to support the model implementation and validation.

1.6. Outline of the thesis

The second chapter of this work is dedicated to the hydraulic modelling of the VFCW of the Evieu plant. In a modelling context, knowing the water flows and hydrodynamics inside a VFCW is essential to better understand and improve its functioning. In addition it is the first step for a global modelling (hydraulic and biological) of this system. To carry out this modelling, some hydraulic parameters have to be determined. The first part of this section concerns the hydraulic parameter assessment. We compare the VFCW hydraulic properties estimated by laboratory direct and inverse methods and those obtained by inverse modelling using water content and outflow data collected from the VFCW. The aim is to determine the most appropriate method in order to estimate the best hydraulic parameters for the VFCW system. Water content evolution within the VFCW is obtained by TDR probes. At the end of this part, the hydraulic modelling is presented. Calibration of these TDR probes is presented in Chapter 3.

We designed an experimental technique aiming at estimating the concentration in autotrophic biomass, and its kinetic and stoichiometric parameters. The fourth chapter of the thesis presents a new respirometric method aiming at measuring biological process parameters for models like HYDRUS/CW2D (Langergraber and Simunek, 2005). It is applied to investigate the nitrification process in unsaturated porous media of samples taken from the VFCW. These latter are required for the next step, the biological modelling of the studied VFCW. Various operating conditions are investigated to determine the biodegradable organic matter quantity and the nitrification capacity. Special attention is devoted to the assessment of the robustness of the method. Therefore, with these biological parameters a better biological modelling allows a better understanding of biological and chemical transformation and degradation processes which take place in VFCWs.

The last part of the thesis concerns the calibration of the biofilm model of HYDRUS/CW2D to predict biodegradation behavior and nitrification essentially in the VFCW. Initial conditions and nutrient fractionations are determined with specific protocols (some of them determined with the respirometric method). A comparison between simulated data and experimental measurements carried out in the effluent of the VFCW of Evieu is presented. Model limits and possible improvements are discussed for gravel VFCW.

Chapter 2

On the characterization of the hydraulic properties of the filtering material of a Vertical Flow Constructed Wetland*

Abstract

Characterizing the hydraulic properties of the filtering material of a VFCW is a prerequisite to model wastewater treatment using process-based filtration models. The filtering material is a matrix of porous mineral material and organic matter that makes hydraulic characterization a difficult task. Here, we present a combined laboratory and *in situ* approach to assess the hydraulic properties of a French VFCW installed at Evieu. The laboratory approach produces prior estimates of the local properties of the various different VFCW system layers. These prior estimates are subsequently refined with *in situ* measurements then inversely modeled using HYDRUS-1D code. Laboratory experiments consisted in both direct (sandbox, pressure chamber experiments, permeameters) and inverse estimation of hydraulic parameters (evaporation method). *In situ* measurements were based on 5.5-day monitoring of the full-scale filter using 24 TDR probes installed at different depths. Applying the methodology with successive optimizations and a large number of experimental data led to a reliable hydraulic parameter-set able to accurately simulate water content at different depths in the VFCW. We conclude that to consistently represent the hydraulic behavior of the VFCW requires *in situ* hydraulic behavior observations combined with inverse modelling. However, to avoid the ill-posedness problem inherent to inverse modelling schemes, the number of parameters that inverse modelling needs to estimate should be kept to minimum (by fixing saturated water content based on local-scale porosity measurements, for instance). In addition, local-scale laboratory measurements should be used to correctly initialize the inverse problem.

2.1. Introduction

This chapter is dedicated to the hydraulic modelling of the VFCW of the Evieu plant with the HYDRUS software, and particularly to hydraulic parameter determination. As presented before, several studies reported on the assessment of the hydraulic properties of VFCWs, but no study compared the performance of different hydraulic assessment methods for the particular case of VFCWs. In addition, no study has evaluated the different assessment procedures for the specific case of the Cemagref type VFCW, where a sludge layer develops at the filter surface. Hence the first part of this section concerns the hydraulic parameter assessment. We compare the VFCW hydraulic properties estimated by laboratory direct and inverse methods and those obtained by inverse modelling using water content and outflow data collected on a French VFCW. The aim of the work is to determine the most appropriate method in order to estimate the best hydraulic parameters for VFCW. Water content evolution within the VFCW is obtained by TDR probes. Calibration of these probes is also presented. In the end of this part, the hydraulic modelling of the VFCW is presented.

2.2. Materials and methods

2.2.1. The VFCW studied

The Evieu wastewater treatment plant (Ain, France) comprises a sequence of vertical and horizontal sub-surface flow constructed wetlands. The plant has been in operation since 2004. It was originally designed for 200 PE, but as only 100 PE are currently connected, the filter surface has been divided in two to work at full capacity. The first stage is made up of three VFCWs receiving raw wastewater. The pump sump at the plant inlet only performs mechanical screening using a 5 cm mesh screen. Each filter is fed according to an infeed/rest regime of 3.5/7 days. Effluent from this first stage is then connected to a second pump sump and separated between the second stage's vertical and horizontal flow constructed wetlands according to the experimental objectives (Molle *et al.*, 2008). All the constructed wetlands are planted with *Phragmites australis* reeds.

This study focuses on one of the filters of the first stage. The selected vertical filter (28 m², 2.9 m wide x 9.7 m long) is designed according to French recommendations. From the bottom to the top, it contains a 15 cm thick drainage layer (grain size of 30-60 mm), a 10 cm transition layer (grain size 15-25 mm) and a 60 cm gravel layer (d_{10} = 2.46 mm; UC = d_{60}/d_{10} = 1.39; average porosity of 40.4%). As the filter has been

working at nominal load for 7 years, a sludge layer of about 20 cm has developed at the top of the filter. The VFCW is fed by raw wastewater in batches of 5 cm at a rate of 1.23 $m^3.h^{-1}.m^{-2}$ on average. During spells of dry weather, 8 separate batches are processed per day. Water is drained by a 160 mm diameter drainage pipe (0.42 m of pipe per m^2), allowing passive aeration from the bottom as well.

2.2.2. *In-situ* monitoring of the hydraulic behavior of the VFCW

The hydraulic behavior of the VFCW was monitored to estimate its hydraulic parameters using inverse modelling. To monitor water contents in the VFCW, a set of 24 time domain reflectometry (TDR) probes was installed one year before the experiment in order to minimize measurement disturbances. Six installation pits were dug in the VFCW, 4 probes were installed at different depths in each pit (Figure 2.1), and the pits were then filled back up. Based on preliminary observations, sludge and gravel proportion varies according to filter depth, with the result that biomass growth and solid entrapment in the porous gravel become increasingly limited with depth. This makes it possible to differentiate several layers, each presenting different hydraulic behaviors. To perform inverse modelling, we hypothesized that the VFCW is composed of 4 horizontal layers (from top to bottom): sludge deposit (layer 1, h_1 = 20 cm thick), biomass-colonized gravel (layer 2, h_2 = 20 cm thick), less biomass-colonized gravel (layer 3, h_3 = 20 cm thick), and almost-clean gravel (layer 4, h_4 = 20 cm thick). Probes were inserted at four different depths corresponding to this layering system, and connected through multiplexers to a TDR100 signal generator/analyzer (Campbell Scientific™). Results were recorded using a CR1000 datalogger (Campbell Scientific™). Measurements were made at a time interval of 1 minute end-to-end throughout the monitoring campaign, including the 3.5 batch feeding days and the first two days of the rest period.

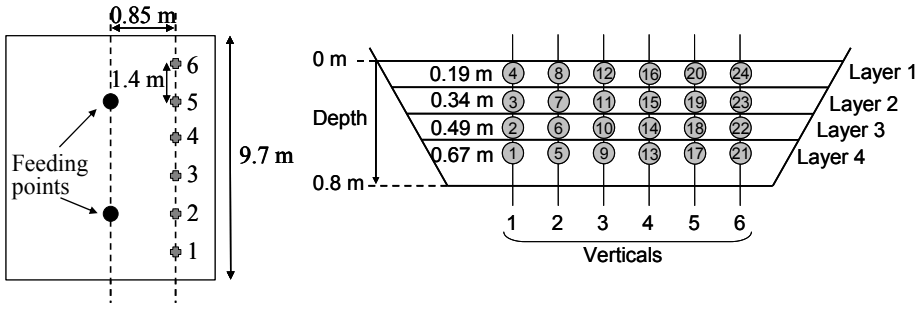


Figure 2.1: Set-up of the *in-situ* experiment: (left) Top view of the VFCW with the six vertical trenches for the TDR probes. (right) Longitudinal section of the VFCW with the 24 TDR probes inserted within the four layers of the VFCW

2.2.3. Hydraulic parameters of the VFCW materials

2.2.3.i. Model and procedure

The hydraulic properties of the VFCW sludge and gravel layers were modelled using the van Genuchten-Mualem closed-form expressions (van Genuchten, 1980; Mualem, 1976):

$$\theta(h) = \theta_r + \frac{\theta_s - \theta_r}{\left[1 + (\alpha h)^n\right]^m} \qquad \text{[Eq. 2.1]}$$

with $h > 0$ and $m = 1 - 1/n$; h (L), the actual pressure head; $\theta(h)$ (L^3/L^3), the actual water content dependent on h; θ_r and θ_s (L^3/L^3), the residual and the saturated volumetric water contents respectively; α (1/L), the fitting scale and n (-), the shape parameter; and

$$K(\theta) = K_S S_e^{\lambda}\left[1 - \left(1 - S_e^{1/m}\right)^m\right]^2 \qquad \text{[Eq. 2.2]}$$

with $S_e(-) = (\theta - \theta_r)/(\theta_s - \theta_r)$, the effective fluid saturation; $K(\theta)$ (L/T), the actual hydraulic conductivity dependent on the actual water content θ; K_s (L/T), the saturated hydraulic conductivity; and λ (-),the Mualem pore connectivity parameter.

The moisture retention equation (Eq. 2.1) contains four independent parameters (θ_r, θ_s, α, and n), while the hydraulic conductivity equation (Eq. 2.2) integrates the saturated hydraulic conductivity (K_s) and the Mualem pore connectivity parameter (λ). According to Ritter *et al.* (2003), λ has little sensitivity to model flow. Consequently, this parameter was fixed at 0.5. In order to limit the total number of

parameters to be assessed during the inversion, and following Ramos *et al.* (2006), we set θ_s for gravel as equal to total porosity. Total porosity is easy to calculate from the dry bulk and particle densities (Flint and Flint, 2002). Setting θ_s as equal to total porosity is challenged by several authors, who suggest that θ_s might be smaller than total porosity due to entrapped air or the presence of flow irregularities (Wessolek *et al.*, 1994; Richard *et al.*, 2001). We hypothesized that this is particularly true for smaller-textured porous media or natural soil. Consequently, we fixed $\theta_{s,gravel}$ to total porosity and only optimized $\theta_{s,sludge}$.
To assess the remaining parameters of Eq. 2.1 and 2.2, different parameter assessments were developed, based on both laboratory and in-situ measurements. The parameter assessment strategy is summarized in Table 2.1.

Table 2.1: Hydraulic parameter assessment strategy

Parameters		θ_r	θ_{s_sludge}	α	n	K_s
Methods						
Direct	Laboratory	Sand box/Pressure chamber. Parameter fitting with the van Genuchten-Mualem equation [Eq. 2.1] (RETC)				Constant Head Soil Core Method
Inverse	Laboratory	Evaporation method used to determine the unsaturated hydraulic conductivity relationship $K(\theta)$ on VFCW core samples (HYDRUS-1D)				
	In-situ	Simultaneous hydraulic parameter determination by numerical inversion from in-situ water content data (HYDRUS-1D)				

2.2.3.ii. Laboratory scale experiments

Samples

Samples were collected at different depths of the VFCW to assess the local-scale hydraulic properties of the different layers presented in section 2.2.2. The use of a sampling technique that minimizes sample compaction is required in order to keep the original sample structure and porosity. Consequently, 7 samples were extracted using PVC cylinders (diameter = 15 cm, height = 11 cm): one sample from layer 1, two samples from layer 2, three samples from layer 4, and one containing clean gravel from another filter that was not yet in use. Samples from layer 3 were not studied because of the damage that occurred during the transport of the sample. The drainage layer was not studied, based on the

assumption that its role in the hydraulic behavior of the filter can be neglected in comparison with the hydraulic role of the upper layers.

Determination of saturated hydraulic conductivity

The saturated hydraulic conductivity (K_s) of the VFCW samples was estimated directly by applying the constant-head soil core method (CHSCM; Klute and Dirksen; 1986; Reynolds and Elrick, 2002). This technique is suitable for measuring the hydraulic conductivity of highly permeable materials like sand and gravel at saturation level (10^0 to 10^{-5} $cm.s^{-1}$). The sample cores were saturated by placing them in a tank filled with water for a 24 h period before measuring K_s. Measurements were repeated three times for each sample (except for the sludge layer that was only measured once due to the slow water flow passing through it). We also measured the volatile matter content for each sample in order to compare K_s values with organic matter content. Subsamples extracted from the core samples using 100 cm^3 stainless steel rings were dried at 105 °C and then 550 °C to assess the dry matter and the volatile matter contents, respectively.

Water retention curves

After determining K_s, undisturbed subsamples were extracted from the core samples using 100 cm^3 stainless steel rings. A sandbox (Stackman *et al.*, 1969) was used to determine water retention at low suctions up to 10 kPa (0.1, 1, 3.2 and 6 kPa). The samples were subsequently moved to a pressure chamber to determine water retention at high suctions up to 1.5 MPa (0.025, 0.1 and 1 MPa).
The van Genuchten-Mualem model (Eq. 2.1) was fitted to the experimental water retention data using the RETC program (van Genuchten *et al.*, 1991). Since θ_s was fixed using the porosity value, only the residual water content θ_r and the shape parameters α and n were fitted for layers 2 and 4.

Evaporation method

The evaporation method is a transient inverse technique for determining unsaturated hydraulic conductivity and water retention curves at laboratory scale (Wind, 1968; Ciollaro and Romano, 1995; Santini *et al.*, 1995; Hopmans *et al.*, 2002). The method inverts the governing flow equation using measured transient evaporation rates from a saturated soil sample.

The evaporation method was applied on the samples directly after the saturated hydraulic conductivity measurements when samples were still saturated. The samples were sealed at the bottom and placed under a free-evaporation boundary condition at the top, i.e. air humidity and temperature were not controlled. Two TDR probes were inserted at two different depths (0.03 m from the top, TDR A, and at 0.03 m from the bottom, TDR B) as illustrated in Figure 2.2. Each TDR probe comprises three rods (100 mm length, 3 mm internal diameter, 15 mm spacing between rods). TDR measurements were performed on a Tektronix^{TM} 1503B oscilloscope. The relationship between dielectric constant and water content was obtained by a soil-specific calibration. Samples were weighed two to three times per day at the beginning of the experiment and only once a day after evaporation rate stabilized. Once daily losses became negligible (less than 10 mg of water evaporated in 24 h), the experiment was stopped. The weight loss due to the loss of organic carbon during the evaporation experiment was neglected compared to the evaporation process.

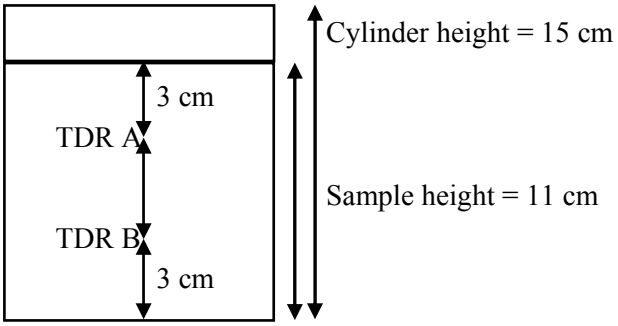


Figure 2.2: Set-up of the evaporation experiment

The hydraulic parameters (θ_r, θ_{s_sludge}, α, n and K_s) of the six samples were determined *via* the inverse modelling tool in HYDRUS 1-D using measured soil water content and evaporation rates. Hydraulic parameter values derived from the earlier constant-head, sandbox and pressure chamber experiments were used as starting values for inverse modelling. Samples were considered as initially saturated. Boundary conditions were expressed in terms of water fluxes: no flux at sample bottom and variable flux at top. The measured cumulated evaporation was interpolated, and the instantaneous fluxes were implemented as top boundary condition. We were able to minimize the objective function in HYDRUS-1D using the Levenberg–Marquardt nonlinear minimization method (Marquardt, 1963).

2.2.3.iii. Inverse modelling using in-situ measurements

We did not use all data from the *in situ* monitoring but instead selected one particular batch with a long drainage period that was recorded at night. On one hand, we reduced the size of the dataset to enable faster optimization. On the other hand, the selected batch presents a sufficiently large water content variation to enable better hydraulic parameter estimation. Hydraulic parameters optimized from the evaporation experiment were used as starting values to inverse-model *in situ* water content data using HYDRUS-1D. In all cases, the flow domain corresponds to an 80 cm-high vertical column composed of four materials: the sludge layer (00-0.20 m), the first gravel-sludge layer (0.20-0.415 m), the second gravel-sludge layer (0.415-0.605 m), and a final practically gravel-only layer (0.605-0.80 m). The transition and drainage layer were assumed to be only negligibly related to flow. The one-dimensional mesh used for simulations consisted of 101 nodes. The top boundary condition is a time-dependent atmospheric boundary condition. Wastewater load duration and flow rate are specified, while evaporation is neglected. If the incoming flow rate exceeds infiltration capacity, the ponding of water above the surface is taken into account. The bottom boundary condition is a seepage face. The five van Genuchten-Mualem parameters (θ_r, θ_{s_sludge}, α, n and K_s) were estimated simultaneously, for each vertical trench. To avoid ill-posedness problems, the parameters were estimated layer-by-layer, from top to bottom.

Furthermore, to evaluate the robustness of the initialization, inverse modelling of the *in situ* data was initialized with hydraulic parameter estimates from direct laboratory experiments and with parameter estimates from generic parameter databases available in HYDRUS.

2.2.3.iv. A global set of parameters

After optimizing the per-layer hydraulic parameters for each vertical trench, we combined the parameters from the different vertical trenches to obtain a single parameter-set for each layer. Both spatial variability and inverse uncertainties are considered in this integration step. Before combining the parameters into a single dataset, any outliers were removed. For each parameter, inversion results give a mean value and a standard deviation. The coefficient of variation (CV) of the standard deviation of each parameter for each layer was used to discriminate outliers. This CV was calculated for each layer according to:

$$CV_i = \frac{\frac{1}{N}\sum_{j=1}^{N}\left(\sigma_{ij}^2 - \left(\frac{1}{N}\sum_{j=1}^{N}\sigma_{ij}^2\right)\right)^2}{\frac{1}{N}\sum_{j=1}^{N}\sigma_{ij}^2} \qquad \text{[Eq. 2.3]}$$

with i, the studied parameter; $j = 1{:}N$, the position index, with N the number of vertical trenches (i.e. N = 6); and σ_{ij}^2 , the standard deviation of the parameter value i, for a given layer and position j, provided by the *in-situ* data inversion. A CV greater than 1 means that one or more standard deviation values are more than twice as high as the average of the standard deviations. Therefore, these values are not taken into account in the parameter-set assimilated. Negative parameter values were also removed.

Assuming that parameter values are normally distributed, we combined the parameter-set of the different vertical trenches for a given layer into one parameter-set whose mean and standard deviation given are by Eq. 2.4.

$$\mu_{GD} = \frac{1}{N}\sum_{i=1}^{N} X_i \;\; ; \;\; \sigma_{GD}^2 = \frac{1}{N}\sum_{i=1}^{N}\sigma_i^2 \qquad \text{[Eq. 2.4]}$$

with $i = 1{:}N$, the number of vertical trenches; μ_{GD}, the mean of the global distribution; X, the mean of the local distribution; σ_{GD}^2 the standard deviation of the global distribution; and σ_i, the standard deviation of the local distribution.

For each layer and each vertical trench, from the mean and the standard deviation of the global distribution of each parameter, we randomly sampled a parameter value. But, HYDRUS 2D failed to simulate water flow within the VFCW. It was mainly because of the sludge layer hydraulic properties. Consequently, all hydraulic simulations were performed with HYDRUS 1D.

2.2.4. Model validation

Following the inverse-modeled parameter identification using a single batch, hydrodynamic modelling and model parameters were validated by applying the HYDRUS 1D software directly onto the remaining fraction of the monitoring dataset. Flow domain and boundary conditions were identical to those used for *in situ* data inversion. Initial conditions can be

specified either in terms of water content or pressure head, although pressure head is the more advisable variable since it is the driving force for water flow (Radcliffe and Simunek, 2010). Here, the only data available was water content (TDR probes), and only at some VFCW depths. We used the following procedure to obtain a realistic and continuous initial pressure head profile: (i) we started from a hydrostatic pressure distribution and simulated several feeding batches separated by the average drainage time interval in order to achieve a pseudo-permanent state; (ii) once the pseudo-permanent state was reached, we selected the time for which water content profile matches the experimentally-observed initial water content. The corresponding water pressure profile was then considered as initial condition for simulating the VFCW during the monitoring period.

2.3. Results and discussion

2.3.1. Parameter optimization

2.3.1.i. Laboratory experiments

Based on porosity estimates, the θ_s values were fixed to 40.6 % for layers 2 and 3, and 44.0 % for layer 4.

Saturated hydraulic conductivity determination

Table 2.2 gives the K_s values and the volatile matter contents for the different layers considered within the VFCW.

Table 2.2: Saturated conductivity and volatile matter content for different layers of the studied VFCW

Layer	K_s (cm/s)	VM (%DM)
1	4.22E-04 (1 value)	26.9 (SD = 20.1; 12 values)
2	1.49E-01 (SD = 4.26E-03; 3 values)	2.4 (SD = 1.21; 12 values)
2	1.45E-01 (SD = 8.32E-03; 3 values)	
4	1.07E-01 (SD = 1.58E-02; 3 values)	1.8 (SD = 0.24; 12 values)
4	1.41E-01 (SD = 1.46E-02; 3 values)	
4	1.57E-01 (SD = 1.05E-03; 3 values)	
Clean gravel	> 2.65E-01*	1.4 (SD = 0.48; 12 values)

SD = standard deviation

* Maximum measurable value

As expected, K_s value was proportional to porosity. However, for layer 1, there are issues over the reliability of the K_s value and the method used. First, the sludge layer is characterized by significant shrinking-swelling behavior. The constant head soil core method is inappropriate for determining the K_s of porous media of variable geometry (Reynolds and Elrick, 2002). Second, the K_s value for layer 1 is close to the lower boundary of the method's range of validity (10^{-5} cm/s). We also note that the K_s values for layers 2 and 4 are very close, which is somewhat surprising given that layer 2 contains more organic matter than layer 4, 2.4 % and 1.8 %, respectively.

Water retention curves

The water retention curves as determined both on the sandbox and in the pressure chamber apparatus are given in Figure 2.3. At equal applied pressure, sample water content increases with increasing proportion of organic matter. The shape of the water retention curve is consistent with Giraldi and Iannelli (2009). For coarse material, when water content is nearly saturated, the shape of the water retention curve varies sharply. These materials generally offer very low water retention. However, the reliability of measurements close to saturation is debatable, particularly for the coarse gravel material, as there may be significant water loss when handling the samples in the sandbox and pressure chamber experiments.

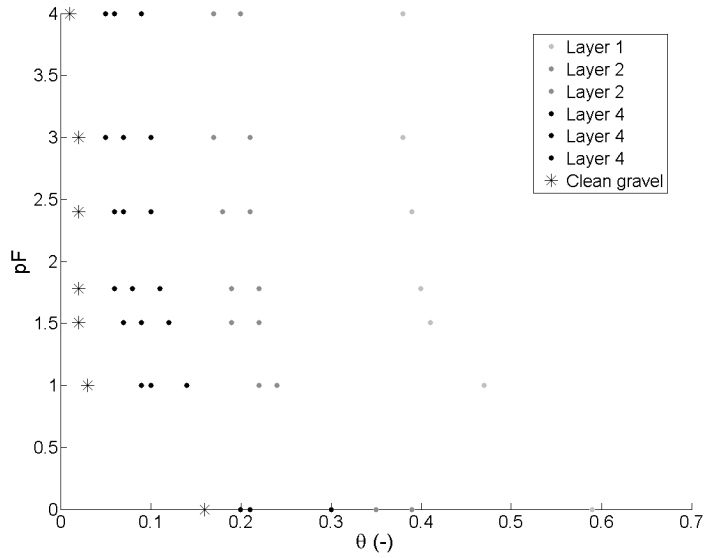


Figure 2.3: Water retention curves determined during the sand box and pressure chamber experiments

Based on these data, and with saturated water content fixed to porosity (except for layer 1), hydraulic parameters were fitted for every sample. Results are presented in Table 2.3. Cross-comparison of hydraulic parameters between each layer 2 sample revealed significant differences for θ_r and α values ($p < 1.10^{-6}$). The Student's *t*-test applied on the water retention curves indicates that the hydraulic properties are significantly different between layers.
Table 2.3 highlights that the parameter values obtained are consistent with a simple physically-based porous flow modelling concept. Indeed, α will be smaller and θ_r will be higher as organic matter content increases, reflecting the impact of organic matter on the structure of the porous medium. n parameter values were similar for all gravel-containing samples. Relatively high sludge proportions had no significant impact on this parameter.

Evaporation method

Table 2.4 presents the hydraulic parameter values obtained from the evaporation experiment. For layer 2, all optimized parameter values are similar ($p > 0.17$). Parameters values were also similar for two out of three of the layer-4 samples ($p > 0.005$). In addition, comparing θ_r, α and n between layers did not emerge any clear trend.

The parameter values from the evaporation experiment (Table 2.4) were generally lower than those estimated by the direct method (Table 2.3). However, the degree of reliability on parameters assessed by the evaporation method should be considered low, as illustrated by the wide confidence intervals obtained from the inverse optimization method. Several problems may explain this low reliability. First, the evaporation method is in general not very reliable for estimating hydraulic properties at near-saturation, and its reliability is even lower when sample cores are initially saturated, as was the case in this study. Indeed, for soils with a high structural porosity, Richard *et al.* (2001) found that the retention properties were overestimated and hydraulic conductivity underestimated when the evaporation experiment started from fully-saturated samples. Solte *et al*. (1994) suggested conducting the evaporation method without the preliminary saturation step.

Table 2.3: Parameter values and confidence intervals (95 %) of the hydraulic properties of the VFCW as obtained from standard laboratory experiments (Eq. 2.1, RETC software)

Layer	1			2			2			4			4			4		
Parameter	Value	95% CI		Value	95% CI		Value	95% CI		Value	95% CI		Value	95% CI		Value	95% CI	
θ_r	0.37	0.35	0.40	0.21	0.20	0.22	0.17	0.16	0.18	0.06	0.05	0.07	0.05	0.04	0.06	0.09	0.09	0.10
θ_s	0.67	0.64	0.70	**0.406**			**0.406**			**0.44**			**0.44**			**0.44**		
α (1/cm)	1.20	0.40	2.14	0.46	0.26	0.66	0.98	0.77	1.20	5.19	2.58	7.80	4.81	3.27	6.36	1.78	1.44	2.13
n	1.51	1.28	1.70	2.13	1.70	2.56	1.68	1.54	1.81	1.56	1.40	1.72	1.59	1.48	1.70	1.689	1.56	1.80

Table 2.4: Parameter values and confidence intervals (95 %) of the hydraulic properties of the VFCW as obtained from evaporation measurements (Eq. 2.1 and 2.2, HYDRUS software)

Layer	1			2			2			4			4			4		
Parameter	Value	95% CI		Value	95% CI		Value	95% CI		Value	95% CI		Value	95% CI		Value	95% CI	
θ_r	0.05	-0.99	1.10	0.02	-0.79	0.83	0.05	-0.41	0.50	0.11	-0.75	0.97	0.03	0.02	0.04	1.0 E-04	-3.0 E-04	5.0 E-04
θ_s	0.84	0.79	0.89	**0.406**			**0.406**			**0.44**			**0.44**			**0.44**		
α (1/cm)	0.51	-0.36	1.37	3.39	1.15	5.63	0.23	-1.29	1.74	4.82	-1.33	10.96	0.17	0.08	0.26	3.29	2.33	4.26
n	1.05	1.00	1.10	1.16	0.71	1.61	1.06	1.00	1.124	1.11	0.78	1.43	2.54	1.80	3.28	1.07	1.06	1.08
K_s **(cm/s)**	6.6 E-03	3.1 E-03	1.0 E-02	0.15	0.14	0.16	0.07	0.05	0.08	0.10	0.10	0.10	0.06	0.04	0.07	0.09	0.09	0.09

Secondly, non-optimal experimental conditions likely biased the evaporation measurements. The contact between TDR probes and porous material may become problematic due to air entry during the measurements. This is particularly problematic for the sludge sample, which shrinks strongly during drying (Vincent *et al.*, 2011). Finally, the evaporation measurements were led in a laboratory that did not have controlled temperature and humidity, which may ultimately have led to transient evaporation demands and more uncertain upper boundary conditions in the inversion model.

2.3.1.ii. In-situ measurements

Figure 2.4 presents the water contents measured at various depths in the VFCW (13, 31, 47 and 62 cm below the VFCW top surface) together with the experimental uncertainties estimated by media-specific calibration. The high organic matter content resulted in fairly significant signal loss in the sludge layer for some water content measurements. Water contents from just a one-night batch are used in HYDRUS-1D to estimate the hydraulic properties.

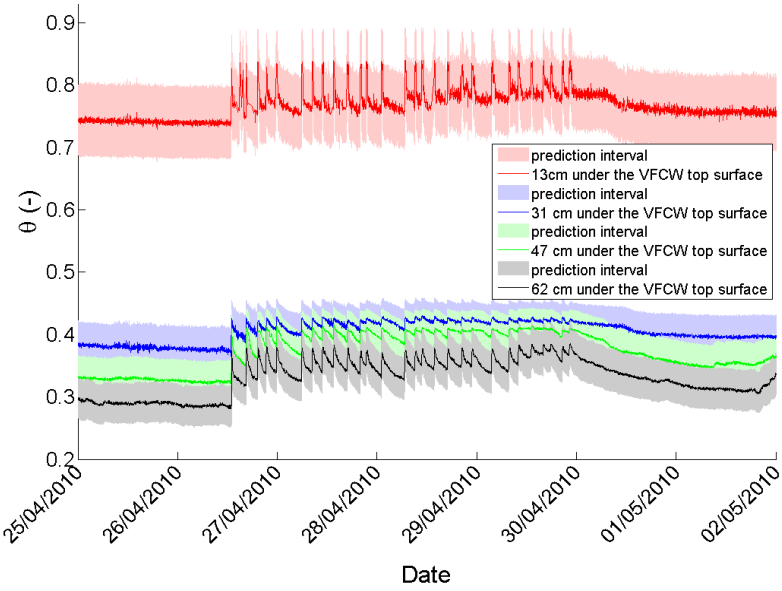


Figure 2.4: Water contents and their uncertainties from TDR probe calibration at various VFCW depths (vertical trench 2) before and during the monitoring campaign

Water content variations monitored by TDR probes allow identifying all the batches (Figure 2.4). Each batch is easily identifiable by the increase of the water content. In addition, the water retention and hence the water content decreases with depth, as organic matter content is lower deeper in the filter.

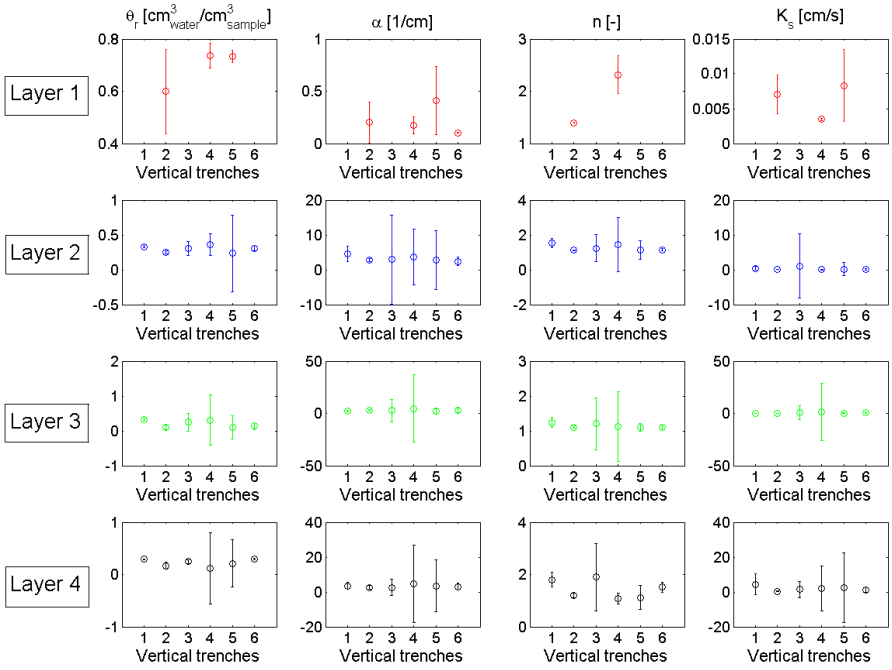


Figure 2.5: Hydraulic parameter estimates and confidence intervals (95 %) from the *in-situ* data inversion for the four layers and all vertical trenches (Eq. 2.1 and 2.2, HYDRUS software)

Results from the *in-situ* data inversion are presented in Figure 2.5. For layer 1, parameters from *in situ* data inversion are dispersed and the confidence intervals for K_s and n values do not overlap for the different horizontal positions in the VFCW. Once the inversion results have been filtered via the coefficient of variation method, mean θ_r values are similar for layers 2, 3 and 4 for all verticals ($p > 0.002$). K_s, α and n parameter values also presented this same similarity between vertical values within a same given layer ($p > 0.0017$), thus demonstrating the reliability of the inversion from field data.

The inverse modelling from *in situ* data could be even more robust if more information (such as measured VFCW outflow) were included in the objective function. However, outflow, as simulated by HYDRUS in the 1D modelling set-up, is evaluated at the interface between the bottom of the

gravel layer and the transition layer, while outflow measurements are only available at the VFCW outlet. Effluent has to drain through a gravel layer and then a 20 m-long drainpipe before reaching the VFCW outlet. Given that flow behavior in the gravel layer and drain pipe was not characterized, we could not include the measured outflow in the objective function.

2.3.1.iii. Parameter integration

The CV effectively discriminated outliers from among parameter values derived from inverted field data. After removing the outliers, the set of parameters validated for each vertical trench was then combined to obtain the overall global VFCW-scale parameter set. Table 2.5 gives the means and the standard deviations of the global hydraulic parameters. Results mostly differ from values obtained by laboratory methods, which is consistent with Mertens *et al.* (2005).

Table 2.5: Parameter values and confidence intervals (95 %) of the hydraulic properties of the VFCW as obtained from the combination of the results of direct laboratory, inverse laboratory and *in-situ* inverse procedures.

Layer		θ_r [$cm^3_{water}/cm^3_{media}$]	θ_s [$cm^3_{water}/cm^3_{media}$]	α [1/cm]	n [-]	K_s [cm/s]	λ [-]
1	Mean	0.64	0.84	0.15	1.80	6.8 E-03	0.5
	SD	0.09	0.17	0.20	0.18	1.2 E-03	
2	Mean	0.32	0.406	3.25	1.28	0.11	
	SD	0.10		1.31	0.50	0.12	
3	Mean	0.22	0.406	2.48	1.18	0.11	0.5
	SD	0.14		1.72	0.10	0.20	
4	Mean	0.26	0.44	2.95	1.31	2.32	
	SD	0.04		1.52	0.31	3.22	

SD = standard deviation

Comparing lab-defined (Tables 2.3 and 2.4) *vs in-situ* measured reference parameters (Table 2.5) showed that laboratory methods gave good estimations of reference K_s value but underestimated the θ_r and α values, and n values were too dispersed to draw any firm conclusions. These patterns contrast with the conclusions of Kumar *et al.* (2010), who showed that field-scale θ_r, θ_s and n parameters could be estimated from laboratory experiments but that inverse modelling with *in situ* data was needed for α and K_s. These

differences with the conclusions of Kumar *et al.* (2010) can mainly be explained by the fact that their study was carried out on soil samples and partly explained by the inappropriate operation conditions of the evaporation method.

2.3.2. Comparison of the different methods

Figures 2.6 and 2.7 present the observed and simulated water contents in the VFCW for vertical trench 2. Simulations were performed with parameters obtained from (i) the direct laboratory method (Figure 2.7, left), (ii) the inverse laboratory method (Figure 2.7, right), and (iii) the inversion of *in-situ* water content data (Figure 2.6). Estimated parameters from this latter method were considered as reference parameters. Figure 2.7 illustrates that parameter-sets obtained by the two laboratory methods are unable to properly simulate the water contents observed in the VFCW.

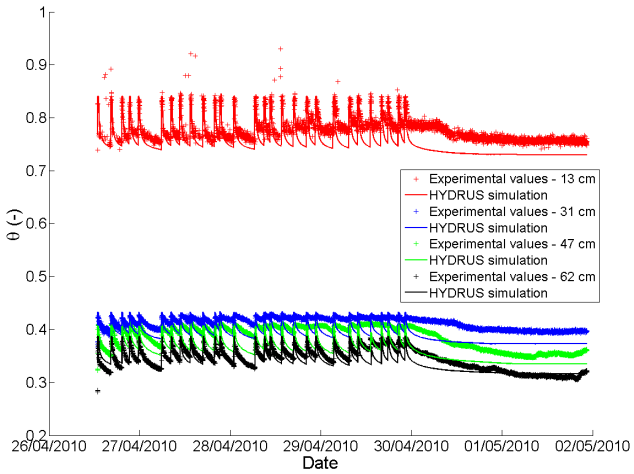


Figure 2.6: Measured and simulated water content evolution in the VFCW at different depths during the monitoring campaign (Simulation performed with hydraulic parameters from *in-situ* water content data inversion)

One advantage of this multi-tier approach consists in improving the identifiability of the badly-posed inversion problem. Indeed, when only parameter estimates from direct laboratory experiments for initialization were used, we were able to obtain a parameter-set by inverse modeling over one batch, but direct model failed to simulate the entire monitoring campaign. When only using generic parameter databases available in HYDRUS, we failed to obtain a parameter-set by inverse modeling.

We found that K_s parameter values were similar for layer 2 for the different approaches that were used (Figure 2.8). As expected, K_s scales to sludge content and consequently increases with depth. This close agreement between the different determination techniques is remarkable, given that K_s can normally vary significantly at short distances. These results contrast with many soil science studies showing that K_s at core scale in the laboratory is not effective for modelling *in situ* transport (e.g. Mallants *et al.*, 1996).

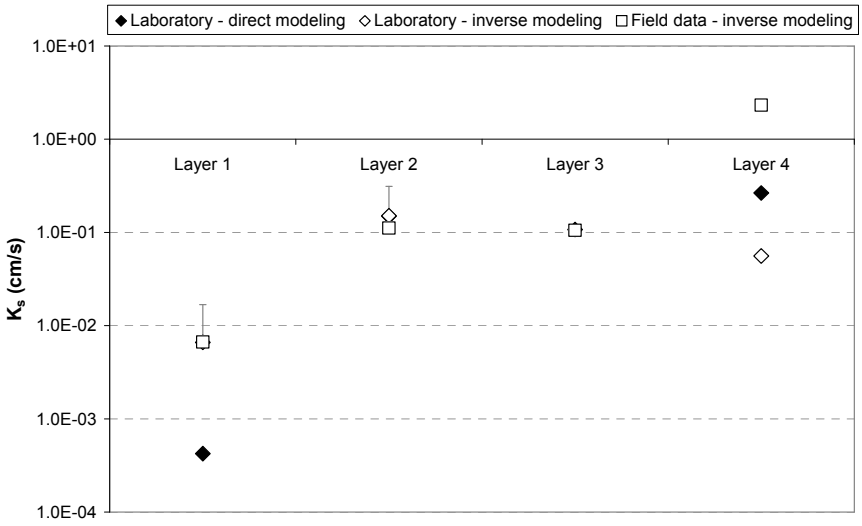


Figure 2.8: K_s values for the four layers through the various optimizations

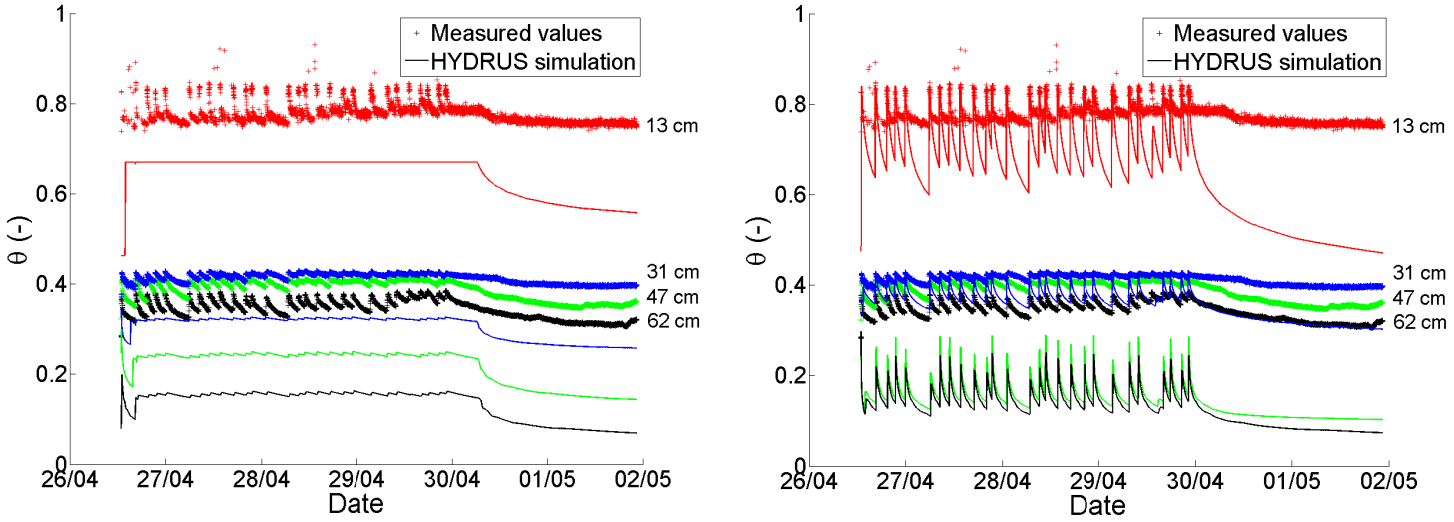


Figure 2.7: Measured and simulated water contents with hydraulic parameters (left) from direct laboratory methods and (right) from inverse laboratory method

θ_r appeared to be difficult to determine with the inverse method (high confidence intervals, Table 2.4), particularly when organic matter content was high, as was the case for layers 1 and 2. For these specific layers, a non-equilibrium flow approach would probably be more appropriate, since not all the porosity would participate in water flow.

The α value was lower for layer 1 than for layers 2 and 3, as expected (Table 2.5). However, the change in values for layers 2 and 4 when switching from the direct to the inverse laboratory method ran counter to our expectations. Again, experimental bias in the evaporation method may explain this pattern. For layers 2 and 4, α was always underestimated by laboratory methods. This could be explained by non-equilibrium flow and hysteresis. Indeed, non-equilibrium preferential flow may have occurred in the VFCW. In such cases, it is expected that $\alpha_{\text{non-equilibrium flow}} > \alpha_{\text{equilibrium flow}}$ due to a significant effect of macropores on unsaturated flow (Feyen *et al.*, 1998). However, it is still difficult to obtain reliable estimates of non-equilibrium flow parameters using inverse modelling data (Simunek *et al.*, 2003; Laloy *et al.*, 2010), and $\alpha_{\text{non-equilibrium flow}}$ is consequently subject to a large degree of uncertainty. Hysteresis may also be involved in the observed differences, since laboratory methods represent drying processes while field measurements represent drying and wetting processes.

Ritter *et al.* (2003) showed that laboratory methods are useful to properly initialize inverse methods for estimating hydraulic parameters. Parameters from laboratory experiments are useful to reduce the parameter dimension in inverse models and to gain a faster convergence of the model. Confidence intervals generally decrease over the course successive hydraulic parameter estimation and optimization processes. Therefore, a stepwise optimization process maximizes information exploitation from the various experiments while and keeping the objective function as close as possible to its global minimum. We experienced convergence difficulties with the inverse modelling of *in-situ* data carried out directly with hydraulic parameter estimations from the direct laboratory experiments.

Both the modelling process and the model parameters were validated on the remainder of the monitoring dataset. As shown in Figure 2.6, the simulation of water contents is good for most of the layers in the first four batches, where predicted water contents stayed close to observed water contents. For later batches, we observed a degree of discrepancy that can be explained by the fact that HYDRUS does not consider water accumulation due to biomass growth, presence of organic matter, and the build-up of total suspended solids in the filter.

During the rest period, model predictions were unable to accurately reproduce the observed decrease in water content. The lowest absolute

difference between observed and simulated water contents was found for layer 4. Nevertheless, for a mature system like the Evieu VFCW plant, we consider that water content can be adequately simulated over a three-days feeding period. This would probably not be the case for a longer simulation or for a less mature system where biomass growth and suspended solid deposits during a given feeding period is expected to have a greater impact on hydraulic parameters. Unfortunately, our experimental set-up did not enable us to validate the model in these conditions.

2.4. Conclusion

VFCW systems are becoming popular engineered systems for wastewater management in rural areas, yet the hydraulic functioning of VFCW systems is still not well known. There are very few studies available that can be used to compare the performance of different parameter identification methods for these artificial systems. In particular, no study has yet been performed to determine the hydraulic properties of the Cemagref-type VFCW, which comprises a different functional layers (sludge, mix between sludge and gravel).

Here, we applied a multi-tier approach to obtain a reliable hydraulic parameter-set for the various layers composing a VFCW. Data from classical laboratory hydraulic determination methods were used to initialize inverse modelling methods. These inverse modelling methods were applied on laboratory and *in situ* data, and initialization was needed to constrain the search space of the inversion at close-to-optimum and thus converge to the optimum faster. As the Cemagref-type VFCW entails strong vertical heterogeneity of hydraulic properties, several layers (four layers in this case) were useful to describe the hydraulic behavior of the filter. However, we did not attempt to optimize the number of layer in the simulation model.
The applied methodology with successive optimizations led to a reliable hydraulic parameter-set that is able to predict water contents at different in-VFCW depths. In contrast, hydraulic properties inferred from either direct laboratory experiments or from *in situ* inversions in which initialization is based on generic literature data, failed to predict the water contents accurately. This latter conclusion suggests that the objective function in the inverse model may be characterized by a set of local minima. The fact that the HYDRUS software only features a local search algorithm makes initialization of the hydraulic function a critical issue when inverting HYDRUS on observed VFCW water data.

Chapter 3

Imaging of Vertical Flow Constructed Wetland using Electrical Resistivity Tomography and Time Domain Reflectometry*

Abstract

Vertical flow constructed wetlands treatment performances may be improved at the cost of a better understanding of the complex geo-chemical phenomena occurring within the filter. An essential issue is the description of water flow within the filter. In this chapter, we present an original approach combining time domain reflectometry (TDR) and time-lapse electrical resistivity tomography (ERT) to study water flow through the first-stage VFCW.

Twenty four TDR waveguides were installed in the filter and allowed monitoring water content changes at different positions within the VFCW. Specific calibration relationships were established for the different constitutive layers of the system. The water dynamics and the progressive clogging of the filter during the loading period could successfully be monitored in the gravel layer. However, despite additional coating of the probes, TDR did not perform very well in the sludge layer, leading to large uncertainties in measured water contents.

The ratio between the inverted ERT resistivity before the beginning of the feeding period and the actual inverted ERT resistivity, i.e. the time lapse ERT resistivity ratio, confirms the overall good repartition of the effluent over the entire system. This can be induced by the 20-cm thick sludge layer that was developed over the 10 years of operation of the system. The time lapse ERT resistivity ratio exhibits large variations which are not observed with the TDR measurements. Direct imaging of the water content, which consists in the application of a material specific petrophysical relationship to ERT time-lapse inverted resistivity images, did not perform well. Thus we suggest to use integration methods instead of direct mapping for combining data because the latter is less sensitive to poorly defined petrophysical relations.

In this chapter, my work dealt with the calibration, installation and monitoring of the TDR probes, as well as the interpretation of field measurements. ERT measurements and inversions were carried out by other co-authors. Experiments presented here are part of a second experimental field campaign, the only campaign for which simultaneously resistivity measurements and TDR measurements were made.

3.1. Introduction

The ability to monitor the volumetric water content with a high space and time resolution with advanced hydrogeophysical techniques can be considered as a new milestone for the better understanding of the functioning of VFCW systems. The use of capacitance probes located in tubes at different depths of a VFCW system was explored both at the laboratory scale (Langergraber, 2003; Forquet *et al.*, 2009a) and at field scale (Giraldi and Iannelli, 2009). In these studies, little attention was devoted to the layer specific calibration of the capacitance probes. Morris *et al.* (2011) presented a small embedded magnetic resonance sensor that allows measuring both hydraulic conductivity and clogging level in horizontal flow constructed wetlands. All these studies implement techniques that have small measurement volumes. Hence, for obtaining representative plant scale observations of hydraulic behaviour of VFCW systems, sensors need to be multiplied at different locations. The usage of geophysical imaging tool permits to overcome this issue. Lillo *et al.* (2011) used electrical resistivity tomography (ERT) to investigate preferential flow in a vertical flow sand filter, but only discussed the raw electrical resistivity tomogram, without quantifying the water content dynamics in the filter.

The purpose of the present study is to combine a reference local scale water content monitoring technique with a proximal hydrogeophysical technique to monitor water content dynamics at the scale of the first stage of a VFCW system. To this end, we combined Time Domain Reflectometry (TDR) and Electrical Resistivity Tomography (ERT).

TDR is a popular technique in the field of near-surface hydrology, which has been proven to be efficient and reliable. It relies on the measurement of soil dielectric permittivity, which is known to be influenced by the volumetric water content of the porous material. Numerous works have been published, especially to answer calibration issues and to estimate sampling volume associated with material inserted TDR probes. An inappropriate calibration is detrimental for accuracy, especially at low water content. Robinson *et al.* (2003a) suggested a classification of the calibration models, distinguishing two main categories: empirical and mixing models. The most popular empirical model has been developed by Topp *et al.* (1980). He suggested to use a second-order polynomial relationship between the permittivity and volumetric water content. Separate equations are used for mineral and organic soils. The latter have different dielectric properties because of higher porosity and bounded water content. However to reduce uncertainty, additional factors of influence must be taken into account, such as the apparent soil density (Malicki *et al.*, 1996). Jacobsen (1993) studied and

ranked the different available methods but concluded that despite including more parameters, general calibration laws will remain less accurate than soil specific calibration. Mixing models are physically based models and therefore more generalizable (Roth *et al.*, 1990; Dirksen and Dasberg, 1993). They may be particularly interesting for adapting calibration formula when the usage of a coating around waveguides is made, e.g. when the dielectric losses are high such as in saline soils (Fujiyasu *et al.*, 2004). Ferré *et al.* (1998), Knight (1992) and Knight *et al.* (1997) numerically estimated the measurement volumes of various waveguide configurations. The latter is generally confined in the space between electrodes. Therefore it is important to install probes a long time before measurements are carried out (Robinson *et al.*, 2003b). The probe length is also of importance: the longer they are, the less they will be sensitive to small cavities that might be created during probe insertion (Gregory, 1995).

Geophysical methods, like ERT, have three main advantages over usual near-surface hydrology tools (Linde *et al.*, 2006): (i) they provide spatially distributed estimates of physical properties; (ii) they are relatively less invasive; (iii) and comparatively cheap. However they present a main disadvantage: the relationship between the measured physical property (i.e., electrical resistivity) and the hydraulic property of interest (i.e., water content) is often weak. In order to overcome this issue, different methods of combining geophysical data and locally measured hydraulic data have been developed. Linde *et al.* (2006) distinguish three categories: (i) direct mapping, which consists in the transformation of geophysical model using petrophysical relationship; (ii) integration methods, which rely on the interpolation of hydraulic properties using the information provided by the geophysical model; (iii) joint inversion, where hydrological data are used in the inversion process of geophysical data and vice-versa. In this chapter, we decided to focus first on the applicability of direct mapping. An example of direct mapping using time-lapse ERT is given by French and Binley (2004). The pretrophysical relationship used in this study is the so-called Archie's law (Archie, 1942). However, calibration data were missing and the default cementation index was used. Petrophysical relationship between electrical resistivity and water content has been an intensive field of research (Lesmes and Friedman, 2005) and, like for TDR, both empirical and conceptual model have been developed (Laloy *et al.*, 2011). The former are often preferred for direct mapping application and are either developed based on laboratory calibration measurements (Yeh *et al.*, 2002) or based on field scale calibration experiments (Michot *et al.*, 2003).

In section 2 of this chapter, we present the experimental site and the protocol used to simultaneously perform TDR and ERT measurements on the VFCW system. Section 3 includes first TDR calibration results. TDR and ERT results are then presented side by side successively for the feeding and the rest period of the functional VFCW. Finally results of direct mapping are given and discussed.

3.2. Materials and Methods

3.2.1. Evieu vertical flow constructed wetland

The Evieu wastewater treatment plant (Ain, France) comprises a sequence of vertical and horizontal subsurface flow constructed wetlands. The plant is in operation since 2004. It was originally designed for 200 PE, but currently only 100 p.e. are connected. As a consequence, the filter area has been divided in two to work at full capacity. The first stage is made up of three VFCWs receiving raw wastewater. Only a mechanical screening using a 5 cm mesh screen is made in the pump sump at the plant inlet. Each filter is fed according to a feeding/rest regime of 3.5/7 days. The effluent from this first stage is then connected to a second pump sump and separated between vertical and horizontal flow constructed wetlands of the second stage according to the experimental objectives (Molle *et al.*, 2008). All the constructed wetlands are planted with *Phragmites australis*. This study focuses on one of the filters of the first stage. The selected vertical filter (28 m², 2.9 m wide and 9.7 m long) is designed according to French recommendations. From the bottom to the top, it contains a 15 cm thick drainage layer (grain size of 30-60 mm), a 10 cm transition layer (grain size 15-25 mm) and a 60 cm gravel layer (d_{10} = 2.46 mm; d_{60}/d_{10} = 1.39; average porosity of 40.4 %). As the filter is working at nominal load since 7 years, a sludge layer of about 20 cm has been developed at the top of the filter. The VFCW is fed by a raw wastewater by batches of 5 cm, at a rate of 1.23 $m^3.h^{-1}.m^{-2}$. Eight distinguished batches per day occur during dry weather. Water is drained by a drainage pipe of 160 mm diameter (0.42 m of pipe per m²) which allows a passive aeration from the bottom as well.

3.2.2. TDR calibration procedure

We performed a site specific calibration of the relationship between water content and material dielectric constant. The dielectric constant is obtained from the travel time in the studied media, along the waveguide:

$$\Delta t = \frac{2L\sqrt{K_a}}{c} \qquad \text{[Eq. 3.1]}$$

with Δt (s), the travel time; L (m), the waveguide length; K_a (-), the dielectric constant; c ($m.s^{-1}$), the speed of light.

Eq. 3.1 can be simplified in order to express the dielectric constant as the ratio of the apparent probe length on the actual probe length:

$$\sqrt{K_a} = \frac{L_a}{L} \qquad \text{[Eq. 3.2]}$$

with $L_a = c \cdot \Delta t / 2$, L_a (m), the apparent probe length. The apparent probe length experimentally measured differs from L_a because it also includes an offset value (L_{a0}) related to the length and the material of probe head. We then first measured the offset value for each probe according to the protocol described by Heimovaara (1993) and withdrew it from the measurements.

TDR measurements were carried out on three disturbed samples extracted from the VFCW (layer 1, layer 2, and layer 4) using a TDR100 signal generator/analyzer (Campbell Scientific^{TM}). Samples from layer 3 were not studied because of the damage that occurred during the transport of the sample. Samples were then packed into PVC cylinders (diameter = 0.4 m, height = 0.15 m) whose volumes were reduced by two PVC plates to obtain a 5 L useful volume. At least 10 different water contents were tested for each material, from saturation to dryness for sample of layer 1 and conversely for samples of layers 2 and 4, in order to cover a large moisture scale. Triplicate tests were performed for each water contents. After each measurement three sub-samples were extracted from samples using stainless steel rings of 100 cm^3 and dried in an oven (50 °C) to assess their water contents. Finally, a third power polynomial function was used to assess the relationship between water contents and dielectric constant measured by the TDR probe.

3.2.3. The experimental setup

To monitor the water content within the VFCW, a set of 24 TDR probes were installed one year before the experiment took place in order to limit installation disturbances on the measurements. Six installation pits were dug in the VFCW, and 4 probes were installed at different depths (0.14 m; 0.28 m; 0.42 m and 0.56 m) in each pit (Figure 3.1). Pits were filled up after probe insertion. The TDR profile was located at 0.85 m from the distribution pipes. All probes were connected through multiplexers to a TDR100 signal generator/analyser (Campbell Scientific^{TM}) and results were recorded using a CR1000 datalogger (Campbell Scientific^{TM}). Measurements were made at a time interval of 1 minute all along the monitoring campaign, including the 3.5 batch feeding days and the 7 days of the rest period. Three PT100 platinum resistance thermometers were also inserted inside the sludge layer at 0.15 m in depth, assuming that the temperature is homogeneous throughout the filter thanks to the short height of material and the contact with the atmosphere through the drain at the bottom. A rain gauge monitored rainfall events and was connected together with the thermometers to a Gantner datalogger (Gantner Instruments Test & Measurement GmbH, Austria) collecting data every minute (Figure 3.2).

The experimental setup included a row of 48 electrodes lined up on the filter surface between the TDR profile (0.5 m) and the distribution pipes. A regular spacing of 0.2 m was used. The row length was 9.4 m. Electrodes were connected to Syscal Pro resistivity meter (Iris Instruments, Orléans, France).

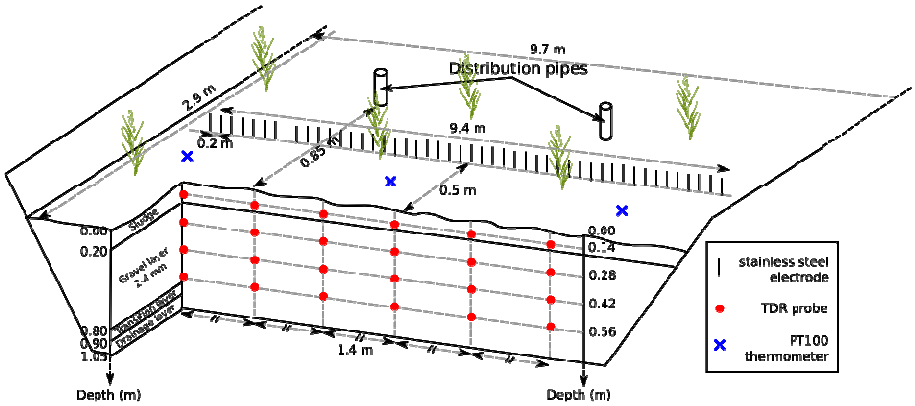


Figure 3.1: Experimental setup for water flow monitoring of a VFCW

Among the different existing arrays for electrode interrogation, the two most popular are Wenner and dipole-dipole arrays. Wenner array is sensitive to vertical changes in resistivity and give the smallest number of possible measurements. Dipole-dipole array is sensitive to horizontal changes in resistivity and is particularly appropriate for multi-channel measurements (Loke, 2009). The combination of the two techniques does not overestimate horizontal nor vertical changes but is, however, very time-consuming. Therefore, a Wenner-Schlumberger array was chosen as a good compromise between the two. A preprogrammed 366-measurements sequence was implemented in the resistivity meter which also provides electrode commutation thanks to an on-board multiplexer. 16 time-lapse measurements were carried out during both the feeding and the rest period. During the feeding period, we waited that most of the water drains out after a load (usually 1 hour and a half) before starting resistivity measurements since quick water flow may disturb it.
Inlet wastewater conductivity was monitored all along the experiments. Values varied from 1490 to 1810 µS cm^{-1} (values compensated in temperature).

3.2.4. ERT and TDR data processing

Outliers were removed from TDR data using Eq. 3.3.

$$\left(X - \mu_X\right) \geq 2.75\sigma_X \qquad \text{[Eq. 3.3]}$$

where X is the TDR dataset, μ_X and σ_X its average and standard deviation, respectively.

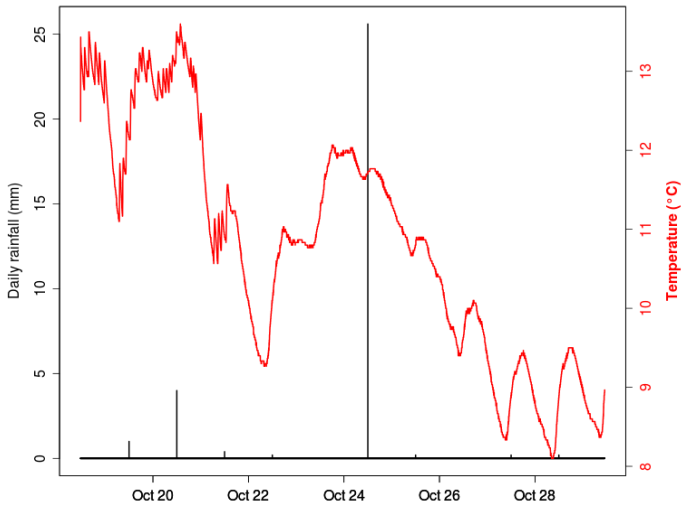


Figure 3.2: Daily rainfall and average temperature in the sludge during the experiment

Erroneous measurements were first removed from ERT dataset if the coefficient of variation of measurement repetitions exceeded 5 %. Then measurements were corrected and related to a reference temperature of 25 °C (Hayley *et al.*, 2007):

$$\rho_{25°C} = \rho_T \left[1 + 0.0183(T - 25)\right] \qquad \text{[Eq.3.4]}$$

where $\rho_{25°C}$ and ρ_T are electrical resistivity at 25°C and at the temperature T (in Celsius degree), respectively.

The inversion was performed using a finite element based algorithm (R2, v2.6), which accounts for three-dimensional current flow in a two-dimensional resistivity field. The inversion domain was restricted to the filter cross-section since the latter is isolated from the surrounding soil by a geomembrane. An unstructured triangular mesh made of 1540 elements was used. The average element length is half the electrode spacing. The first dataset was processed alone using a linear filter for regularization. Then other datasets were inverted using a difference regularization technique based on the results of the first inversion as starting model. This technique permits to better constrain the inverse procedure (Binley and Kemna, 2005).

3.2.5. Direct mapping

Combination of TDR and ERT data was done using a direct mapping approach. From each TDR dataset, we selected the values that correspond to the start time of time-lapse inversion. From each ERT model, we selected the values that correspond to the cells where TDR probes are located. The aim is to setup a petrophysical relationship between water content data and electrical resistivity values. The data were further divided between those related to the sludge layer and those corresponding to gravel. Finally we randomly selected couples of ERT/TDR data that were used for calibration; others were employed to verify the obtained relationship.

3.3. Results and Discussion

3.3.1. TDR calibration

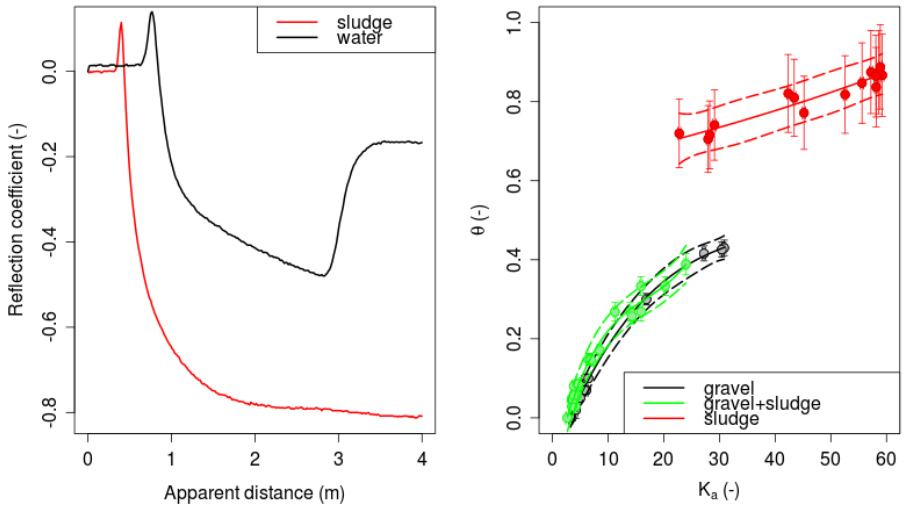


Figure 3.3: Reflection coefficient of TDR signal versus apparent distance for probes inserted in sludge and water (left). Material specific calibration curve of water contents versus dielectric constants (right). Dashed lines represent 95 % confidence intervals

Figure 3.3 (right) displays the results of the calibration for the three studied materials. Gravel and gravel/sludge materials have closed relationships. However a *t*-test performed on the residuals of the difference between the two curves shows that they significantly differ, featuring the influence of organic matter on the calibration curve. The obtained equations are:

Gravel: $\Theta = 7.49.10^{-6} K_a^3 - 8.57.10^{-4} K_a^2 + 3.68.10^{-2} K_a - 0.11$

[Eq. 3.5]

Gravel+sludge: $\Theta = 5.92.10^{-5} K_a^3 - 2.99.10^{-3} K_a^2 + 5.98.10^{-2} K_a - 0.14$

[Eq. 3.6]

Obtained values are of the same order of magnitude than those obtained by Topp *et al.* (1980) for mineral soils.

The calibration of TDR probes for the sludge layer is a particular issue. In the sludge layer, the signal is attenuated to a point where the reflection cannot be distinguished from the background noise. Figure 3.3 (left) compares the signal obtained in water and in sludge. In the former media, we observe a clear reflection peak at an apparent distance of 3 m while nothing is observed in the case of the sludge, even at larger apparent distances. This phenomenon is likely to happen in presence of high ionic concentration. Despite the relatively moderate values of conductivity observed in the effluent (≈ 1000 µS cm^{-1}), ionic concentration in sludge seems to be high enough to disturb the measurement. We therefore decided to coat the rods of TDR probes inserted in sludge. Coating made of plastic thermoretractable material is suppose to provide electrical isolation and therefore to reduce signal attenuation. The drawback of this technique is that it reduces measurement sensitivity (Robinson *et al.*, 2003a). The measured dielectric constant is no more the one of the surrounding material but the one of the association of the coating and the surrounding material. In order to compare values of calibration with those of the literature, we filtered the measured apparent dielectric constant (K_{app}) values for the influence of coating using the approach presented by Fujiyasu *et al.*, (2004) (Eq. 3.7).

$$K_a = \frac{K_{coat} K_{app} \cosh^{-1}(s_1 / r_1)}{K_{coat} \cosh^{-1}(s_0 / r_0) - K_{app}\left[\cosh^{-1}(s_0 / r_0) - \cosh^{-1}(s_1 / r_1)\right]}$$

[Eq.3.7]

where s_0 is half of center-to-center spacing of rods without coating, r_0 is the radius of rods without coating, s_1 is half of center-to-center spacing of rods

with coatings and r_1 is the radius of rods with coatings (Figure 3.4). K_{coat}, K_a and K_{app} are the coating, the soil and the measured dielectric constants, respectively.

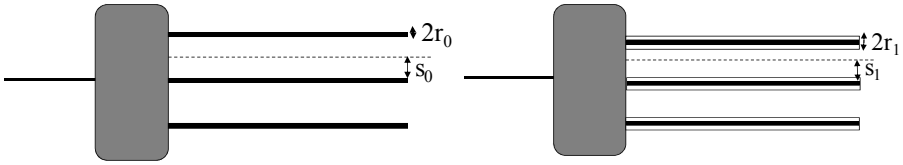


Figure 3.4: Schemes of a TDR probe without coating (left) and a TDR with coating (right) with half of center-to-center spacing of rods without and with coating (s_0 and s_1, respectively) and the radius of rods without and with coating (r_0 and r_1, respectively)

Once corrected, the calibration relationship for sludge becomes Eq. 3.8.

Sludge: $\Theta = 6.78.10^{-10} K_a^3 - 1.14.10^{-7} K_a^2 + 3.18.10^{-3} K_a - 0.63$

[Eq. 3.8]

Coefficients greatly differ from those obtained by Topp *et al.* (1980) for organic soil that are often taken as reference. We also point out the large confidence intervals and errors associated to the measurement. Despite coating, the reflection coefficient remained low making it very sensitive to noise. An alternative to coating for limiting signal attenuation may be to use shorter rods but it will make probes more sensitive to cavities like shrinkage cracks that are likely to happen in sludge.

3.3.2. The feeding period

3.3.2.i. Water front infiltration

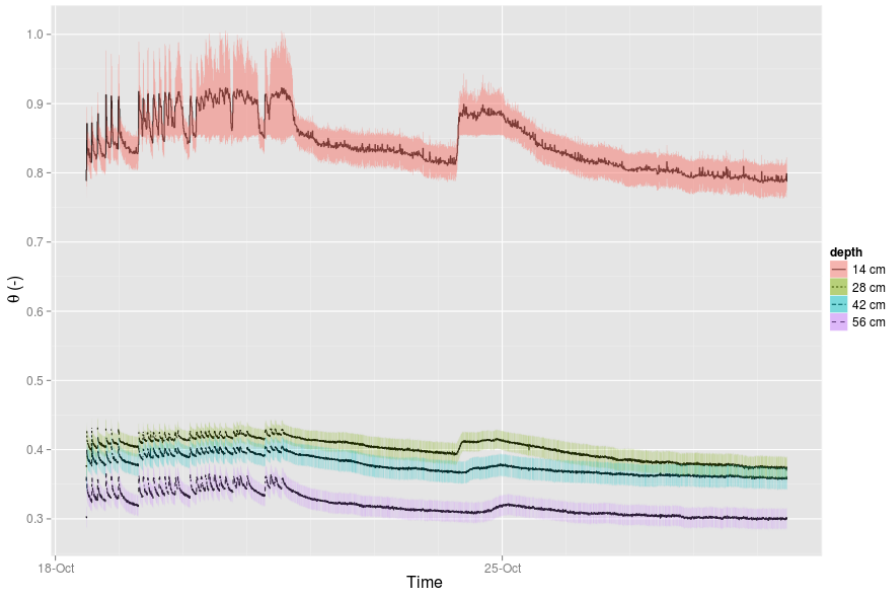


Figure 3.5: Evolution of water content during the experiment at vertical trench 4. Shaded area corresponds to confidence intervals

Evolution of the water content during the experiment at vertical trench 4, which is representative of the global behavior of the system, is depicted on Figure 3.5. The feeding period distinguishes itself from the rest period by its frequent peak corresponding to loads. There is no significant decrease of the water content during the rest period which may be explained by the season and by an important rain (25 mm) that occurred on the 24th of October (Figure 3.2).

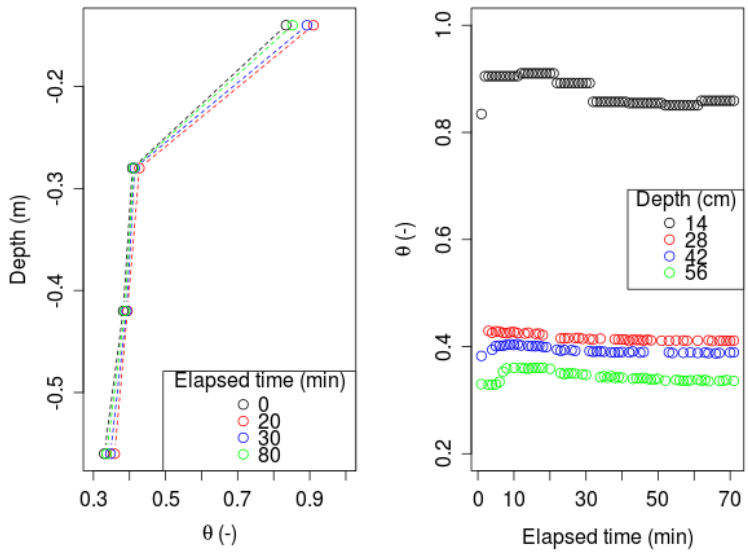


Figure 3.6: (left) Water content versus depth at different times after a load. (right) Water content versus time at different depths after a load

Figure 3.6 provides a detailed description of what is happening during a load and the following drainage during the feeding period. On the right figure, increases in water content correspond to the arrival of the water infiltration front at the TDR depths. There is a lag time of about 8 minutes between the peak at a depth of 14 cm and the one at 56 cm. This corresponds to a rather quick flow supporting the assumption that preferential flow occurs in such coarse systems. On the left picture, peaks corresponding to infiltration front progression can not be observed. We observe that the hydraulic properties of the materials differ significantly in depth. The maximum water content achieved on a lower layer never exceeds the minimum water content at the layer above. This supports the development of different calibration functions for different layers.

3.3.2.ii. The dynamics of the filter clogging

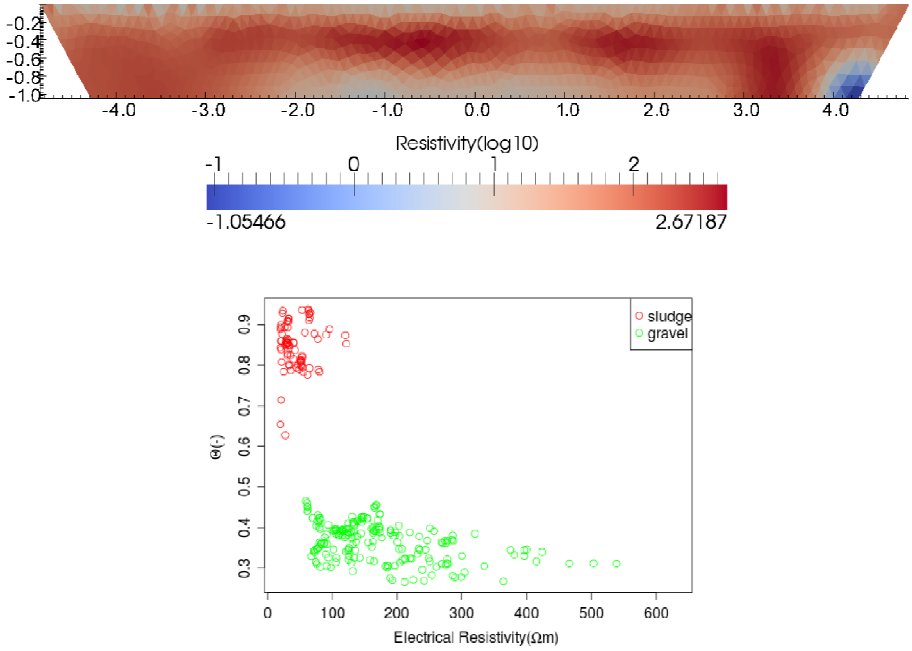


Figure 3.7: (top) Reference cross-section resistivity image (in log scale), (bottom) water content versus electrical resistivity at TDR positions for all time-lapse measurements

Using the reference cross-section resistivity image (Figure 3.7, top), we identify the separation between the sludge deposit and the gravel filter in the first 15-20 centimeters. Sludge has a very low electrical resistivity and a very high water content, as shown on Figure 3.7 (bottom), where water content and electrical resistivity values at location of TDR probes are plotted for all time-lapse measurements. The gravel has a higher resistivity compared to the sludge. The resistivity drops at the bottom of the filter, which may be explained by the presence of a seepage face (saturated media) around the drainage pipe. We do not have any explanation for the low resistivity values on the bottom right corner of the filter and we assume that it is more likely to be an artifact related to the inverse problem, combined with a poor drainage at this location. The sludge layer plays an essential role in VFCW systems that are fed with raw wastewater, especially on hydraulic balance (Molle *et al.*, 2005). Indeed, the low hydraulic conductive sludge deposit improves the influent distribution over the surface. In addition, fresh suspended solid deposit tends to clog the small pores of the sludge deposit. On Figure 3.5 we

observe a clear trend over the feeding period towards an increase of the water content. This phenomenon can be explained by: (i) the progressive wetting of the filter before its water content reaches a steady periodic state typical of VFCW (Forquet *et al.*, 2009b); (ii) the progressive clogging of the filter surface due to TSS deposition.

3.3.2.iii. Influent distribution

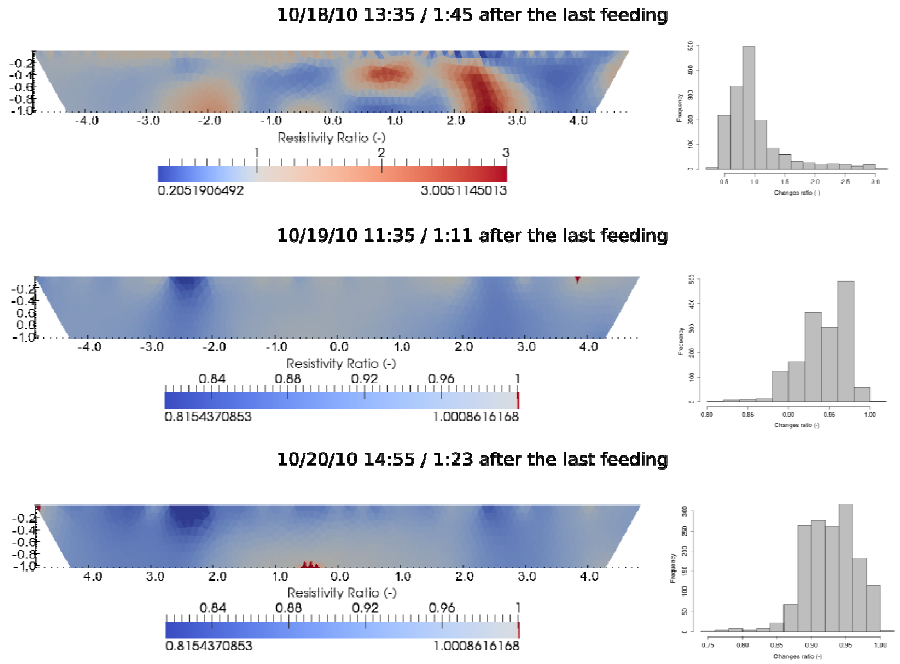


Figure 3.8: (left) Resistivity ratio tomograms at three selected time lapses during the feeding period. (right) Distribution of change ratio values

As mentioned in the previous section, the enhancement of influent distribution over filter surface is one of the benefits of sludge deposit. We suggest verifying this assertion for the studied filter using ERT. If we compare the change in resistivity between before and after the feeding period begins (Figure 3.8), we observe that it is quite homogeneous (around 0.96) over the cross-section except near the inlet pipes (at x = -2.5 m and x = 2.5 m) where it can reach 0.8. This difference is small as all observed changes in water content (Figure 3.5).

3.3.3. The rest period

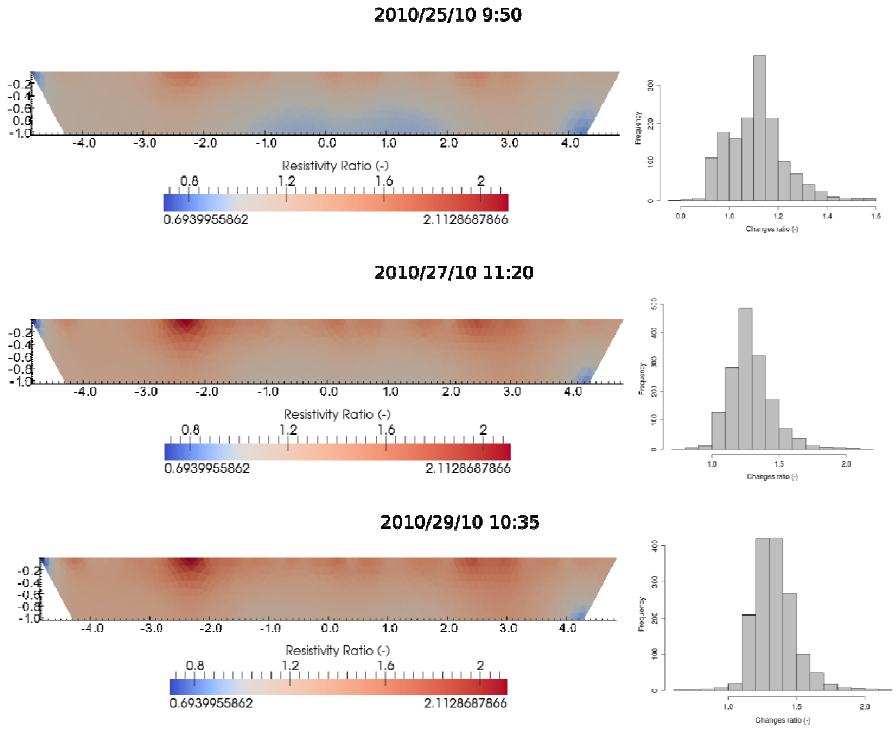


Figure 3.9: (left) Resistivity ratio tomograms at three selected time lapses during the rest period. (right) Distribution of change ratio values

The rest period exhibits larger changes in resistivity ratio (taking as reference value the last tomogram of the feeding period) as shown on Figure 3.9. Over the three days that followed the rain event, the resistivity ratio increased over the entire filter with the average value moving from 1.18 to 1.4, while the water content only slightly changed except near the surface in the sludge deposit where it dropped by 10 percent.

3.3.4. Direct mapping

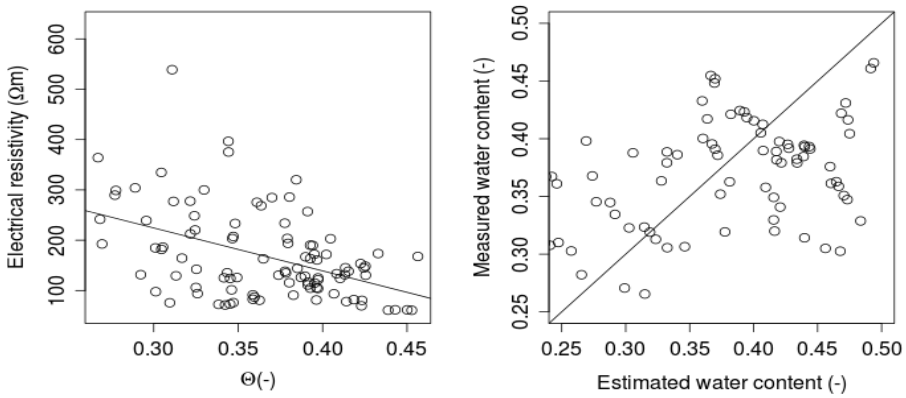


Figure 3.10: (left) Calibration relationship between electrical resistivity and water content for the gravel layer estimated using the calibration set. (right) Measured water content versus estimated water content obtained by applying the calibration relationship on the validation dataset

We only analyzed the petrophysical relationship in the gravel layer. Results of the fitting are shown in Figure 3.10. Despite the petrophysical relationship is normally formalized using a non-linear empirical equation, it does not permit to improve the fitting compared to a linear equation. Therefore we kept the latter linear analysis in our analysis. The linear relationship may be justified by the relatively short range of water content variations that we observed. The validation plot displays a large dispersion around the bisectrix confirming the poor prediction abilities of the model.
Different factors may contribute to this result: (i) the short range of water content variations; (ii) an non-uniform media: material properties change quickly with depth; (iii) the influence of water flow during the feeding period: flow rate at the end of a load is still important especially compared to the time taken by an ERT measurement (about 20 minutes).

Michot *et al.* (2003) demonstrate that direct mapping is possible if calibration relationships are established for each layer. An alternative method could be the use of integration methods like cokriging (Rucker, 2010).

3.4. Conclusions

We observed the hydraulic behavior of a VFCW using advanced hydrogeophysical monitoring. We combined local observations of TDR measured water content with proximal ERT imagery.

The TDR methodology performed rather well for the gravel layer of the VFCW. The gravel layer specific calibration is close to the classical calibration curve established by Topp *et al.* (1980) for mineral material, but is statistically significantly different. Our calibration model therefore provides a better accuracy for volumetric water measurements in the gravel layers of VFCW systems. The calibration for the sludge layer demonstrated that the normal 0.30 m waveguides are not suited for measurement in this media, due to high signal attenuation. To solve this issue, a coating was added to probes located in sludge, but results remained imperfect leading to a poor calibration for water content, and hence large confidence interval in predicted water contents. Other solutions like the reduction of the length of the waveguides must be investigated.

At the scale of a load, TDR measurements efficiently reproduced the water front progression towards the bottom of the filter. Eight minutes are enough to the infiltration peak to reach the deepest TDR probe suggesting the existence of preferential flows. At the scale of the loading period, the water content progressively increased as the system became clogged.

Time-lapse ERT images gave a qualitative picture of the efficiency of water distribution over the filter. The ratio of resistivity change after one day of feeding was lower near the inlet pipes but only of 20 per cent compared to the rest of the filter and this value tends to diminish with time. ERT time-lapse measurements showed the drying dynamic during the rest period with ratio of resistivity change up to 2 compared to the resistivity distribution at the end of the feeding period. Such sharp changes are surprising when compared to the almost stable TDR values.

Finally, direct mapping between TDR and ERT images led to disappointing results. No significant correlation between water content and ERT data could be found in sludge and in gravel the relationship is too weak to perform any prediction. Improvements might be obtained by faster measurements and layer-specific calibration but also by using integration methods instead of direct mapping: the latter being less sensitive to weak relationship (Rucker, 2010).

Chapter 4

A - Measuring the nitrification rate

For understanding the conversion processes in VFCW, methodologies are needed for measuring the nitrification rate of organic materials. A large variety of methods exists for measuring degradation rates in saturated liquid conditions. For VFCW systems however, nitrification rates should be measured in solid unsaturated materials (Langergraber, 2003; Andreottola *et al.*, 2007; Ortigara *et al.*, 2010). Solid respirometry is a promising methodology for measuring this nitrification rate.

Most of the methods published for measuring the nitrifying activity of an organic matrix were developed for liquid materials, sampled in process systems with suspended growth biomass such as activated sludge process or membrane bioreactor (Nowak *et al.*, 1994). The protocols were later adapted for saturated process systems with attached biomass such as submerged biofilters, moving bed bioreactors, after the biofilm has been detached prior to the nitrification measurement (Fdz-Polanco *et al.*, 2000; Vigne *et al.* 2011).

A comprehensive review of the various methods that are available was carried out. The details are provided in Table 4A.1, with the respective advantages and disadvantages of each method.

The principles of the methods are presented below, and summarized in the following pages:

- Measuring temperature variations (self-heating test);
- Measuring pH (titration experiments) or chemical forms like production of nitrates;
- Measuring oxygen uptake (respirometry liquid (saturated) or solid (unsaturated)).

.

Table 4A.1: Advantages and disadvantages of the various methods available for both nitrification and carbon degradation studies

Method	Material	Inaccuracy sources	Measurement	Measurement phase?	Activity of the studied media	Continuous feeding (gas/liquid)	Adjustable to a solid phase?	Commentaries
Self-heating test	Controlled temperature reactor (accurate thermometer)	Other endo/exothermic reactions Thermal balance of possible in/out	Heat produced by the reactive environment	Liquid	Low (no continuous feeding)	No/No	Difficult	Means of temperature measurement very precise Thermal insulation of reactors needed
Acid-base titration	pH probes and pump dispenser for pH regulation	Material heterogeneity	Solution pH → carbonate and ammonium consumption	Liquid	Low or high	Yes/No	No	Necessary to well-know the reaction stoichiometry
Nitrogen forms monitoring	Important analysis means	Analysis method. Nitrogen storage in the solid phase difficult to estimate	Consumption and production of various nitrogen forms	Solid/liquid	Low or high	Yes/Yes	Yes in percolates and out-gases	Necessary to be certain of the reaction stoichiometry
Static respirometry	Closed reactor and gas analysis (dissolved or not)	Measurement device Intrusive reactions	O_2 consumption, CO_2 production	Solid/liquid	Low	No/No	Yes	Necessary to re-circulate the gases to have an adequate diffusion
Dynamic respirometry	Provision of gas Gas analysis	Complex mass balance. Measurement device accuracy for flows, composition, intrusive reactions	O_2 consumption, CO_2 production	Solid/liquid	High	Yes	Yes	Never used for nitrification study but method largely used for biological activity measurements

4A.1. The self-heating test (calorimetry principles)

This method consists of the monitoring of temperature variations into an adiabatic chamber (isolated from outside temperature). It is used to determine the energy production rate, and so the global rate of the endo/exothermic reactions which take place inside (Daverio *et al.* 2003). Nitrification and denitrification processes are exothermic ($\Delta H° = -259$ kJ.mol N^{-1} for the nitritation process, and $\Delta H° = -99.4$ kJ.mol N^{-1} for the nitratation process (Daverio *et al*, 2003)). However, calorimetry does not allow differentiating the cell respiration from other exothermic phenomenon usually present in reactors, such as chemical exothermic or biochemical reactions (Barrena *et al.*, 2006). To provide measurement accuracy, calorimetry can be used only in a closed environment and with sludge with a high biological activity.

4A.2. Measuring chemical forms

4A.2.1. Acid-base titration

The nitrification of one ammonium ion is accompanied by the production of two hydrogen ions, so the solution is acidified ($NH_4^+ + 2O_2 \rightarrow 2H^+ + H_2O + NO_3^-$). In a liquid reactor where the nitrification reaction takes place, the pH control can be carried out by acid-base addition. The added acid-base quantity gives then an estimate of the nitrification rate of an organic matrix (Gernaey *et al.*, 2001; Ficara et Rozzi, 2001; Gapes *et al.*, 2003) (Figure 4A.1).

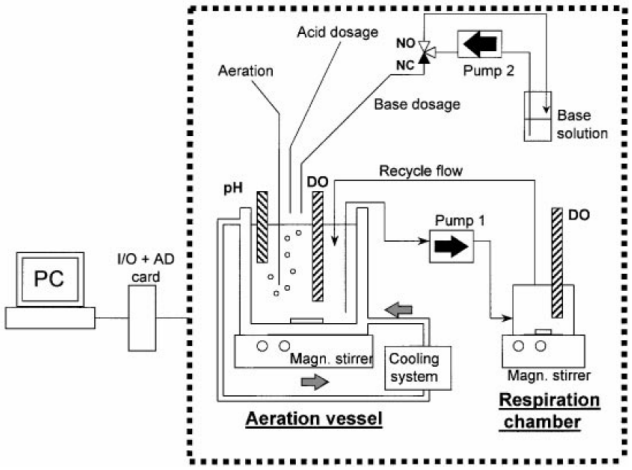


Figure 4A.1: Example of a device combining respirometry and titrimetry measurement for activated sludge study (Source: Gernaey *et al.*, 2001)

This method must be performed under immersed conditions applied to solid samples with monitoring of nitrate concentrations. However, due to the nitrate storage in the media from VFCW and the saturated conditions of the experiment, results should be biased.

4A.2.2. Monitoring nitrate

With this method, an organic mixture is continuously mixed with a magnetic stirrer and aerated with a diffuser. Initial conditions are applied to prevent limitations due to dissolved oxygen (concentrations > 6 $gO_2.m^{-3}$), NH_4-N substrate (addition of 15 $gNH_4\text{-}N.m^{-3}$) or alkalinity (addition of 120 $gHCO_3^-.m^{-3}$) maintaining pH in the range 7 - 8. Samples of liquid are taken every 10 minutes for 1 h, immediately filtered on glass-fibre filters (0.7 µm). The NO_3-N concentrations are analyzed. The slope of the NO_3-N concentrations vs. time give the maximum nitrification rate [$R_{V,max\ nit}$ expressed in $kgNH_4\text{-}N.m^{-3}_media.d^{-1}$] as it corresponds to the non-limiting nitrification rate conditions (WERF, 2003).

Concerning submerged biofilters, the nitrification rate was assessed by monitoring the nitrate production (Tschui *et al.*, 1994; Jeong *et al*., 2006). These studies did not consider the media heterogeneity that occurs due to the solid phase distribution caused by erratic flow pattern, hydraulic channelling, irregular transfer of substrates and difference in the distribution of the biological activity.

4A.3. Respirometry

4A.3.1. Respirometry for saturated conditions (liquid respirometry)

For liquid matrices, respirometry can be carried out by the measurement of the dissolved oxygen uptake rate. This technique is used for both measuring the respiration linked to the organic carbon degradation (Spanjers and Vanrolleghem, 1995) and the nitrifying activity, using or not inhibitors such as allylthiourea and chlorates (Surmacz-Gorska *et al.*, 1995) or using non nitrying conditions (Souef, 2008).

To differentiate the two processes involved in nitrification (nitritation and nitratation), inhibitors can be applied (Ginestet *et al.*, 1988; Chandran *et al.*, 2000; Souef, 2008). A supply of nitrites at the beginning of the nitrification process versus a supply of ammonium allow to differentiate the nitritation from nitratation by subtracting the activity recorded from nitratation measured previously (Souef, 2008).

Andreottola *et al.* (2007) presented a respirometric technique for VFCW using saturated columns, mainly to measure the rate of oxidation of COD. With this technique, the maximum rate of nitrification can also be determined (Appendix IV). Despite the promising combination of these rates with CW2D model simulations (Langergraber, 2008), the proposed method is carried out under immersed conditions applied to solid samples with monitoring of dissolved oxygen concentrations (not gaseous oxygen). Results should be completely different from the ones that can be observed under unsaturated conditions.

4A.3.2. Respirometry for unsaturated conditions (solid respirometry)

Solid respirometry for CW is less described in literature. Research papers were published for characterizing biological activity of compost, for carbon conversion (Tremier *et al.*, 2005; Adani *et al.*, 2004). Studying nitrification of solid matrixes by respirometry is therefore a novelty and was carried out at the Cemagref Lyon during this study. On-going works were also carried out at the Cemagref Rennes for nitrification in compost (de Guardia *et al.*, 2008).

Optimal and controlled conditions are required (Adani *et al.* 2001) such as moisture, oxygen content, temperature, and nutrient content.

Water content. For many authors (Haug 1993; Adani *et al.*, 2003), water content is the most influent parameter for a respirometric test. Paletski and Young (1995) showed that the oxygen uptake is linked to the water content of a solid matrix. The optimal water content prevents the decrease of the optimal microbial activity when water content is too high (anaerobic conditions promoted) or too low (lower potential microbial activity). Generally, the volumetric water content in respirometric tests is limited below 45 % (Berthe *et al.*, 2007).

Porosity. Authors emphasize the link between respiration and porosity measurements (Berthe *et al.* 2007). The optimum free air space (FAS) differs between the authors (Madejon *et al.*, 2002; Rudrum *et al.*, 2002; Mohee *et al.*, 1998), but commonly the FAS has to be higher than 30 % for not being a limiting factor. Berthe *et al.* (2007) pointed out that a sample with both low FAS and high water content has some difficulties to be uniformly aerated. A bulking agent is therefore needed. Tremier *et al.* (2005) mixed biological sludge with pine barks (1/1 wet mass ratio) to obtain such a bulking agent.

Air-flow rate. For Adani *et al.* (2001), 140 $mL.L_{FAS}^{-1}$ in the outlet airflow is the minimum airflow to ensure aerobic conditions during the dynamic respiration index (DRI) measurement.

Temperature. Biological activity is dependent on temperature. Thus this is a critical parameter for the respiration index determination (Iannotti *et al.*, 1993; Lasaridi *et al.*, 2000). There is no agreement in the literature on the optimal temperature that has to be applied during a respirometric test. The available data for sludge respiration tests suggests that temperature should situate between 30 °C and 37 °C (Iannotti *et al.*, 1993; Paletski and Young, 1995; Lasaridi and Stentiford, 1998).

Hence, to study the conversion of ammonium into nitrates by autotrophic biomass (nitrification) it is still necessary to design a new technique for the measurement of nitrification rates in partially saturated medium. Indeed, the available techniques consist in the immersion of biofilm in liquid conditions (WERF, 2003; Dold *et al.*, 2005; Choubert *et al.*, 2009; Surmacz-Gorska *et al.*, 1995; Ficara and Rozzi, 2001) that leads to significant disturbance of the nitrification activity of biofilm. The purpose of the following chapter is therefore to present a novel respirometric tool (solid respirometry), designed to measure the maximum nitrification rate in a VFCW as a way to yield a-priori estimates of the biological process parameters of models like HYDRUS/CW2D.

Chapter 4

B - Solid respirometry to characterize the nitrification kinetic: a better insight for modelling nitrogen conversion in vertical flow constructed wetlands*

Abstract

We developed an original method to measure nitrification rate at different depths of a VFCW with variable contents of organic matter (sludge, colonized gravel). The method is specifically adapted for a matrix operated under partially saturated conditions and is based on respirometric principles. The oxygen demand is determined from the analysis of the oxygen concentration, measured by an on-line analyzer equipped with a paramagnetic detector. The composition of the gas passing through a reactor containing a mixture of an organic matrix mixed with a bulking agent (wood) is analyzed versus time while a regular addition of liquid containing ammonium is applied on the mixture. In this chapter we present the overall methodology, the factors influencing the measurement (sample volume, nature and concentration of the applied liquid, number of successive application), and we studied the robustness of the method. The combination of the method with a mass balance approach led to original results of concentration and maximum growth rate coefficient for the autotrophic biomass in different layers of a VFCW, that are critical inputs for the VFCW plant modelling.

*Adapted from: Morvannou, A., Choubert, J.-M., Vanclooster, M., Molle, P. (2011).
Solid respirometry to characterize nitrification kinetics: A better insight for modelling nitrogen conversion in vertical flow constructed wetlands. *Water Research* 45(16), 4995-5004

4B.1. Introduction

The purpose of this chapter is to present a novel respirometric tool (solid respirometry) designed to measure the maximum nitrification rate in a VFCW as a way to yield a-priori estimates of the biological process parameters of models like HYDRUS/CW2D (Langergraber and Simunek, 2005). The novelty is based on the fact that the solid respirometric method allows handling matrices in partially saturated conditions, such as those found in the porous media of VFCW. The effects of the addition of substrates, the hydraulic retention time, and the injected nitrogen (ammonium) load on the measured nitrification rate are assessed. Special attention is given to interpret the phenomenon of nitrogen (nitrate) release and storage. Then, the robustness of the developed method was evaluated. Subsequently, the method is applied to assess turn-over parameters of the autotrophic biomass at different heights in a full-scale VFCW.

4B.2. Materials and methods

The solid respirometric equipment was set-up for partially saturated samples collected from a VFCW. This equipment is first presented in section 4B.2.1. Then the method developed for measuring the maximum nitrification rates as well as the data for evaluating its robustness are presented in section 4B.2.2. Finally, the application of the method for a full-scale VFCW plant is illustrated in section 4B.2.3.

4B.2.1. The solid respirometer

4B.2.1.i. Equipment and operating conditions

The respirometric system (Figure 4B.1) was adapted from a concept developed for characterizing household waste (Tremier *et al.*, 2005). The system consists of six stainless steel, temperature controlled (double envelope), cylinders of an overall height of 0.40 m and an internal diameter of 0.22 m. The temperature of the reactor was maintained at 20°C with a cooler (Lauda WKL903). The VFCW sample was mechanically mixed with a woody bulking agent (wood chips of average size 3 x 2 x 0.5 cm) that was previously immersed in tap water for 24 hours, using an end-over-end tumbler (Firlabo, operated at 60 rpm for 2 minutes). For colonized gravel

from the VFCW (e.g. d_{10} = 2.46 mm; UC = 1.39; initial porosity of 40 %), the volumetric ratio bulking agent/sample yielded 50/50, allowing to maximize both porosity and oxygen uptake. For sludge, a volumetric ratio bulking agent/sample of 75/25% was used. The application of a mechanical mixing was found to be essential to obtain a good repeatability. A total volume of 3 L of the mixture was then introduced in each cell of the solid respirometer, and the reactors were hermetically closed.

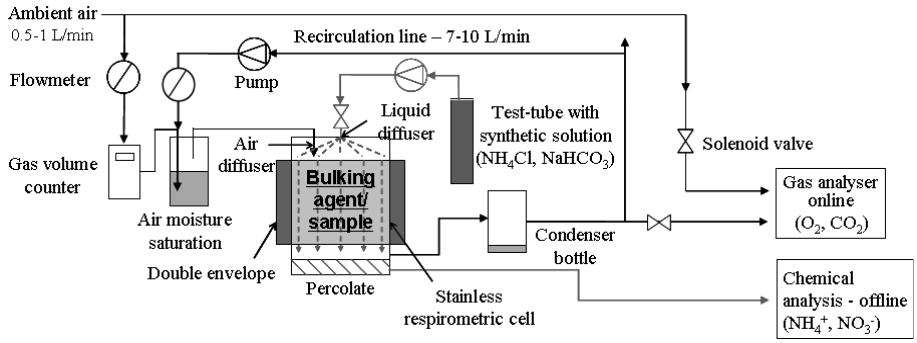


Figure 4B.1: Solid respirometer device

Each reactor was subsequently subjected to a continuous supply of ambient airflow (0.5-1 L/min) mixed with recycled air (7-10 L/min). These conditions led to a ratio between recycled and ambient air between 10 and 20, allowing to obtain perfect mixed conditions and no limiting oxygen rates (Berthe *et al.*, 2007). Gas flow rates applied to every reactor were quantified by volumetric sensors (Gallus 2000, Actaris).

After a previous cooling stage (Peltier, PKE 511), allowing to eliminate the humidity of the gases, the outgoing gases of every reactor were analyzed with an on-line analyzer (Servomex 4900) equipped with a paramagnetic detector for oxygen (0-100 %) and with optical sensors for the analysis of carbon dioxide (CO_2, 0-3000 ppm), methane (CH_4, 0-500 ppm) and nitrous oxide (N_2O, 0-500 ppm). The outgoing gas of each reactor was analyzed every hour for 8 minutes, and the incoming gas was analyzed every hour for 12 minutes. Oxygen content was monitored to calculate the nitrification rate, while CH_4 was monitored to verify that anaerobic conditions did not occur.

4B.2.1.ii. Sensitivity of the method

The bulking agent improved the porosity and thus the aeration efficiency of the sample (Tremier *et al.*, 2005), without extra oxygen uptake. It also maintained the humidity for the growth of microorganisms (Berthe *et al.*, 2007).
The calibration of the gas analyzer was carried out twice a week and before starting a new experimental campaign. This guaranteed an absolute gas measurement precision of 0.01 %. To improve the reliability of the method, connecting pipes were changed regularly to limit supplementary oxygen uptake caused by microorganisms that develop in the connection pipes of the recirculation line (oxygen uptake called “intrusive” uptake). Moreover, the total "intrusive" oxygen uptake (blank test) of each reactor and connecting pipe were systematically measured before filling the reactors. This intrusive uptake was subtracted from the uptake measured with the mixture introduced in the reactor. With this protocol, a relative standard deviation between two replicates smaller than 20 % was obtained.

4B.2.1.iii. Respirometric index

In the following equations, the oxygen uptake rates were expressed in terms of dry matter (DM). For the measurement of DM, the water of collected samples (sludge and colonized gravel) was evaporated until dried in a drying oven (105°C) for at least 24 h. DM was calculated by the difference of weights before and after drying according to the standardized method published by APHA (2005). Duplicate determination coincided with the 5% of the measured weight.

The difference in the oxygen concentration between the reactor entrance ($O_2^{in}(t)$, [%]) and the reactor exit ($O_2^{out}(t)$, [%]) provided the oxygen uptake rate by mass unit (noted *DRI*, [mg O_2/kg DM/h]) as shown in Eq. 4B.1. This variable was related to the biomass activity within a reactor. The total consumed oxygen mass during the period t_F ($CO(t_F)$, [mg O_2/kg DM]) was calculated by integrating *DRI* (t) from t = 0 to t_F, as shown in Eq.4B.2.

$$DRI(t) = \frac{dO_2(t)}{dt} = \frac{\left[O_2^{in}(t) - O_2^{out}(t)\right] \times Q_{air}^{in} \times 60 \times 1000 \times 32}{V_{molar(T°)} \times M_{sample}} \quad \text{[Eq. 4B.1]}$$

$$CO(t_F) = \int_0^{t_F} DRI(t).dt \quad \text{[Eq. 4B.2]}$$

with Q_{air}^{in} [L/min], the gas flow rate applied to a reactor; $V_{molar(T°)}$ [L/mol] the molar volume of the outgoing air considering its temperature (T [°C]); M_{sample} [kg DM] the mass of dry sample to characterize; and t_F the length of the experiment. The conversion factors are as follows: 60 to convert from minute to hour; 1000 to convert from g to mg O_2; 32 to convert from mol O_2 to g O_2.

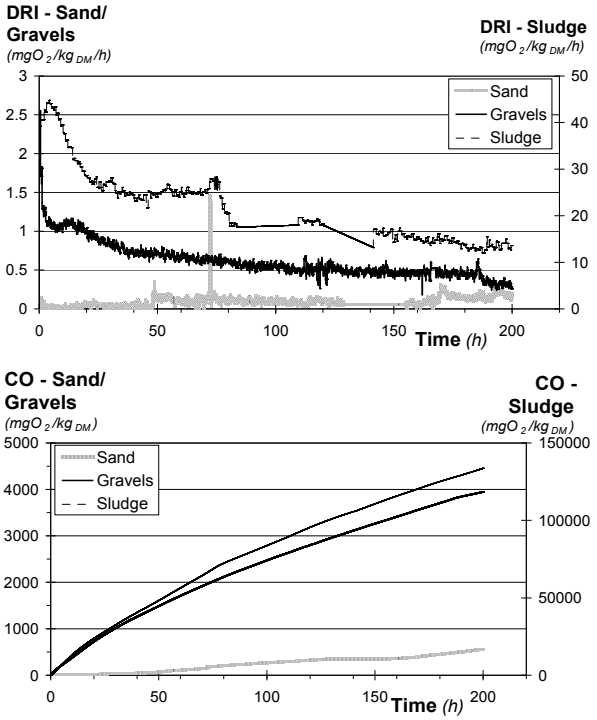


Figure 4B.2: Examples of *DRI(t)* and *CO(t)* results for carbon degradation in three organic wastes (colonized sand and gravel, sludge)

Figure 4B.2 illustrates examples of the measured time course of *DRI(t)* and $CO(t_F)$ for three materials like sand, colonized gravel and sludge. For sand containing few biodegradable organic matter (lab-scale columns fed with synthetic wastewater, Rolland *et al.*, 2009), *CO* (t_F=200 h) ranges between 480 and 1000 mg O_2/kg DM. For such low $CO(t_F)$, the difference between

replicates was about 40 % which prevented using the proposed method for samples with a too low amount of organic matter. For colonized gravel sampled at the first stage of a VFCW (situated in Evieu (France) described in Molle *et al.*, (2008), we found $CO(t_F = 200\ h)$ that ranged between 3 840 and 6 400 mg O_2/kg DM. As for sludge from a drying reed bed situated in Andancette (France), described in Troesch *et al.*, 2009, we found $CO(t_F = 200\ h)$ that ranged between 48 000 and 320 000 mgO_2/kg DM. For both organic matrices, the difference between replicates was lower than 20 %.

4B.2.2. Determining of the nitrification rate

4B.2.2.i. Liquid addition, percolate release, and nitrification index

To study nitrification, each reactor was equipped with a spraying system (2 L/min) allowing a uniform supply of liquid solution to the sample. To limit the dissolution of the oxygen when spraying, and to limit the sur-saturation phenomenon for oxygen, the liquid was first aerated during 12 h and, subsequently, at rest for 1 h before being injected in a reactor. A typical time course of *DRI(t)* recorded with an addition of liquid is shown in Figure 4B.3. The DRI_{max} was determined by the most important difference between the oxygen concentrations entering and leaving the reactor. The $CO(t_F)$ (Eq. 4B.2) was equal to the area located between the *DRI(t)* curve and the endogenous respiration baseline.

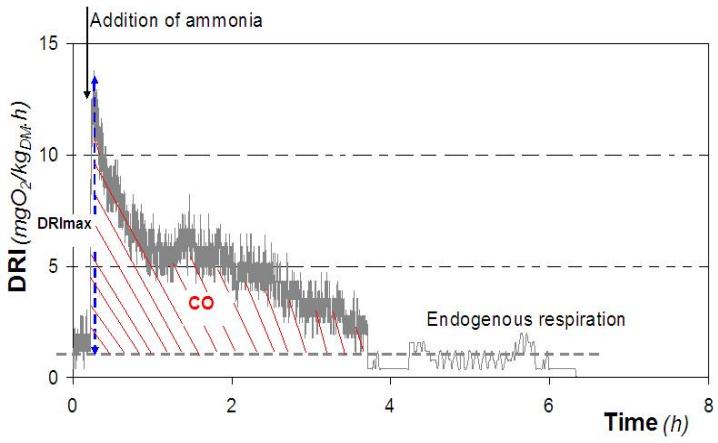


Figure 4B.3: Respirogram obtained after addition of ammonia for the nitrification study

4B.2.2.ii. Calculating nitrification rates from DRI_{max} and $CO(t_F)$

The actual oxygen uptake rate ($\frac{dO_2}{dt}$, [mg O_2/kg DM/h]) in local conditions can be calculated using conceptual models as shown in Eq. 4B.3, drawn from activated sludge models (Henze *et al.*, 1987) and extended to VFCW (Šimůnek *et al.*, 1999). Five parameters are used, such as the maximum autotrophic growth rate ($\mu_{A,\,max}$, [1/h]), the cellular yield coefficient (Y_A, [g $COD_{biomass}$/gNH_4-N $_{nitrified}$]), the saturation/inhibition coefficients for oxygen ($K_{ANs,O2}$, [mg O_2/L]), nitrogen ($K_{ANs,NH4}$, [mg NH_4-N/L]) and inorganic phosphorus ($K_{ANs,IP}$, [mg P/L]). Also four variables are used like the concentration of oxygen (C_{O2}, [mg O_2/L]), the concentration in ammonium (C_{NH4}, [mg N/L]), the concentration in inorganic phosphorus (C_{IP}, [mg P/L]) and the concentration of biomass (C_{XA}, [mg $COD_{biomass}$/kg DM]):

$$\frac{dc_{O_2}}{dt} = -\frac{4.57 - Y_{AN}}{Y_{AN}} \mu_{A\max} \cdot \frac{c_{O_2}}{K_{ANs,O_2} + c_{O_2}} \cdot \frac{c_{NH_4}}{K_{ANs,NH_4} + c_{NH_4}} \cdot \frac{c_{IP}}{K_{ANs,IP} + c_{IP}} c_{XA} \qquad \text{[Eq. 4B.3]}$$

When no limiting conditions occur in terms of oxygen, nitrogen and phosphorus, the previous equation can be simplified into Eq. 4B.4.

$$\left(\frac{dO_2}{dt}\right)_{\max} = -\frac{4.57 - Y_A}{Y_A} \cdot \mu_{A,\max} \cdot C_{XA} = DRI_{\max} = R_{s,\max} = \rho . R_{v,\max} \qquad \text{[Eq. 4B.4]}$$

From the value of DRI_{max} Eq. 4B.4, the maximum nitrification rates $R_{s,\,max}$ [mg O_2/kg DM/h] were determined. This value was linked to the maximum volumetric nitrification rate $R_{V,max}$ [mg O_2/L_{sample}/h] using the concentrations of solids in the layer noted ρ [g DM/L_{sample}] (concentration of dry matter once it was get rid off of dead leaves, roots).

$CO(t_F)$ and DRI_{max} gave the nitrified mass using the conversion factor of 4.3 gO_2 consumed for 1 gNH_4-N nitrified (= 4.57-Y_A). An alternative method in determining the nitrified mass was to carry out a mass balance on chemical analysis data. After passing through the mixture made of the bulking agent and sample, each percolated solution was collected and immediately filtered. The composition of the percolate was determined by using chemical analysis COD, NH_4-N, NO_3-N and NO_2-N, according to standardized methods (APHA, 2005).

4B.2.2.iii. Experimental conditions tested to adjust liquid injection

The strategy carried out to adjust, evaluate and apply the solid respirometric method is summarized in Table 4B.1. The effects of the concentration and the volume of the liquid solution on nitrification were studied in detail for the colonized gravel from a VFCW.

Table 4B.1: Strategy to adjust, evaluate and apply the solid respirometric method

Design of the solid respirometric method for nitrification *- Testing of the influence of experimental conditions on respiration rates -*	**Evaluation of the method** *- Testing for the robustness and comparison with "classical" protocols or literature -*	**Application to a VFCW plant**
– Impact of the injected volume of liquid; – Impact of injections of ammonium-free water, and subsequent injections of water with ammonium; – Impact of injections of water with ammonium only (no previous addition of ammonium-free water); – Impact of injected mass of nitrogen (ammonium).	– Comparison with NO_3-N production rate in liquid conditions (batch test) with biofilm (taken off from gravel by a mechanical step), immersed in liquid and excess of oxygen; – Comparison with NH_4-N uptake and NO_3-N release with analysis in percolates of respirometer; – Comparison with literature values from other methods.	– Measurement of the maximum nitrification rate *(Rv, max)* [with *DRI* measured after four successive injections of 1 L of liquid solution (90 mgNH_4-N/L); – Mass balance calculated with input and output nitrogen fluxes calculated [inflow rate (19 m^3/d) and nitrified mass (420 $gN_{nitrified}$/d)]. This aims at characterizing the autotrophic degradation process in a full-scale VFCW; – Determination of $\mu_{A,max}$

Two types of liquids were studied to measure the nitrification rate: an ammonium-free tap-water to study the need to clean the organic matter from CW before measuring nitrification; and tap water containing ammonium. The chemicals that were considered in the liquids were ammonium chloride (NH_4Cl) to feed nitrifiers, and sodium bicarbonate ($NaHCO_3$) to prevent from mineral carbon limitation. Different concentrations and volumes of injected water were evaluated in order to study the role of the mass of nitrogen applied on nitrification rate. The storage and depletion (release) phenomenon of nitrogen were studied following the chemical analysis of batches.

Samples of colonized gravel collected within the first stage of the VFCW from a plant located in Evieu (France) (Molle *et al.,* 2008), were mixed with the bulking agent (see preparation method in section 4B.2.1.i.), and were characterized in the reactors of the solid respirometer device at 20°C. The *DRI(t)* curves were determined under the following supply conditions (Table 4B.1):

- injections of three different volumes (250, 500 and 1000 mL) with two concentrations of ammonium (30 and 60 mg NH_4-N/L), implying four thresholds nitrogen concentrations (7.5, 14.3, 28.5, 60.0 mg N). Among them, two threshold concentrations (14.3 and 28.5 mg N) were applied with two different volumes (Figure 4B.4);
- injections of ten successive volumes of 1 L of liquid ; six of them were carried out with ammonium-free water (tap water). Then, four batches were carried out with water containing ammonium (60 mgNH_4-N/L) and bicarbonate in stœchiometric quantity (2 batches/day);
- injections of six successive volumes of 1 L of water containing ammonium (90 mg NH_4-N/L) and bicarbonate in stœchiometric quantity (2 batches/day); and,
- injections with different masses of nitrogen (8, 15, 28, 55, 90 mg) applied to five samples of colonized gravel, and determined after the application of a succession of a 1 L-batch with water containing ammonium.

For each experimental condition detailed above, the maximum specific nitrification rates (Rs_{max}, [mg O_2/kg DM/h]) were determined as explained in section 4B.2.2.ii. Moreover, the mass of released ammonium and nitrates was calculated from the chemical composition of the liquid that percolated.

4B.2.2.iv. Other conventional protocols for comparing solid respirometry results

The maximum volumetric nitrification rates ($R_{S,max}$, [mg O_2/kg DM/h]) obtained from solid respirometry experiments were compared to the values obtained with a common protocol generally applied to assess the maximum nitrification rate of an activated sludge. The batch test consisted in measuring the NO_3-N production rate in liquid conditions (noted $R_{S,liq}$) under non limiting conditions (mixing, aeration, ammonium availability, no COD added, carbonate addition, T° = 20 °C) as detailed in the protocol published by Water Environment Research Foundation (WERF, 2003). The batch test was applied after a mechanical removal of the biofilm composed of organic matter and biomass, attached to the gravel. The biofilm was removed by a rigorous mixing 1 L of colonized gravel placed in 3 L of water. This step was repeated three times successively, until clean gravel was obtained. The nitrification rate was converted as detailed in section 4B.2.2.ii. The experiment was carried out for 5 samples of colonized gravel, collected every two weeks.

4B.2.3. Determining maximum nitrification rate and concentration of autotrophic biomass developed in a VFCW plant

In the VFCW, three horizontal layers were differentiated: only sludge deposit (1st layer, h_1 = 20 cm of thickness), colonized gravel with biofilm (2nd layer, h_2 = 30 cm of thickness), and almost clean gravel (3rd layer, h_3 = 30 cm of thickness) with a negligible activity. The section below describes sampling, measurement, and calculation strategies that were implemented in order to determine the turn-over parameters of the autotrophic biomass.

4B.2.3.i. Sampling and preparation

Samples of sludge and colonized gravel were shovelled up (1-20 cm depth and 20-40 cm depth for sludge and colonized gravel samples, respectively) at two locations of the first stage of the VFCW. Hence, one sample was collected for each 15 m^2 of filter. Both sampling points were located at 2 meters of the feeding point, providing raw waste water input to the VFCW. The duplicate samples collected for each layer are merged, then subsequently prepared with the bulking agent (as described in 4B.2.1), and introduced in the reactors of the solid respirometer device.

4B.2.3.ii. Determining the maximum nitrification rate ($R_{S,max}$) with solid respirometry

The *DRI(t)* and DRI_{max} were determined at 20°C for the two samples (sludge and colonized gravel) after four successive batches of 1 L, containg a solution of 90 mg NH_4-N/L, was applied. The maximum specific nitrification rates, $R_{S,max}(h_1)$ and $R_{S,max}(h_2)$ [mg N/g DM/h], were then determined. The concentrations of solids in each layer, ρ_1 and ρ_2 [g DM/L_{sample}], were used to convert the individual values into volumetric nitrification rates noted $R_{V,max}(h_1)$ and $R_{V,max}(h_2)$. By weighting with the respective thickness (h_1 and h_2) of each layer, the global value (for the two first layers), $R_{V,max}$ [mg N/L_{sample}/h], was calculated.

4B.2.3.iii. Calculating the autotrophic concentration (C_{XA}) by means of nitrogen mass balance

The daily net growth of the autotrophic biomass that accumulated in the system was modelled with an approach adapted from Nowak *et al.* (1994) presented in Eq. 4B.5. It used the daily nitrified nitrogen fluxes in a wastewater treatment plant as determined from the flow rates and the concentrations of different nitrogen forms of raw and treated water. The amount of the autotrophic biomass produced each day by nitrification, $M_{XA}(t)$, [g COD], was estimated by the sum of daily nitrified nitrogen ($\varphi N_{nitrified}$, [g Nnitrified/d]), assuming that the autotrophic biomass input from the influent was negligible. The fraction that disappears each day was estimated from a decay process (b_A, [1/d]) and from the evaluation of the mass removed by treated effluent ($\varphi XA_{effluent}$, [g COD/d]), as there was no regular withdrawal of the excess sludge, but resting period with no feed. Moreover uptake of nitrogen by reeds and denitrification were considered as negligible as shown by Molle *et al.* (2008) and Tanner (1996). The typical decay rate value (b_A) was chosen similar to thoses determined for secondary sludge from an activated sludge process [0.0071 h^{-1} (=0.17 d^{-1}) at 20°C (Dold *et al.*, 2005)], as it is not easily measurable. The daily net growth of the autotrophic biomass yields:

$$\frac{d\,M_{XA}(t)}{d\,t} = Y_A.\varphi N_{nitrified} - b_A.M_{XA}(t) - \varphi_{XAeffluent} \qquad \text{[Eq. 4B.5]}$$

This equation was applied to the VFCW from Evieu that treated 19 m^3/d of water and yielded a daily nitrogen nitrification flux ($\varphi N_{nitrified}$) of 420 g $N_{nitrified}$/d (14 g $N_{nitrified}/m^2$.d). This latter value was computed from

concentrations of different nitrogen forms in daily average, flow proportional, composite samples. Assuming an initial autotrophic concentration of 100 g $COD_{biomass}$, the successive mass balances converged towards a reliable value, independent of the initial value (Nowak *et al.*, 1999). The global concentration of autotrophic biomass accumulated in the VFCW (C_{XA}) was calculated by dividing the mass of autotrophic biomass (M_{XA}) by the volume of the active biological reactor (V_1+V_2), located from the surface layer to the bottom of the second layer of gravel (h_1+h_2= 50 cm height), assuming that the third layer (30 cm at the bottom of VFCW) had no biological activity (almost clean gravel).

4B.2.3.iv. Calculating the maximum autotrophic growth rate ($\mu_{A,\,max}$)

Using the previous calculations explained in section 4B.2.3.iii. (C_{XA}) and in section 4B.2.3.ii. (global $R_{V,\,max}$), the maximum autotrophic growth rate ($\mu_{A,\,max}$ [h^{-1}]) was determined with Eq. 4B.6.

$$\mu_{A,\max} = Y_A \cdot \frac{h_1 . R_{v,\max}(h_1) + h_2 . R_{v,\max}(h_2)}{h_1 + h_2} \cdot \frac{1}{M_{XA} / V_1 + V_2} \qquad \text{[Eq. 4B.6]}$$

with Y_A the cellular yield coefficient (0.24 g $COD_{biomass}$/g NH_4-$N_{nitrified}$, Henze *et al.*, 1987).

4B.3. Results and discussion

4B.3.1. Impact of injecting liquid and consequences on measuring nitrification

The conditions of injections were studied as described in section 4B.2.2.iii.

4B.3.1.i. Impact of the injected volume and the concentration of nitrogen

Figure 4B.4 presents $CO(t_F)$ and DRI_{max} for batches of 250 mL, 500 mL and 1 L of tap water containing either a concentration of 30 or 60 mgNH_4-N/L with bicarbonate, for a nitrogen mass applied of 7.5 to 60 mg N. Relative standard deviation indicates the discrepancy around the mean values.

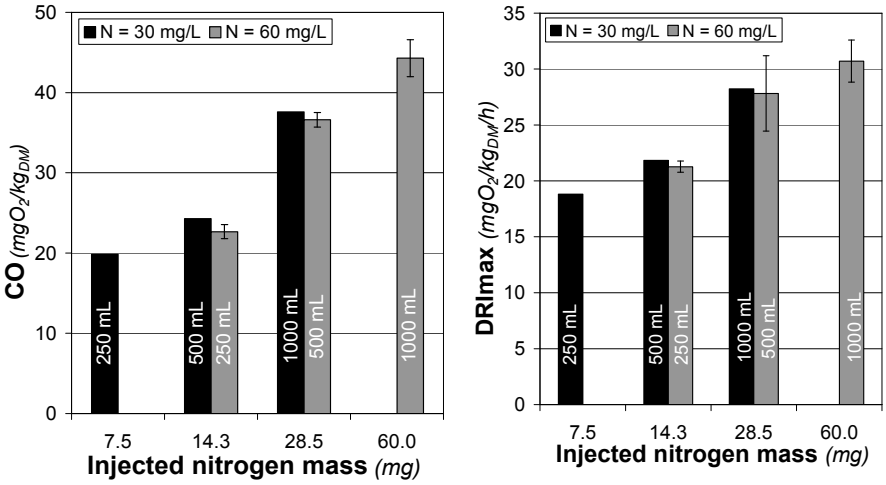


Figure 4B.4: *CO* (left) and *DRImax* (right) measured for different batches loaded with different nitrogen load

For a given injected nitrogen mass of 14.3 and 28.5 mg N, the $CO(t_F)$ and the DRI_{max} remain rather constant and independent of the injected volumes or the nitrogen concentrations that was applied. No differences were observed for different injected volumes. Also, no influence of the hydraulic retention time was observed. Only the injected nitrogen mass had an impact on $CO(t_F)$ and consequently on the nitrification rate. No influence of the hydraulic retention time was measured. Further investigations are presented in section 4B.3.1.iv.

When the injected volume increased from 250 to 500 mL, and from 500 mL to 1 L, for a given nitrogen concentration (30 or 60 mg NH_4-N/L), the $CO(t_F)$ and the DRI_{max} increased by 20 to 50 %, while the injected mass of nitrogen doubled. Similar observations were carried out when the nitrogen concentration increased from 30 to 60 mg NH_4-N/L for a given injected volume of water (250, 500 or 1000 mL). Thus we can conclude that the increase was not proportional to the injected volume or to the NH_4-N concentration, probably due to a limitation in the mixture coming from the oxygen transfer or due to the hydraulic retention time.

4B.3.1.ii. Impact of adding "ammonium-free" water, and subsequent water containing ammonium

Figure 4B.5 presents the mass of nitrate nitrogen (NO_3-N) and ammonium (NH_4-N) released in the percolates, when successive 1 L batches were applied to a respirometric reactor. Six batches of ammonium-free water (tap water) were first applied, and then four batches of water containing ammonium and bicarbonate were injected. The nitrified mass calculated from $CO(t_F)$ (conversion with 4B.2.2.ii) is also shown.

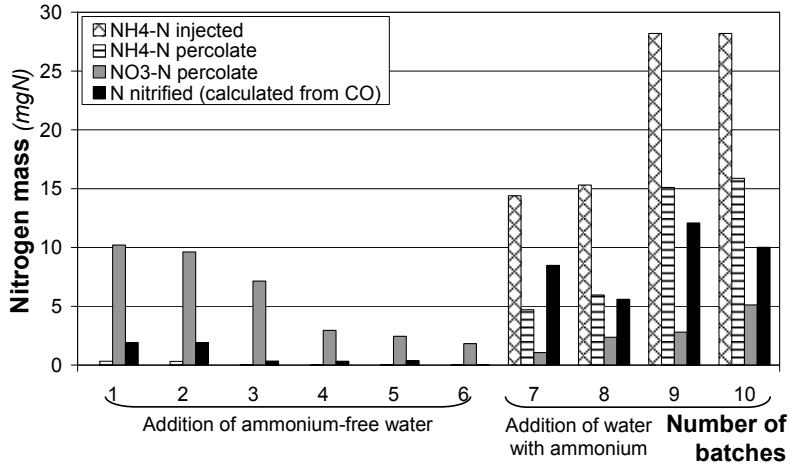


Figure 4B.5: NH_4-N, NO_3-N and equivalent *CO* measured (mgN) for the successive addition of water with or without ammonium

As the number of applied batches without ammonia increased, we measured a release of nitrates. The individual mass of nitrates decreased from 10 mg NO_3-N (batches 1 and 2) to 2 mg NO_3-N (batches 5 and 6). At the same time, a small release was measured for ammonium (0.3 mg N for batches 1 and 2, and almost no release for the others). The nitrified mass, calculated from *CO*, decreased from 2 mg N, for batches 1 and 2, to 0.1 mg N for batches 5 and 6. When batches of water containing ammonium were applied, subsequently after batches with ammonium-free water, a storage process of nitrogen occurs through the reactor for an amount of 2 to 5 mg N per batch, varying in terms of the injected mass. Indeed, a removal of 10 mg NH_4-N occurred for batches 7 and 8, and 15 mg NH_4-N for batches 9 and 10 (NH_4-$N_{injected}$-NH_4-$N_{percolate}$). Though, the released mass of nitrates was about 2 and 5 mg NO_3-N for batches 7 to 10. The nitrified mass (calculated from *CO*) was between 5 and 10 mg N. Consequently, depletion and then storage of nitrogen are two processes that disturb the measurement

of the nitrification rate in the biofilm. The application of successive batches of water containing nitrogen only is thus studied in the following paragraph.

4B.3.1.iii. Impact of adding only water containing ammonium (no previous ammonium-free water)

Figure 4B.6 presents the results obtained with six successive 1 L batches of water containing ammonium and bicarbonate, with no previous addition of ammonium-free water. Water contained in the material porosity was not considered because injection and percolate volumes were similar.

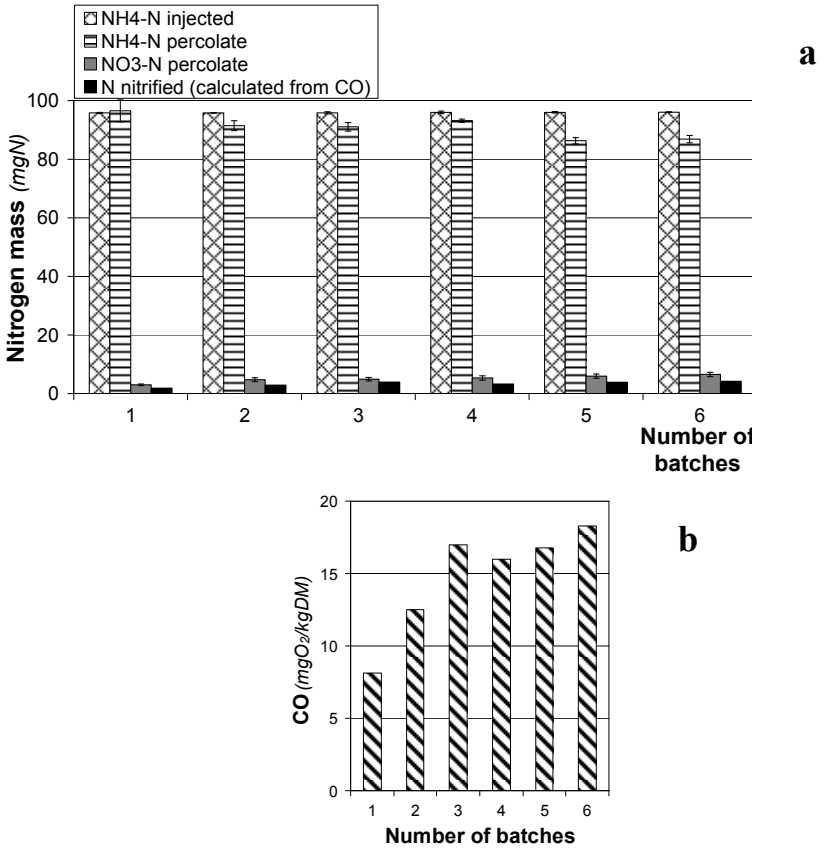


Figure 4B.6: (a) Mass of NH_4-N (injected and released), NO_3-N (released), nitrified nitrogen (mg N) and (b) *CO* measured for the successive addition of water with ammonium

As the number of injections increased, we observed a decrease in the mass of nitrogen released through the percolates from 95 to 87 mg NH_4-N. At the same time, the released mass of NO_3-N increased from 1 to 6 mg NO_3-N, and the nitrified mass (calculated from *CO*) increased from 1 to 5 mg N. In this protocol where water containing ammonium was used, we did not observe a storage of nitrogen during the injections. We still observed a difference of 1 mg N between the nitrates produced and the oxygen consumed by nitrification. This is in accordance with the accuracy of the respirometric method and chemical analysis.
The $CO(t_F)$ increased from 7 to 17 mg O_2/kg DM for the batches 1 to 3, and remained almost constant, approximately 17 ± 2 mg O_2/kg DM for batches 3 to 6 (Figure 4B.6, b). This observation suggests that a saturation was reached of the nitrogen stock in the biofilm, after application of at least four batches. However, the application of water containing ammonium, after previously cleaning the organic matter from CW with "ammonium-free" water, would require more than four batches to restore the depleted nitrogen stock.

4B.3.1.iv. Influence of the injected nitrogen mass

Figure 4B.7 presents the values of mean and relative deviation of the specific oxygen uptake rate ($R_{S,max}$, [mg O_2/kg DM/h]), determined for five injected nitrogen masses in the range 8 to 90 mg N (noted *LoadN*, [mgN]). These values were obtained after applying four 1L batches of water containing ammonium.

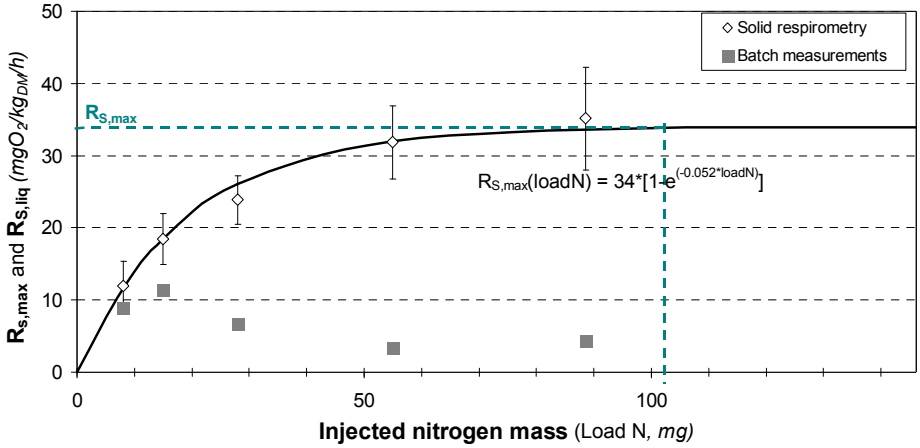


Figure 4B.7: $R_{S,\,max}$ and $R_{S,liq}$ measured at different injected nitrogen mass for a colonized gravel sample

The maximum oxygen uptake rate ($R_{S,\,max}$) increased as the injected nitrogen mass increased. We observed that the uptake rate reached an approximate constant value of 34 mg O_2/kg DM/h, that represents 41 mg O_2/L/h. Thus, the maximal nitrification rate of the sample of colonized gravel was reached in such conditions (no oxygen limitation, 20°C). A logarithmic regression was performed using Eq. 4B.7.

$$R_{S,\max}\left(loadN\right) = R_{S,\max}.\left[1 - e^{\left(-k_{Rv\max}.loadN\right)}\right] \qquad \text{[Eq. 4B.7]}$$

with $R_{S,\,max}$ the maximal oxygen uptake rate [mg O_2/kg DM/h], $k_{Rv\,max}$ the rate coefficient [1/mg N], and *loadN* [mgN] the injected nitrogen load. The following parameter values were estimated from this regression: $R_{S,\,max}$ = 34 mg O_2/kg DM/h and k_{Rvmax} = 0.052 /mg N.

For further experimentations, we can chose to apply an injected nitrogen mass of 100 mg N to work at the conditions of the maximum level of nitrification rate, which corresponded to 40.8 g N/g DM injected.

4B.3.2.Evaluation of the proposed method

4B.3.2.i. Comparison with a conventional method

Nitrification rates obtained with the proposed solid respirometry ($R_{S,max}$) were compared to batch measurements carried out by immersing the detached biofilm in liquid conditions ($R_{S,liq}$) (see section 4B.2.2.iv.). As shown in Figure 4B.7, the results of liquid conditions were located between 3 to 11 mg O_2/kg DM/h. A difference with the solid respirometry method of 5 to 30 mg O_2/kg DM/h was obtained, suggesting that nitrifying biomass reacts differently. It was supposed that the mechanical detachment of the biofilm from gravel did not damage nor stress the biomass cells and did not affect their nitrification rate. When partially saturated conditions were regularly applied, we thus suggest that the solid respirometry was more appropriate for assessing the nitrification rate in such systems. However, the solid respirometry was much more complex to implement. In addition, the use of nitrates produced and released through the percolates did not improved results either, due to the depletion and storage phenomenon.

4B.3.2.ii. Comparing existing literature values

In order to discuss our results, the values of maximum specific nitrification rates ($R_{S,max}$, [mg O_2/DM/h]) were converted into volumetric rates ($R_{V,max}$, [mg O_2/L_{sample}/h]), that were compared to literature values in Table 4B.2.

Table 4B.2: Comparison of $R_{V,\,max}$ to literature values [mg O_2/L_{sample}/h]

Method of $R_{V,\,max}$ measurement	**Solid respirometry** (partially saturated conditions)	**Nitrates production rate** (batch liquid conditions)	**Respirometry**[*] (liquid conditions)	**Simulations**[**]
Source	(this study)	(this study)	(Andreottola *et al.*, 2007)	(Langergraber and Šimůnek, 2005)
Results	32-50 (mean = 41) (SD = 9; 2 values)	13 – 25 (mean = 19) (SD = 6; 5 values)	1.8	30.5

[*] respirometric method applied to the liquid passing continuously through a colonized filtering column (Andreottola *et al.*, 2007)

[**] calculated with a conversion of the predicted autotrophic biomass concentration (150 mgCOD/L once HYDRUS/CW2D was calibrated by inverse modelling with inflow/outflow pollutants fluxes of a VFCW) using the values of $\mu_{A,\,max}$ and Y_A (Langergraber and Šimůnek, 2005).

We observe that the maximum nitrification rate evaluated from the solid respirometric technique differed considerably with the results published by Andreottola *et al.* (2007) of 1.8 mg O_2/L_{sample}/h. Notwithstanding the injected nitrogen amount was almost similar (90 mg), the respirometric method, carried out by Andreottola *et al.* (2007), involved passing liquid continuously through a colonized filtering column. On the contrary, our results are consistent with the maximum nitrification rate proposed by Langergraber and Šimůnek (2005) of 30.5 mg O_2/L_{sample}/h. They obtained maximum nitrification rates from inverse modelling with the HYDRUS-CW2D model, which used inflow/outflow pollutant fluxes from a VFCW.

4B.3.3. Determining the concentration and the maximum growth rate of autotrophic biomass

Table 4B.3 presents the maximal volumetric nitrification rate ($R_{v,max}$) obtained with the solid respirometric technique applied to the samples collected and prepared as described in section 4B.2.3.i. For the sludge layer (1st layer, ρ_1= 187 g DM/L_{sample}), a maximum volumetric nitrification rate of 16.3 g N/L_{sample}/h was obtained. For the colonized gravel (2nd layer, ρ_2= 114 g DM/L_{sample}), a maximum volumetric nitrification rate of 21.7 g N/L_{sample}/h was obtained. Assuming a negligible nitrification rate for the deep layer of the VFCW, we calculated a global volumetric value $R_{V,\,max}$ of 19.5 g N/L_{sample}/h, from the two individual values weighted by the thickness of the two layers (section 4B.2.3.ii.).

Table 4B.3: Maximum nitrification rate ($R_{v,max}$), concentration (C_{XA}), fraction released by treated effluent and maximum growth rate ($\mu_{A,max}$) for the autotrophic biomass

Layers	□ [g DM /L_{sample}]	$R_{v,max}$ [g N /L_{sample}/h]	C_{XA} **in reactor** [mg $COD_{biomass}$ /L_{sample}]	C_{XA} **in treated effluent** [mg $COD_{biomass}$ /L] *(Fraction of the mass contained in reactor)*	$\mu_{A,max}$ [1/h] *(1/d)*
Overall VFCW	143	19.5	123**	0.04 *(0.2 %)*	0.037 *(0.88)*
1st layer (h_1= 20 cm sludge)	187	16.3	103***	-	-
2nd layer (h_2= 30 cm colonized gravel)	114	21.7	137***	-	-
3rd layer (h_3= 30 cm clean gravel)	negligible	negligible	negligible	-	-

Dashed line when no value was determined

* wet density of pure submerged biofilm is 1 kg/L (i.e. density of water) (Vigne *et al.* , 2010). ρ includes the biofilm concentration in each layer, that is to say the concentration of dry matter once it was get rid off of dead leaves, roots

** calculated according to 4B.2.3.iii. with mass balance

*** calculated with the value of $\mu_{A,max}$ and the individual values (each layer) of $R_{v,max}$ (Eq. 4B.4)

A negligible biomass concentration of 0.04 mg $COD_{biomass}/L$ released in the treated effluent was determined (calculated from BCOD and TSS concentrations of the effluent (Stricker, 2000)). This represented only 0.2 % of the amount of autotrophic biomass stored in the VFCW. This level was very low compared to the usual values in treated water released by the activated sludge process (Feray *et al.*, 1999; Vigne *et al.*, 2010). A value of 123 mg $COD_{biomass}/L_{sample}$ was obtained for the global autotrophic biomass concentration (C_{XA}) in the filter according to the method presented in section 4B.2.3.ii.

The maximum growth rate coefficient ($\mu_{A,\ max}$) was calculated, using the approach presented in section 4B.2.3.iv. A value of 0.037 h^{-1} (i.e. 0.88 d^{-1}) was obtained. This value is in accordance with usual values used for modelling of activated sludge process as reviewed by Choubert *et al.* (2009). Consequently, the concentration in autotrophic biomass in the two first layers of the VFCW was estimated to be 103 and 137 mg COD/L_{sample}, respectively. Therefore a comparison with the predicted values of the HYDRUS-CW2D model could be carried out. These values are very close to the values of 110 g $COD_{biomass}/L_{sample}$ predicted by Langergraber and Šimůnek (2005) with the CW2D model.

4B.4. Conclusions

A novel respirometric tool was developed and applied to measure the nitrification rate in partially saturated, porous samples, collected from a VFCW, composed of sludge and colonized gravel. The best operating conditions for injecting liquids (volume, composition) were studied. The use of ammonium-free water before injecting water containing ammonium led to a depletion of the nitrogen storage in the initial system and impeded correct nitrification rate measurements. The use of water containing ammonium only led to equilibrating the depletion/storage phenomenon. The comparison with liquid batch experiments indicates that the solid respirometry was more appropriate for the partially saturated conditions and was therefore closer to the conditions of their original medium. The method was compared to some conventional protocols and literature data. As compared to protocols using liquid conditions, the data were found to be more appropriate to fit within the range of simulated maximum nitrification rates reported in the literature. Indeed the autotrophic concentrations were closer to the values given by simulation once calibrated by inverse modelling with inflow/outflow pollutant fluxes of a VFCW. Then, the protocol was successfully applied to obtain the parameters of the autotrophic biomass of a VFCW. A value of

maximum growth rate similar to the value of activated sludge process was determined. With this respirometric system it was pointed out that the maximum autotrophic growth rate from activated sludge process can be directly used in the modelling of VFCW. As the temperature can be controlled during respirometric essays, increasing or reducing it should allow assessing the maximum nitrification rate under other temperatures. Finally, we conclude that data provided with the solid respirometer are appropriate for a finer calibration of models of constructed wetlands.

Chapter 5

Nitrogen removal modelling in the first stage of a French-type vertical flow constructed wetland with CW2D: ability and limits*

Abstract

CWs are attractive system for waste water treatment for small communities, but the removal processes are often badly understood. Modelling of CW systems is a way to unravel the pollutant removal processes in the CW and improve their design. A study was carried out on a French vertical flow constructed wetland (VFCW) system. The observed laboratory and field data were processed with a multi-component reactive transport module (CW2D) to simulate the conversion processes occurring in the operational VFCW system. Particular attention was devoted to the nitrogen fate and cycling processes (nitrification, adsorption, and denitrification). During a feeding period (3.5 days), influent and effluent concentrations were measured (COD, NH_4-N, NO_3-N) as well as in-situ concentrations of microorganisms and oxygen contents. Measured and simulated concentrations were compared. Some initial CW2D kinetic parameters for modelling wastewater treatment were modified and adapted to the specific treated wastewater and the sludge layer. Simulation results showed that the model agreed with measured data and the best results were achieved with a high nitrogen adsorption coefficient. Finally, some proposals are presented to improve the quality of modelling using the process based model.

*Adapted from: Morvannou, A., Choubert, J-M., Vanclooster, M. and Molle, P.
Nitrogen removal modelling in the first stage of a French vertical flow constructed wetland
– *In preparation*

5.1. Introduction

Mechanistic models allowing to describe the fate and transport of water, solutes, heat and chemicals in artificial CW are nowadays becoming available and may become excellent engineering tools for CW design and control. One of these models is HYDRUS/CW2D (Langergraber and Simunek, 2005). Many modelling studies carried out with HYDRUS concerned natural soils (Jacques *et al.*, 2005, 2008; Jiang *et al.*, 2010) and most of them on water flow during rainfall events (Dittmer *et al.*, 2005; Zhang *et al.*, 2010). Only a few of the HYDRUS studies dealt with the analysis of domestic wastewater treatment systems (Langergraber and Simunek, 2005; Toscano *et al.*, 2009) and none dealt with the specific French VFCW system, as designed by Molle *et al.* (2003). Hence the validation status of HYDRUS/CW2D is currently still poorly described.

The objective of the present work is to evaluate the ability of the HYDRUS/CW2D model to predict carbon and nitrogen concentrations in the effluent of a VFCW treatment. The novelty of the wok consists of the calibration for a VFCW filled with gravel fed with raw wastewater, whereas the available knowledge is only available for VFCW filled with sand and fed by primary treated effluent. To reach a good agreement between predicted and observed values, a specific strategy was developed. It combined data collection at full-scale VFCW plant (raw and treated wastewater) and investigations at a laboratory scale with chemical analyses of autotrophic biomass characteristics (Morvannou *et al.*, 2011).

5.2. Material and methods

5.2.1. The VFCW plant

The Evieu wastewater treatment plant (Ain, France) comprises a sequence of vertical (first stage VF) and horizontal (second stage, HF) subsurface flow constructed wetlands (CW). The plant has been in operation since 2004, and currently 100 PE are connected. The first stage is made up of three units of VFCWs receiving raw wastewater. Each filter was fed according to a feeding/rest period of 3.5/7 days. We studied one of the filters of the VF stage (28 m², 2.9 m wide and 9.7 m long) that was designed according to French recommendations. Eight batches per day were applied. A more complete description of the studied VFCW was presented in Chapters 2 and 3.

5.2.2. Strategy of sampling and analysis

A sampling and measurement campaign was carried out from 26 to 29 April 2010 using online and offline measurements to collect data for comparison with simulation results. Each day of the 3.5 day-feeding batch period, two batches were particularly monitored (raw and treated effluents) with sampling and chemical analysis; all other batches were monitored with samples (raw wastewater) and online sensors (treated wastewater). Figure 5.1 indicates locations where measurements and samplings were carried out. Table 5.1 summarizes analyses made on raw wastewater and on effluent samples.

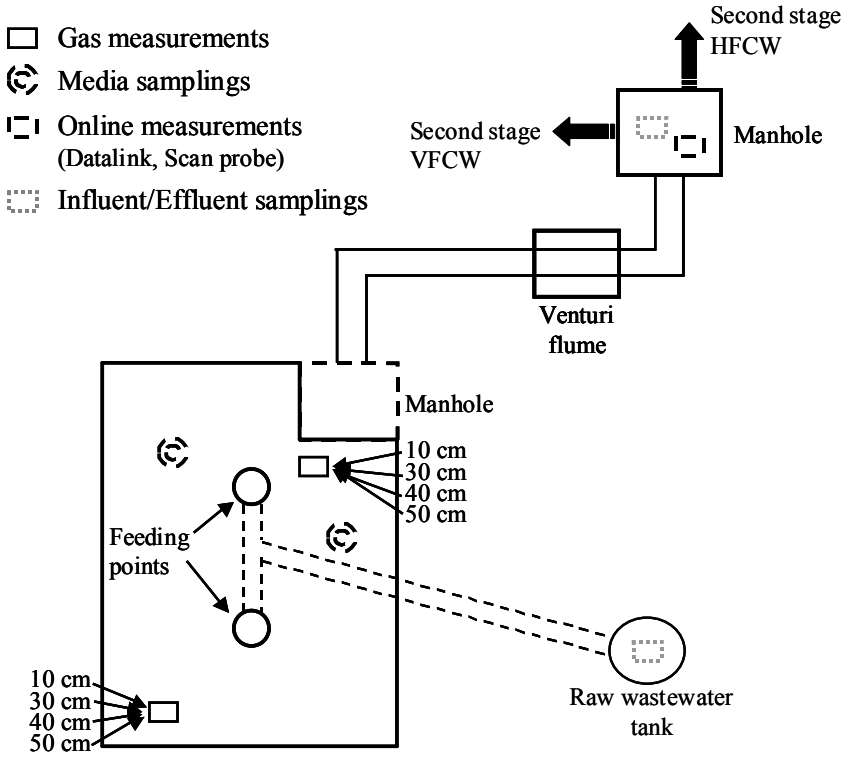


Figure 5.1: Scheme of the studied VFCW, locations of measurements and sampling points (not on scale)

Table 5.1: Analyses carried out on raw wastewater and VFCW effluent samples

	Raw wastewater	Outflow
Online measurements	-	$COD_{raw,filtered}$ / NH_4-N / NO_x-N
Offline measurements	$COD_{raw,filtered}$ / NH_4-N / KN / PO_4-P / TSS	

5.2.2.i. Offline analysis

Concentrations of raw wastewater for each batch during the feeding period

An automatic sampler cooled at 4 °C, containing 24 sample bottles (containers) of 1 L, was installed at the entrance of the VFCW (Figure 5.1) to determine the composition of the raw wastewater. Sampling was carried out only when batch feeding started. The containers were replaced every day. An average flow proportional composite sample was also set-up by mixing a fraction of the content of the eight daily batches that were sampled.

Chemical analyses (APHA, 2005) were carried out on the samples on each individual batch and onto the 24h-flow proportional sample, in order to assess the VFCW efficiency for the following parameters: chemical oxygen demand (COD), total and filtered (0.7 µm), phosphorus (PO_4-P), total suspended solid (TSS), Kjeldahl nitrogen (KN) and ammonium nitrogen (NH_4-N); (NOx-N were verified equal to zero at the inlet).

COD fractions of raw wastewater

This procedure aims at dividing the total COD of raw wastewater into six different variables as defined for ASM1 (COD fractionation) characterized by their aptitude for being rapidly (CR)/slowly biodegraded (CS), by heterotrophic (XH)/autotrophic (XA) biomasses, inert soluble (CI)/particular (Xi) (Henze *et al.*, 1987). From the automatic sampler located at raw wastewater, four samples were taken at various times of the day (morning 08:22; midday 13:30; evening 19:58; and night 00:01). It was possible thus to determine the variations of the COD fractions versus time, during a 24h-period.

Total COD was first determined for each sample using standardized chemical analysis (APHA, 2005). Then the biological method with BOD-tests (Roeleveld and Van Loosdrecht, 2002) was applied to determine the biodegradable COD fraction (BCOD) defined as CR+CS. Finally the physicochemical method with coagulation and 0.7 µm filtration (Mamais *et al.*, 1993) was applied to determine the soluble fraction (COD_{cf}) defined as CR+CI. CI fraction was determined by measurement of the filtered 0.7 µm COD in the effluent leaving the entire process of Evieu plant: a concentration of 30 $mg.L^{-1}$ was assigned (quantification limit).

Assuming that no biomass was present in wastewater (Henze *et al.*, 2000; Pasztor *et al.*, 2009), total COD (COD_{total}) was the sum of the other fraction concentrations (Eq. 5.1), the different fractions can be calculated as presented in Eq. 5.2 to 5.4:

- $COD_{total} = CR + CS + CI + Xi$ [Eq. 5.1]
- $CR = COD_{cf} - CI$ [Eq. 5.2]
- $CS = BCOD - CR$ [Eq. 5.3]
- $Xi = COD_{total} - BCOD - CI$ [Eq. 5.4]

Gas measurements

Oxygen and carbon dioxide contents were measured within the gaseous phase of the filter each day (DrägerSensor XS), one hour after the two particularly monitored batches. Gases were pumped at four different depths (10, 30, 40 and 50 cm) at two places into the VFCW (at 1 and 2 m of the feeding points, see Figure 5.1). Before the beginning of the campaign a measurement of the initial gas content was carried out in order to monitor the renewal of oxygen and the carbon dioxide released during the campaign. Results are expressed in percent of the air phase ±0.2 % (oxygen saturation in air being 21%).

Autotrophic biomass concentration assessment

The solid respirometric technique was applied to samples of sludge deposit and colonized gravel collected 4 rest days after the sampling campaign. They were shovelled up at two locations of the VFCW. Hence, one sample was collected for each 15 m^2 of VFCW. Both sampling points were located at 2 m of the feeding point. Solid respirometry was used to determine the maximum growth rate and the concentration for the autotrophic biomass as published by Morvannou *et al.* (2011).

5.2.2.ii. Online recording

The inflow rate was measured recording the pump functioning time (previously calibrated), and the outflow continuously recorded with a flowmeter (ISCO bubble type) that equipped the Venturi flume. TDR probes installed within the filter were used to monitor the water content within the VFCW (Chapters 2 and 3).

After the flume a manhole allowed collecting the effluent from the VFCW (Figure 5.1). Several on-line analyses were carried out:

- Ammonium concentrations were determined with an on-line analyzer (Datalink intruments AM200 France) every five minutes;
- COD (total and filtered) and NOx-N were determined with an on-line UV-vis probe (S::can Messtechnik, GmbH, Vienna Austria) every one minute (Rieger *et al.*, 2004). Specific calibration based on partial least-squares (PLS) regression (Aji *et al.*, 2003) was carried out using grab samples taken during the experiment (26 for NOx-N, 18 for total COD and 26 for dissolved COD).

During the campaign, for each daily monitored batches, grab samples were taken at 5, 10, 15, 25, 35 and 45 minutes after the batch end in order to check the correlation between the on-line analyzer data and the reference laboratory data.

5.2.3. Conceptual dynamic model CW2D and simulations of the VFCW behavior

The simulation software used was HYDRUS/CW2D version 1.11 (Simunek *et al.*, 1999; Langergraber and Simunek, 2005). The model was applied to model and better understand the biochemical reactions occurring within the Evieu VFCW plant. The model study was designed to better predict carbon and nitrogen concentrations in the effluent. The large setup installed on the Evieu plant, as well as the laboratory-scale experiments allowed to monitor the concentrations inside the VFCW and in the filter effluent.

An important feature is the dynamic multi-component reactive CW2D model to simulate the VFCW from detailed wastewater characteristics and specific off-line protocols. This model, represented in Figure 5.2, integrates the main physical and biological mechanisms occurring in VFCW systems: it considers different phases (solid, immobile and mobile water, and air) involved for one filter layer, as well as processes predicted through the layers. A total amount of 46 parameters is needed for the CW2D model.

Spatial representation. Four horizontal layers were differentiated (from top to bottom): the sludge deposit (layer 1, 00-0.20 m), highly colonized gravel by biofilm (layer 2, 0.20-0.415 m), colonized gravel by biofilm (layer 3, 0.415-0.605 m) and a drainage layer practically exclusively composed of gravel (layer 4, 0.605-0.80 m), the whole forming a 2D-space of 0.80 m

height and 10 cm width. The two-dimensional mesh used for simulations consisted of 305 nodes and 480 parametric triangular finite elements.

Hydraulic model (24 parameters). The hydraulic behavior of the Evieu VFCW was carried out thanks to a multi-tier approach (Chapter 2).

Oxygen transfer (2 parameters and 4 parameters for temperature dependency). The oxygen re-aeration rate applied to the biofilm was maintained constant along the simulation. The temperature was fixed to 20 °C and the saturation concentration of oxygen was equal to 9.18 $mg.L^{-1}$.
Biofilm (8 composition parameters concerning the nitrogen and phosphorus contents of the organic matter and biomass). All micro-organisms are assumed to be attached (immobile) to the solid phase. The CW2D model further assumes that the organic matter is present only in the aqueous phase and that the reaction products are immediately consumed and released in this aqueous phase (mobile phase). The biofilm thickness and its evolution through the time are not considered. In addition, the modifications of hydraulic properties mainly due to biomass growth are not considered.

Biological conversion of substrates (6 stoichiometric + 26 kinetic parameters). Nutrients assimilated by plants are neglected in CW2D model. Biological conversion is considered through nine biokinetic processes. They consist of Monod-type ASM-like equations (Langergraber and Simunek, 2005) and rule hydrolysis of organic matter, conversion of organic matter, conversion of ammonium into nitrites and nitrates, denitrification (using nitrite and nitrates) and microorganisms decay. Moreover, chemical adsorption/desorption are considered for ammonium and inorganic phosphorus (linear or Freundlich type) and the adsorption rate can be specified. For each layer, twelve variables are calculated: 9 for the liquid phase (O_2, CR, CS, CI, NH_4-N, NO_2-N, NO_3-N, N_2-N, and IP) and 3 for the solid phase (heterotrophic biomass (XH) and two autotrophic biomasses, (XANs and XANb).

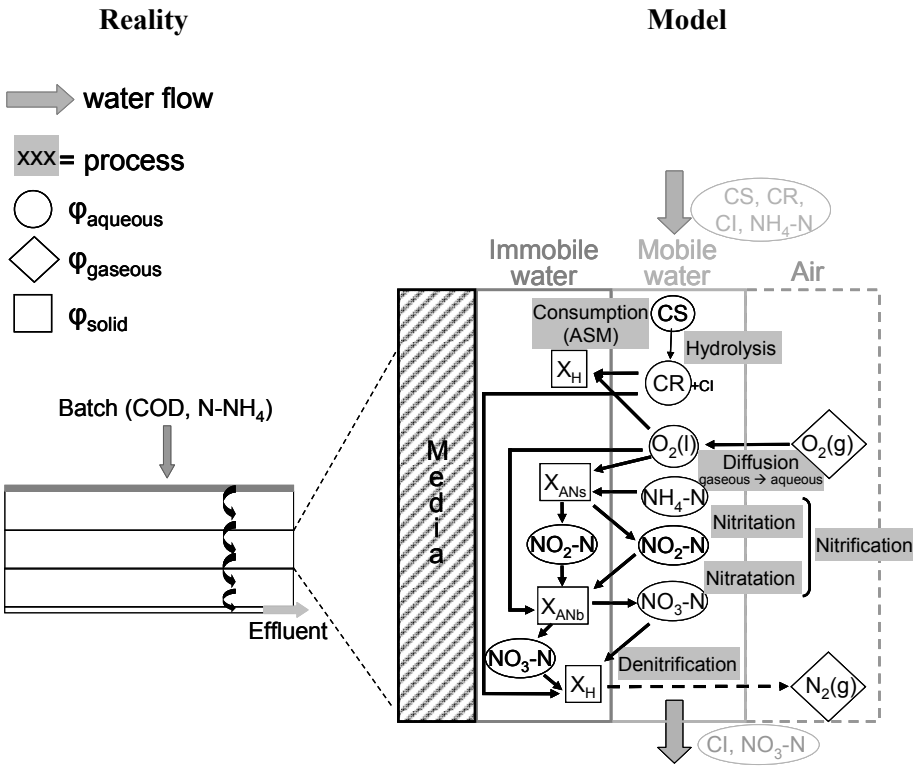


Figure 5.2: Scheme of VFCW layers phases, compounds and processes predicted by CW2D (Adapted from Langergraber and Simunek, 2005)

5.2.4. Calibration strategy and simulations

COD fractions and particularly nitrogen compounds outflow concentrations during the monitoring period were simulated using the HYDRUS/CW2D model according to the calibration loop presented in Figure 5.3.

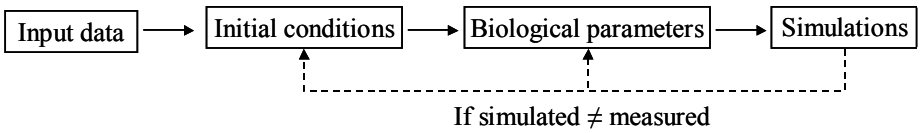


Figure 5.3: Various stages to calibrate CW2D (Adapted from Delrue *et al.*, 2010)

The CW2D model considers two autotrophic biomasses (Figure 5.2) but in this study, no distinction was made between the two autotrophic micro-organism populations. Similar values were used for their concentrations and their biological parameters values (kinetics and stoichiometric).

5.2.4.i. Input data

In addition to instantaneous water flow, the composition of the wastewater (COD fractions, nitrogen compounds and phosphorus concentrations) was given for each batch applied to the VFCW. COD fractions, CR, CS and CI concentrations were calculated from the fractions obtained with the method presented previously. Concentrations of organic compounds (nitrogen, phosphorus) are predicted as part of the particulate COD. We assumed that the concentration in nitrates, oxygen and biomasses were negligible in raw wastewater when compared to the amount present in the VFCW (Henze *et al.*, 2000).

5.2.4.ii. Initial and boundary conditions

Initial conditions were imposed (oxygen) or assessed either with the concentrations measured with the off-line measurements: concentrations in the treated water and concentrations of autotrophic biomass in the VFCW. Table 5.2 presents initial conditions considered.

Table 5.2: Initial conditions for simulations

O_2 ($mg.L^{-1}$)	COD fractions ($mg.L^{-1}$)	NH_4-N and NO_3-N ($mg.L^{-1}$)	XH ($mg_{COD}.L^{-1}$)	XAN ($mg_{COD}.L^{-1}$)
Saturation in the whole VFCW	- CR = 60 in the whole VFCW - CS = 60 in the whole VFCW - CI = 30 in the whole VFCW	Distribution in all layers according to **outflow concentrations** measured during the four first batches No sorbed ammonium was initially considered in the VFCW	Calculated from BCOD (270 $mg.L^{-1}$) of the raw wastewater and TSS concentrations of sludge deposit (20 %DM and 70 %VM) after four days of rest, fraction of biomass = 0.15 (Stricker, 2000); distributed between: - 80 % XH for layer 1 - 20 % XH for layers 2, 3 and 4	Respirometric experiment: Layer 1 : 103 Layer 2 : 137 No XAN were considered for layers 3 and 4

Cauchy boundary conditions at the VFCW top and bottom were applied: the component flux through the system boundaries is calculated according to the load. This boundary condition is equivalent to specify a solute flux limited by a concentration.

5.2.4.iii. Simulations

Following the concept suggested in Figure 5.3, various simulations were carried out with biological parameters modified from the parameters initially included in the CW2D model, based on the comparison between measured and simulated outflow concentrations (trial-and-error strategy). To represent the conversion and transformation processes, 46 parameters are needed and some of them were modified in order to have a better match between simulated and measured data: the maximum aerobic growth rate assessed with solid respirometry experiments and valid for the two autotrophic microorganisms types, the saturation/inhibition coefficient for oxygen during the denitrification process (if the oxygen contents and nitrate outflow concentrations were too low and too high respectively), the oxygen re-aeration rate (when the nitrification process was underestimated) and

adsorption parameters for ammonium. In a simple approach the linear adsorption isotherm was used.

Simulated concentrations were compared with measured concentrations for filtered COD, ammonium and nitrate in the effluent. The comparison was carried out in terms of average concentrations, weighted with the outflow calculated for each batch. Into the VFCW, comparison between measured and simulated values was carried out for the concentration of autotrophic microorganisms and the oxygen contents. As these latter were measured in the gaseous phase, dissolved oxygen contents provide by CW2D were simply converted into gaseous oxygen contents thanks to the Henry's law at 20 °C.

The average difference between simulated and measured concentrations, the mean absolute error (MAE, Eq. 5.5) and the mean absolute relative error (MARE, Eq. 5.6) were calculated for each variable and each scenario as defined in Hauduc *et al.* (2011).

$$MAE = \frac{1}{n}\sum_{i=1}^{n}\left|X_{simulated} - X_{measured}\right| \qquad \text{[Eq. 5.5]}$$

$$MARE = \frac{1}{n}\sum_{i=1}^{n}\frac{\left|X_{simulated} - X_{measured}\right|}{X_{measured}} \qquad \text{[Eq. 5.6]}$$

with, $i = 1{:}n$, the number of average concentrations (i.e. n = 23); $X_{simulated}$ and $X_{measured}$ [mg.L^{-1}], the average simulated and measured concentrations, respectively.

We calculated the assimilated, nitrified, adsorbed, denitrified nitrogen fluxes, as well as ammonium and nitrate fluxes removed from the VFCW for the feeding and the total (feeding and rest) periods.

- From the equation used in the CW2D model (Eq. 5.7) we calculated the nitrified nitrogen flux for each layer and each time step. The reactive liquid volume was fixed to the maximal water content for each layer, calculated from the dry bulk and particle densities (100.0 % for layer 1, all the volume participating to the nitrification process, 40.6 % for layers 2 and 3, and 44.0 % for layer 4).

$$\frac{d\phi NH_4 - N}{dt} = \frac{dNH_4 - N}{dt} \cdot V_{layer} = \frac{\mu_{A-\max}}{Y_A} \cdot c_{XA} \cdot \frac{c_{O_2}}{K_{AN,O_2} + c_{O_2}} \cdot \frac{c_{NH_4}}{K_{AN,NH_4} + c_{NH_4}} \cdot \frac{c_{IP}}{K_{AN,IP} + c_{IP}} \cdot V_{layer} \qquad \text{[Eq. 5.7]}$$

with $\mu_{A,\ max}$, [min^{-1}], the maximum growth rate; Y_A, [$mg_{COD,BM}/mg_{NH4\text{-}N}$], the cellular yield; C_{O2} [$mgO_2.L^{-1}$], the oxygen concentration; C_{NH4}, [$mg_N.L^{-1}$], the ammonium-nitrogen concentration; C_{IP}, [$mg_P.L^{-1}$], the inorganic phosphorus concentration; C_{XA}, [$mg_{COD}.L^{-1}$], the biomass concentrations; $K_{AN,O2}$, [$mg_{O2}.L^{-1}$] the saturation/inhibition coefficient for oxygen; $K_{ANs,NH4}$, [$mg_{NH4}.L^{-1}$], for nitrogen; $K_{ANs,IP}$, [$mg_{IP}.L^{-1}$], for inorganic phosphorus; and V_{layer} [L], the liquid volume of each layer.

The total nitrogen mass nitrified was calculated considering the sum of the nitrified ammonium mass of the four layers.

- The denitrified nitrogen mass was calculated from the nitrified nitrogen mass and the nitrate mass removed from the VFCW: $M_{denitrified} = M_{nitrified} - M_{nitrate\text{-}outflow}$

- The assimilated nitrogen mass was calculated from the BOD_5 mass removed. It was assumed that the assimilated nitrogen mass represents 5 % of the mass of BOD_5 removed (Henze *et al.*, 1996; Choubert *et al.*, 2008, exposed in 1.2.4.iii);

- The adsorbed nitrogen mass was calculated from the incoming KN mass, the nitrified, the assimilated nitrogen masses and the ammonium mass removed from the VFCW: $M_{adsorbed} = M_{KN\text{-}in} - M_{assimilated} - M_{nitrified} - M_{ammonium\text{-}outflow}$. It means that $KN_{particular}$ in the effluent was considered to be negligible. Molle *et al*. (2005) noticed that the percentage of N in the SS of sewage is about 5 % and about 0.7 % in the sludge deposit, the KN removal observed is assumed to be due to nitrification only. Nitrate assimilation can also be neglected. Moreover, in this approach no nitrate adsorption was considered.

To evaluate the simulation and the model robustness, simulated final values achieved at the end of the rest period were used as initial values in order to simulate a new feeding period. Biological parameters were unchanged from the first simulation. As, no measurement was specifically carried out, this simulation attempt was called “fictive” campaign, but the results were compared to the previous measurements, considering that the system operates in a pseudo-permanent regime.

5.3. Results and discussion

5.3.1. Input data

5.3.1.i. Individual concentrations

Table 5.3 presents the average concentrations and standard deviations of the various components arriving on the VFCW for the 3.5 feeding days (28 individual batches).

Table 5.3: Average concentrations and standard deviations ($mg.L^{-1}$) of the components contained in the raw wastewater applied to the VFCW for the 3.5 feeding days (28 samples)

Influent	Hydraulic load ($m.d^{-1}$)	COD_{raw} ($mg.L^{-1}$)	$COD_{filtered}$ ($mg.L^{-1}$)	KN ($mg.L^{-1}$)	NH_4-N ($mg.L^{-1}$)	PO_4-P ($mg.L^{-1}$)	TSS ($mg.L^{-1}$)
Average	0.46	493	223.8	78.2	63.5	5.0	193
SD	0.12	69.5	44.5	10.0	7.7	0.2	56.7
Max/Average ratio(daily scale)	1.24	1.3	1.3	1.1	1.3	1.0	1.7
Number of values	3	28	21	8	28	2	28

Effluent	Outflow ($m^3.d^{-1}$)	COD_{raw} ($mg.L^{-1}$)	$COD_{filtered}$ ($mg.L^{-1}$)	NOx-N ($mg.L^{-1}$)	NH_4-N ($mg.L^{-1}$)
Average	62.2	95.2	67.1	29.4	15.9
SD	49.1	28.9	9.1	11.5	10.1
Number of values	4490	4490	4490	4490	4490

Those results were in the order of magnitude similar to values reported in the literature (Molle *et al.*, 2008; Mercoiret *et al.*, 2010, see Table 1.1) during dry weather flow. The ratio between the maximum values and the average values reveal that concentrations were generally constant during the monitoring campaign, except for TSS concentrations.

COD fractions

COD fractions are presented in Figure 5.4. The results were obtained with the protocol presented in section 5.2.2.i. The COD fractions are different to reported literature data (Figure 5.4, Pasztor *et al.*, 2009) mainly taken from grab samples.

The main relative differences with the literature data come from the repartition between CR (readily biodegradable) and CS (slowly biodegradable) fractions. The average CR and CS fractions were practically six times larger and two times lower, respectively, in the fractionation of this present study than in the literature data. In addition, among the four sample COD fractionations, large variations were observed for the CS and Xi fractions. They are probably due to the sampling period and the modification of the discharges into the sewer network. These large variations over a day have been observed but no study has been published yet.

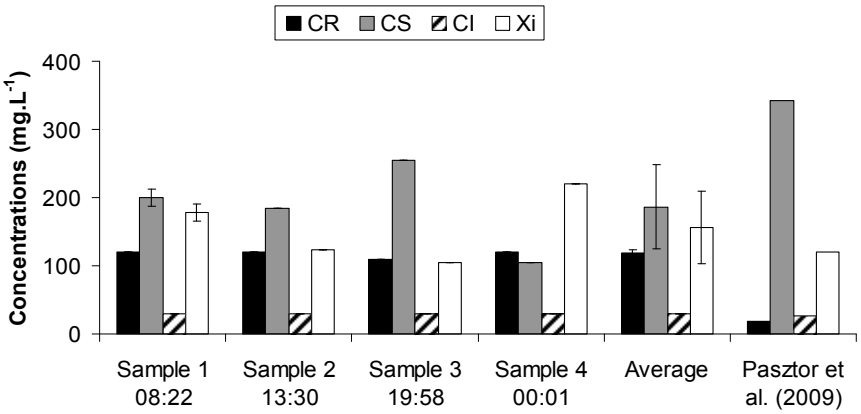


Figure 5.4: COD fractions of raw wastewater of Evieu samples and literature data (from Pasztor *et al.*, 2009)

The results point out the importance of using COD fractions for each batch to model such a system, especially for small communities where variations can be supposed larger than for large communities due to the smaller sewer network.

In the HYDRUS/CW2D model, Xi is not considered because this fraction is mainly retained in the previous primary settling tank in the conventional configuration of VFCW with sand. Consequently, in this study, this fraction was not used. In order to upgrade the model, it could be interesting to consider it coming to a VFCW, to predict the sludge deposit. Particles transport and probably clogging of the VFCW could in such cases be simulated.

The oxygen re-aeration rate

When the nitrification process was underestimated, the oxygen re-aeration rate (K_La, [d^{-1}]) was modified. Table 5.4 indicates the initial value of K_La in CW2D and the modified value in order to fit the observed ammonium and nitrate concentrations in the effluent. No experiment was carried out to measure this input.

Table 5.4: Oxygen re-aeration rate modified compared to CW2D initial value

Oxygen transfer		Initial value (20 °C) (CW2D, Langergraber and Simunek, 2005)	Calibrated value (this work)
K_La [d^{-1}]	Oxygen re-aeration rate	240	576

The oxygen re-aeration rate value was calibrated to correctly represent the nitrification process. This value is twice larger than the initial value but it is in accordance with the value used by McBride and Tanner (2000) (600 d^{-1}) in constructed wetland mesocosms with fluctuating water levels. In this study the choice was to only modify this parameter whereas the nitrification potential depends on various factors: oxygen re-aeration rate, mass of autotrophic biomass, temperature (constant in this study). The mass of autotrophic biomass was not measured and the calibration parameter b_A (decay rate) was not modified. Considering the difficulty of measuring the parameter b_A in these systems, the K_La was arbitrarily modified. Therefore, in this study, K_La is a global parameter whose calibration reflects a need to better define processes. However the simulated oxygen contents were underestimated compared to the measured ones (see 5.3.2.ii). Moreover, there is no spatiotemporal modification of parameter K_La. It can not be adapted neither for feeding and rest periods or top and bottom of the VFCW. The aeration concept could be modified if the oxygen transfer is adapted according to the organic matter content (larger the content organic matter is, lower the oxygen transfer is).

5.3.1.ii. Calibrated parameters values

The best fitting parameters to simulate NH_4-N and NO_3-N concentrations at the exit of the VFCW are presented in Table 5.5 and Table 5.6. The parameters not mentioned were used with default values proposed in CW2D (Langergraber and Simunek, 2005).

Table 5.5: Parameters values (adsorption) modified in order to simulate the measured values

Symbol	Meaning	Default value (Simunek *et al*, 1999)	Calibrated value (this work)
Adsorption parameters (HYDRUS software)			
Kd [d$m_{water}^{3}.kg_{solid}^{-1}$]	Adsorption isotherm coefficient	0	Layer 1: 900 Layer 2: 650 Layer 3: 400 Layer 4: 0
Alpha [d^{-1}]	First-order rate coefficient for one-site non-equilibrium adsorption; mass transfer coefficient for solute exchange between mobile and immobile liquid regions	0	Layers 1 to 3: 0.8 Layer 4: 0

NS: not specified

Table 5.6: Parameters values (biological) modified in order to simulate the measured values (20 °C)

Symbol	Meaning	Default value (Langergraber and Simunek, 2005)	Calibrated value (this work)
Kinetic parameters (CW2D model)			
$\mu_{AN_s}[d^{-1}]$	Maximum aerobic growth rate on NH_4-N	0.9	0.88 (Morvannou *et al.*, 2011)
$\mu_{AN_b}[d^{-1}]$	Maximum aerobic growth rate on NO_2-N	1	With decay rate: b_A= 0.15 d^{-1}

The maximum aerobic growth rate (for nitrification) comes from the respirometric measurements (Morvannou *et al.*, 2011). Changes in fitting parameters mainly concern adsorption parameters. As a decrease in NH_4-N was not directly correlated to an increase in NO_3-N, an increase in adsorption parameters appeared obvious. This point is in accordance with the model developed by McBride and Tanner (2000) about the nitrogen removal in constructed wetland. They stated that adsorption on organic matter is the main cause of the rapid initial ammonium decrease. Moreover, Kadlec *et al.* (2005) indicated through tracer experiments on gravel-bed wetlands with horizontal subsurface flow, the rapid adsorption of ammonium into sediments (28-37 % of the tracer mass injected). Therefore, the *Kd* parameter is proportional to the sludge content, but no adsorption is considered for layer 4.

Birkinshaw and Ewen (2000) studied the nitrogen transformations in a subsurface variably saturated heterogeneous region for nitrate transport modelling, with a term for ammonium adsorption. In a simple approach, they assumed a linear adsorption isotherm with an adsorption coefficient equals to 60 $dm^3.kg^{-1}$. Other studies about nitrogen transformations carried out in systems for wastewater treatment also used a linear adsorption isotherm but the selected adsorption coefficients were lower (2.79 and 1.38 $dm^3.kg^{-1}$ for Yamaguchi *et al.* (1996) and Martin and Reddy (1997) studies, respectively). We used decreasing values for the adsorption coefficients for layers 1 to 3 (900, 650 and 400 $dm_w^3.kg_s^{-1}$, respectively) in order to better fit ammonium concentrations in the effluent. These values would need further studies (laboratory-scale studies) to be confirmed but are consistent with the high organic matter content in the first stage of the French VFCW fed with raw wastewater.

5.3.2. Comparison between simulated and measured data with calibrated parameters

5.3.2.i. Online monitoring (COD, nitrogen forms)

We first calculated the simulated concentrations into flow-proportional composite samples corresponding to each batch applied, using on-line COD monitoring (section 5.2.2.ii.).

Filtered COD concentrations

We compared the dissolved COD (CR + CS + CI) simulated at the VFCW exit to the values measured by online sensor (Figure 5.5). The average value for MARE reaches 15 % and individual values varied from 3 to 50 %. Hence, the CW2D initial conditions and parameters related to COD were considered as suitable for further simulations.

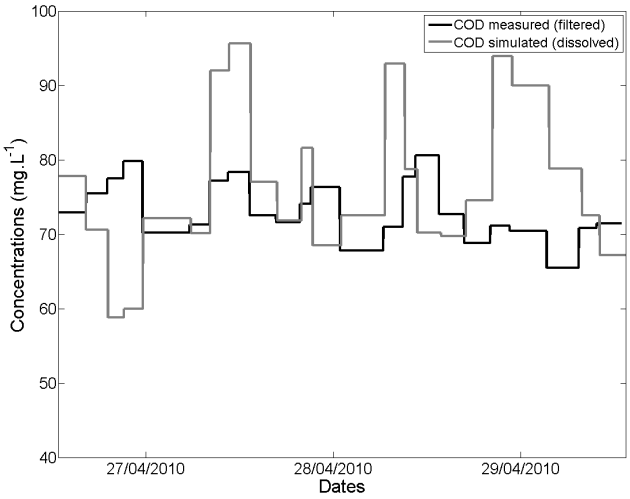
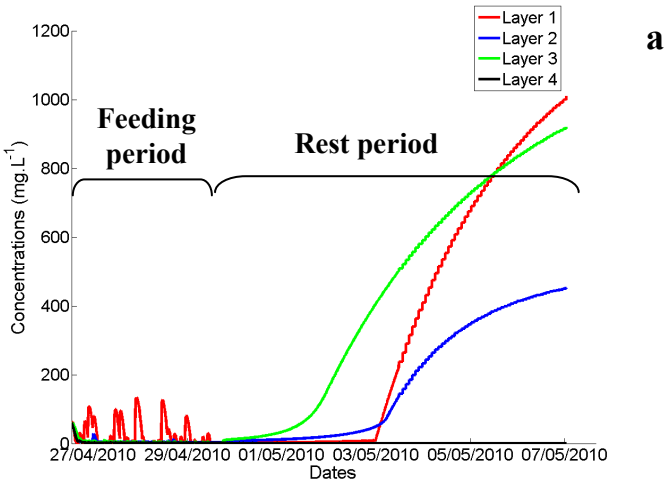


Figure 5.5: Simulated and measured dissolved COD concentrations in the effluent for 3.5 day-period of the FP

During the rest period, the CR and CI concentrations increase in all layers and particularly in layer 1: from 2.5 (end of the feeding period) to 1000 $mg.L^{-1}$ (end of the rest period) and from 6 to 64 $mg.L^{-1}$, respectively (Figure 5.6).



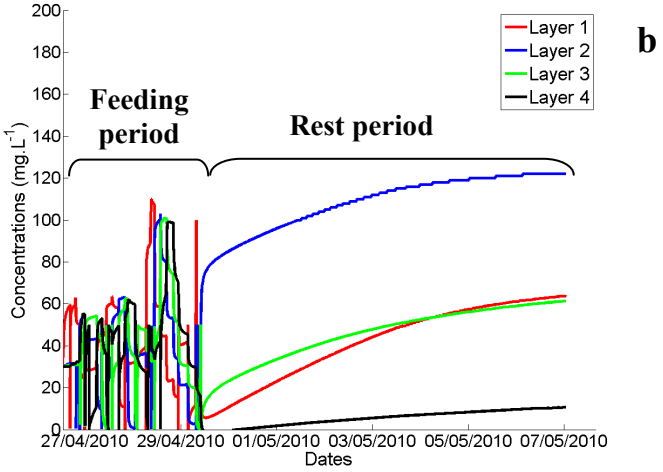


Figure 5.6: (a) CR concentrations simulated in the four layers during both feeding and rest periods. (b) CI concentrations simulated in the four layers during both feeding and rest periods

The predicted accumulation was due to the decay of heterotrophic microorganisms (section 5.3.2.ii); while their growth is very slow due to a preferential uptake of ammonium by nitrification. Indeed the CW2D model uses a growth rate that contains a Monod function that turns to zero when ammonium is lacking (degradation of CR is inhibited in CW2D at low NH_4-N concentration). This result to the accumulation of CR and CI should not fit with reality. Indeed, solid respirometric tests carried out on sludge and colonized gravel have always shown low oxygen uptake rate.

NH_4-N and NO_3-N concentrations

Figure 5.7 presents the evolution of the simulated and measured NH_4-N (a) and NO_3-N (b) concentrations in the effluent of the VFCW during the measurement campaign with the calibrated parameters.

We calculated average relative differences (MARE values) of 27.1 % and 21.3 % for NH_4-N and NO_3-N concentrations, respectively. These relative differences correspond to average absolute differences (MAE values) of 5.5 and 6.5 $mg.L^{-1}$. This was the best adequacy between simulated and measured concentrations. A widespread magnitude of the MARE was recorded between 0.3 % to 63.9 % differences.

The solution obtained confirms the importance of ammonium adsorption for nitrification on the French system, as proposed by Molle *et al.* (2008). The increase in outlet ammonium concentration until reaching a “plateau” could

be explained, in reality, by a saturation of adsorption sites and/or a lack of oxygen for nitrification. Nevertheless, the adsorption model based on a linear adsorption with constant kinetics (no saturation) can not simulate the saturation of adsorption sites. In the model the nitrification limitation could be attributed to oxygen depletion (see section 5.3.2.ii.). Not to mention the model limitation of ammonium adsorption, these results point out the role of the rest period in renewing oxygen content and ammonium adsorption sites as well.

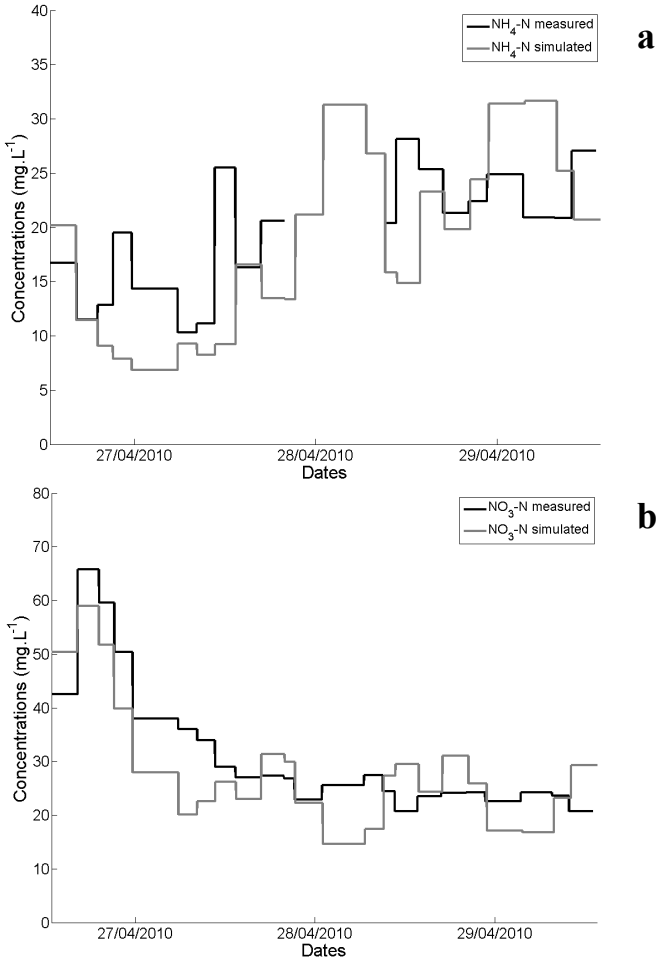


Figure 5.7: Simulated and measured average concentrations for NH_4-N (a) and NO_3-N (b) in the effluent for 3.5 day-period of feeding

Despite the consistency between simulated and measured values on a batch average basis, the instantaneous values for predicted NH_4-N and NO_3-N concentrations are very variable. They are difficult to fit on the observed instantaneous measured values (Figure 5.8, a, b). Concentrations peaks observed at the beginning of each batch can not be reproduced by CW2D. This disparity is probably due to non-equilibrium preferential flow, already underlined in the VFCW hydraulic modelling (Chapter 2.) which rapidly discharge NH_4-N and NO_3-N in the outflow (short circuit like).

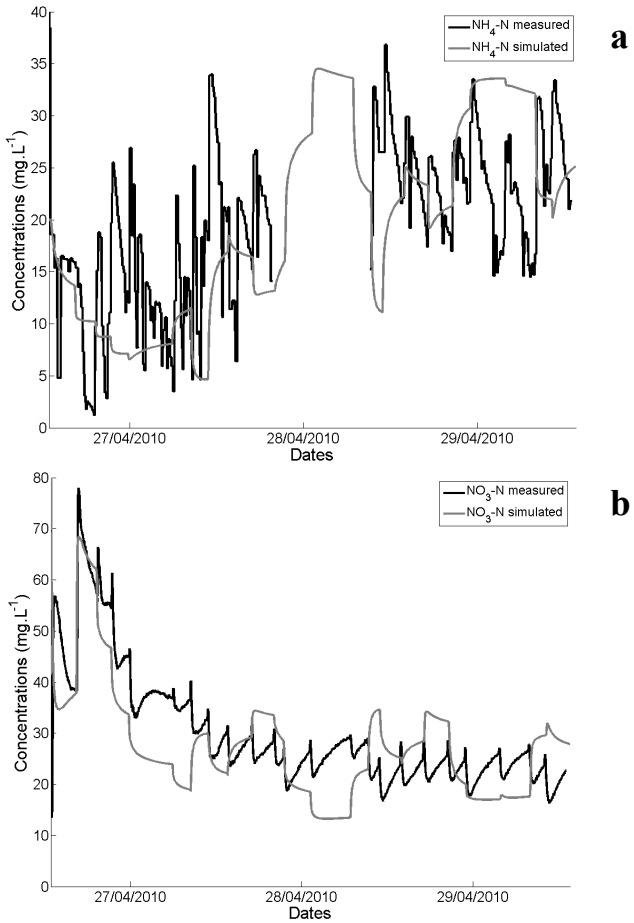


Figure 5.8: Simulated and measured instantaneous concentrations for NH_4-N (a) and NO_3-N (b) in the effluent for 3.5 day-period of feeding

5.3.2.ii. In-situ monitoring (off-line)

Gaseous oxygen contents

Figure 5.9 presents the gaseous oxygen contents calculated from simulated values at different VFCW depths and the measured oxygen contents for the measurement point 1 close to the manhole (a) and 2 away from the manhole (b).

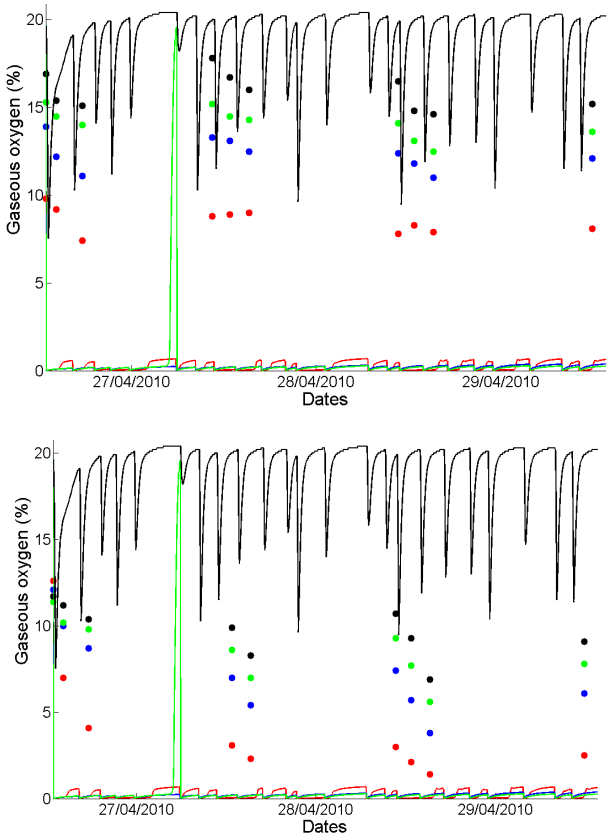


Figure 5.9: Calculated (continuous curve) and measured (spots) oxygen contents at different depths of the VFCW for the two measurement points (red: layer 1; blue: layer 2; green: layer 3; black: layer 4)

Simulated oxygen contents differ from measured values by 5%-unit (layer 4) to 10 to 15%-unit (layers 1, 2 and 3). Simulated oxygen values were close to zero for the three first VFCW layers. These low oxygen contents most probably limit nitrification and microorganisms growth, and consequently explain, as well the adsorption/nitrification competition, the limited nitrification after 3 days of functioning shown in the section 5.3.2.i. The difference between simulation and measurement can lead to two observations:

- In reality nitrification seems to be more limited by a saturation of adsorption sites than low oxygen contents;
- Uncertainty on water content values in sludge due to the poor calibration of TDR probes in this layer. We earlier highlighted that preferential flows occurring in reality are not taken into account by the model. Therefore, in the reality the desaturation of macropores is faster and the access to oxygen easier.

Simulated oxygen contents increase during the rest period and reach up to the saturation concentration of oxygen (i.e. 9.2 $mg.L^{-1}$) (results not shown).

Heterotrophic and autotrophic biomasses

Figure 5.10 presents the evolution of the heterotrophic (XH, Figure 5.10(a)) and autotrophic (XAN, Figure 5.10(b)) biomasses at different VFCW depths and time periods.

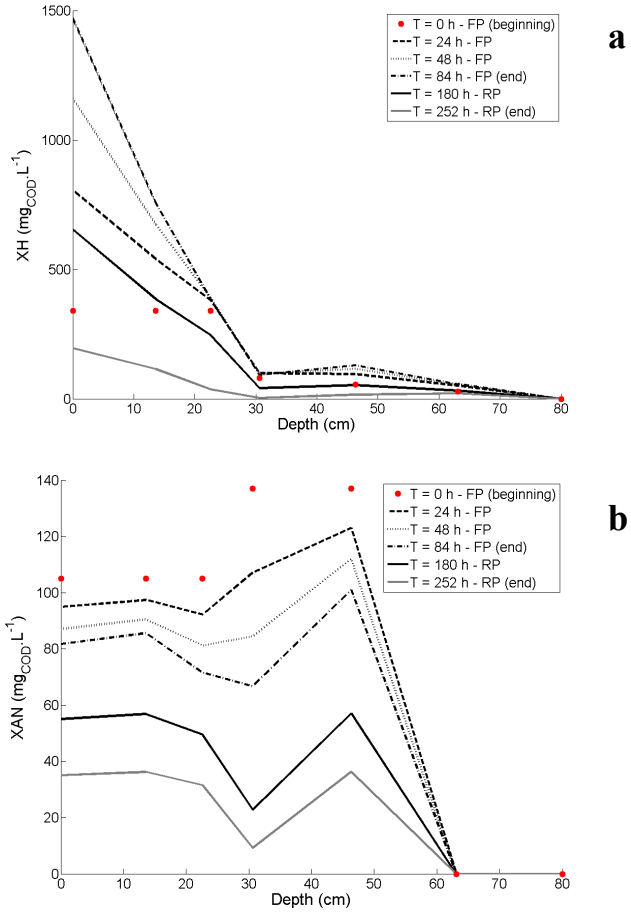


Figure 5.10: Simulated XH (a) and XAN (b) concentrations at different depths and times after the monitoring campaign beginning (FP = feeding period, RP = rest period)

Most of the simulated heterotrophic biomass is present in layer 1 and a significant decrease versus depth is pointed out. As for various other processes treating both COD and ammonium, the microbial community is mainly composed by heterotrophic biomass. With the help of modelling, we can notice that heterotrophic biomass is in the first 30-cm, whereas autotrophic one is in the first 50-cm of the filter.

For the concentrations of heterotrophic biomass, we see that:

- After 4 days of the rest period (T = 180 h), the simulated concentrations of heterotrophic microorganisms are quite close to the initial values determined from total COD and TSS concentrations after 4 days of rest.

- But, at the end of the rest period (T = 252 h), the simulated concentrations are lower than the initial conditions determined (T = 0 h; Table 5.2.).

For the concentrations of autotrophic biomass, the predicted values were always below the initial conditions and they continuously decrease with time, even during the feeding period. A too high decay rate of autotrophic biomass could explain this decrease. In the model concepts, the microorganism decay mainly produced COD (CR, CS and CI) which is in agreement with the increase in CR and CI concentrations mentioned in section 5.3.2.i.

5.3.3. Discussion

5.3.3.i. Fate of nitrogen during feeding and feeding+rest periods

This section discusses the different ways of eliminating the KN, considering the feeding and feeding+rest periods separately. We calculated that 3549 gN were applied to the VFCW during the feeding period. This represents a mean KN load of 36 $gKN.m^{-2}.d^{-1}$ on the operational filter. Carrying out nitrogen mass balances on a VFCW is a difficult task because ammonium and nitrate were already present in the VFCW before the feeding period. These quantities were not determined. Nevertheless, a mass-balance approach has been carried out (section 5.2.4.iii.) to determine the different fluxes involved in the VFCW, among which the assimilated, adsorbed, nitrified, denitrified or released (outflow) nitrogen fluxes. This mass-balance was based on simulated results, except for the ammonium and nitrate outflow fluxes. Figure 5.11 presents the fate of nitrogen through the system for feeding and feeding+rest periods.

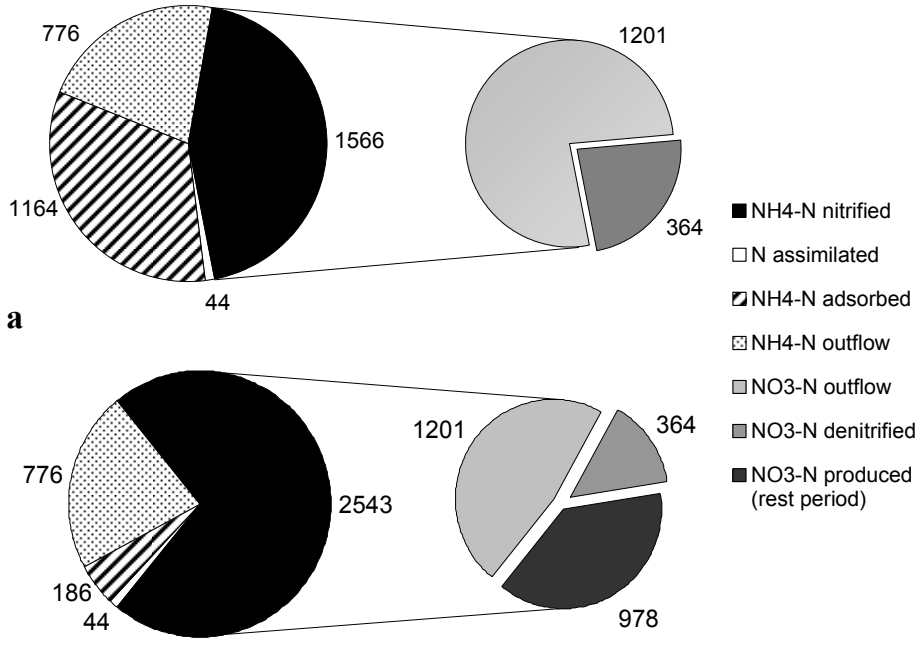


Figure 5.11: Nitrogen fluxes (gN) calculated for feeding (a) and feeding+rest (b) periods

For the feeding period, 776 gKN are released with the effluent, 1164 gKN are adsorbed, and 1566 gKN are nitrified. The nitrified flux causes a release of nitrate of 1201 g whereas 364 g are denitrified. The total KN removal reaches 78.1 % during the feeding period. The adsorbed and nitrified nitrogen quantities represent 32.8 % and 44.1 % of the input KN, respectively. On the same plant, Molle *et al.* (2008) observed a KN removal of about 55.6 % for the same KN load in this study. Langergraber *et al.* (2009b) observed KN removal of mechanically pre-treated wastewater in a two-stage constructed wetland system filled with sand. In such systems, removal efficiency was of 68.9 % for KN and nitrification of about 76.6 % in the first stage.

Nitrogen quantity previously adsorbed in the VFCW is reduced by 84.0 % during the rest period and transformed into nitrate (nitrified nitrogen quantity increased by 62.4 %). These observations explain and confirm the significant nitrate flux generally measured in the VFCW effluent during the first batches (Figure 5.8, right) (Molle *et al.*, 2006). On one feeding+rest period we calculated mean removal efficiency with the CW2D model of 78.1 % for KN which is higher than what is generally observed on a 24 h composite sample during feeding period (Molle *et al.,* 2005).

As simulated, dissolved oxygen is limiting, the simulated denitrified nitrogen quantity represents 23.2 % of the nitrogen nitrified and 10.3 % of the input KN. In our monitoring campaign, the denitrification rate is estimated to be about 3.71 $gN.m^{-2}.d^{-1}$, assuming that denitrification occurred for 3.5 days of feeding. This denitrification rate lead to a denitrified nitrogen quantity estimated to 10.2 % of the input KN which is close to the predicted amount of denitrified nitrogen. Simulated CR (Figure 5.6) and NO_3-N (Figure 5.11) concentrations accumulated during the rest period suggest that denitrification should occur but no denitrification is simulated. To represent this process a layered biofilm model could be used: the outer layers with an easy contact with oxygen present within the VFCW and deeper layers with no or little access to oxygen.

5.3.3.ii. Additional simulation consecutive to a previous simulation period

This section deals with the simulation of a feeding period that is applied immediately after the period previously studied ("fictive" campaign), and hence with new initial values of the different components. This second simulation was carried out with initial conditions similar to the final conditions of the first simulation.

With this "fictive initialization", COD fractions simulated in the outflow globally match measured values (results not shown). Nevertheless, during the first 24 h of the feeding period, CR and CI fractions are much higher than the ones measured due to their high concentrations produced by microorganisms decay during the previous rest period. Henrichs *et al.* (2007) observed also this increase of CR and CI fractions during the rest period. In their study, the CS fraction adsorbed during the feeding period was transformed into CR fraction by hydrolysis and CI fraction was produced and accumulated in dry period by lysis processes of XH and XAN.

For nitrogen (Figure 5.12), despite a decrease of autotrophic microorganisms concentrations during the first feeding at rest period, ammonium concentrations are as well-simulated (MARE = 28.9 %). On the other hand, for nitrate concentrations the MARE reaches 67.8 % and the model over-estimate the nitrate release during the first batches. These first batches are the most difficult to predict. After the release of nitrate the time variation of the concentration fits with measured values.

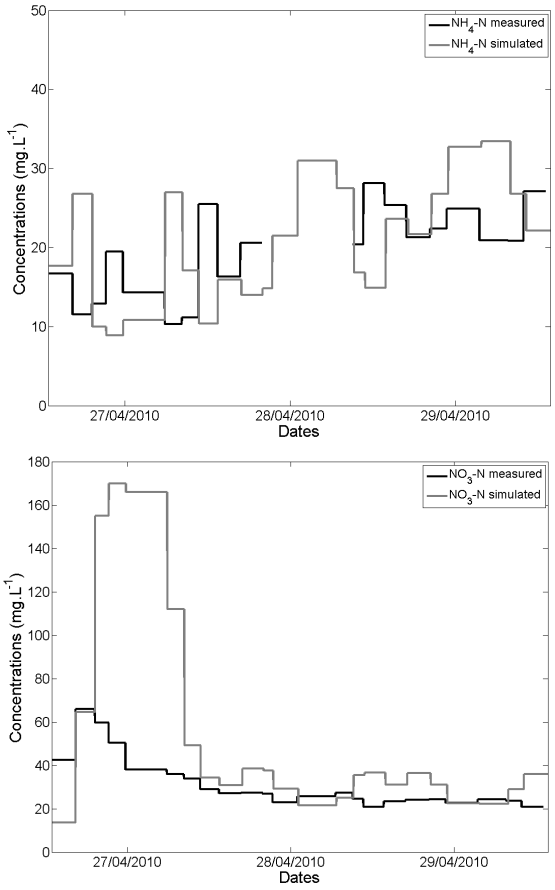


Figure 5.12: Simulated NH_4-N (a) and NO_3-N (b) concentrations for additional simulation ("fictive" feeding period) consecutive to the previously simulation period

In addition, the simulated oxygen contents within the VFCW are higher than those predicted for the first simulation and better match the measured oxygen contents (Figure 5.13). These higher simulated values are probably due to the smaller biomass concentrations within the VFCW after the rest period previously simulated (Figure 5.10). The nitrification process is therefore not limited by the oxygen transfer through the biomasses.

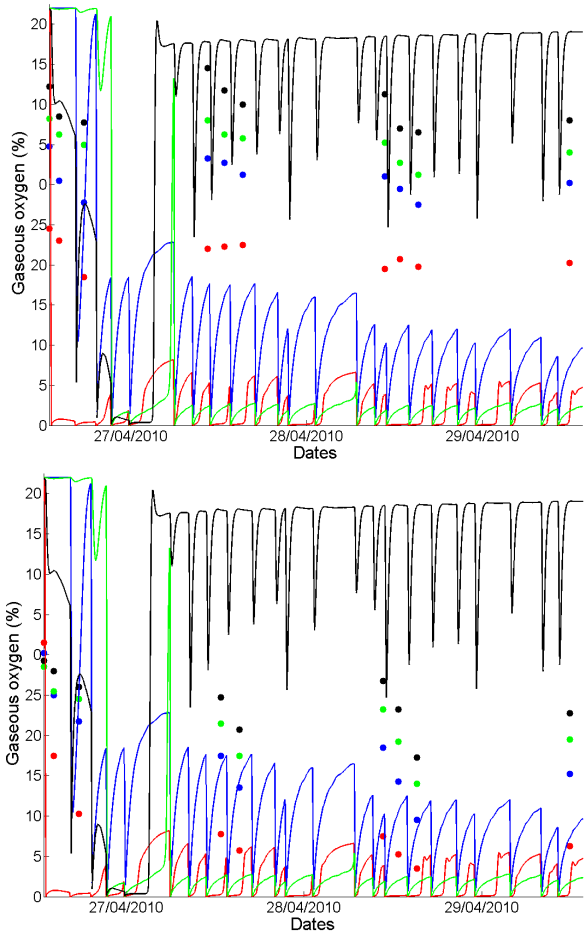


Figure 5.13: Calculated (continuous curve) and measured (spots) oxygen contents at different depths of the VFCW for the two measurement points for the second simulation (red: layer 1; blue: layer 2; green: layer 3; black: layer 4)

The model calibration and the CW2D model were suitable to simulate the concentrations of nitrogen forms in the VFCW outflow. Nevertheless, some difficulties to reproduce correctly storage and release of nitrogen forms in the VFCW have been highlighted.

5.3.3.iii. Improving quality of modelling: additional measurements, modification of model

This section deals with the different ways that would lead to better simulations. Additional measurements and modifications of the model are proposed.

Our research work showed that it is possible to model COD removal and nitrification on a batch average basis, but only if ammonium and nitrates concentrations in the outflow are known for the first batches. Indeed, both ammonium and nitrate concentrations have to be accurately monitored, particularly during the first 24 h where nitrogen concentrations are the most difficult to reproduce. In addition, these concentrations are used to establish their initial concentrations in the VFCW. Even if the pertinence of the different initial conditions can be discussed, the various simulations point out that the model has some difficulties to represent storage and release of the different nitrogen forms. For that, further studies are needed, in particular related to a better COD characterization. Oxygen measurements at different depths and locations of the VFCW are needed to determine the relevance of the model.

Influent COD characterization

A higher data resolution of COD fractionation would improve simulation results due to low hydraulic residence times (few minutes). Indeed, large differences were observed among the different sampling times. The concept of inert particular organic matter (Xi) is linked to a range of activated sludge retention times (SRT, from 5 to 50 days). This fraction of COD, which is refractory to biological treatment in this range of SRT, should not be correct for high SRT processes like those that develop on the French VFCWs (5 to 10 years). A "very slowly biodegradable fraction" might be defined to account for the observed biodegradability at very long SRT. There is a clear need for the improved tracking of inorganic materials, especially those involved in precipitation/dissolution (sulphide, magnesium, calcium, iron, aluminum). Simulation experience indicates that introducing inert suspended solids (ISS) like into the ASM models would improve the simulation of the sludge production.

Effluent characterization frequency

As the filtered COD concentrations are almost the same in effluent during the whole feeding period (batch average basis), monitoring the COD every minute in the effluent is not necessary. Only batch average concentrations comparisons are necessary. If the aim is to better simulate the time course of nitrogen (e.g. as observed with online measurements), then the extent of adsorption and knowledge of the hydraulic behavior of the filter need to be improved.

A deeper analysis of effluent components, as TSS content and granulometry measurements, would lead to a better understanding of both filtration process and detachment rate determination.

VFCW characterization

Some adsorption measurements on medias (sludge and gravel+sludge) of the VFCW would improve the simulation of nitrogen fate, since this mechanism is predominant in this kind of system. Adsorption coefficients were manually calibrated and could be overestimated. A protocol should be set-up to measure this coefficient.

No measurement of the oxygen re-aeration rate was carried out in this study and it was only adjusted according to the nitrogen concentrations in the VFCW effluent. Moreover, it was constant through the whole simulation, whereas it could be modified according to the oxygen contents between the different layers. A protocol should therefore be carried out to measure this coefficient for the oxygen transfer rate. Tyroller *et al.* (2010) carried out some gas (propane) tracer experiments in order to determine the oxygen transfer rate.

A system should be design to carry samples and help determining the initial conditions in the system, for COD and nitrogen forms. Moreover, measurement of *in-situ* nitrogen conversion rate should be developed, using for example CO_2 and/or N_2O emission. Moreover the measurement of denitrification rate should be developed to calibrate denitrification. The evaluation of the concentration of biomass (microbiological techniques such as DNA extraction and denaturing gradient gel electrophoresis, Tietz *et al.*, 2007) should also help the calibration process.

5.4. Conclusion

In this chapter, we use a process based mechanistic model to assess the behavior of an intensively monitored VFCW filled with gravel. Different components, of the raw/treated wastewater, and in the filter were measured during the feeding period of 3.5 days, aiming at calibrating biological parameters of the CW2D model (HYDRUS software). Dynamic behavior of nitrogen forms, COD and oxygen were simulated with a good match on a batch average basis with the model. The model achieved to simulate the intensities of adsorption and nitrification of ammonium occurring during both feeding and rest periods. It was found that during the feeding period, adsorbed nitrogen mass was almost equivalent to the nitrified mass. During the rest period, the previously adsorbed mass is nitrified, resulting consequently to high concentrations of nitrate during the next first batches. However, due to interconnection between each process, the change of only

one parameter can modify various processes. Different parameter combinations could still lead to a match between simulated and measured data. Practical knowledge of the VFCW systems remains essential to correctly calibrate the CW2D model. Further developments were pointed out and seemed to be necessary for a proper prediction of ammonium adsorption and nitrate release phenomena. Improving the hydraulic representation including preferential flows, measurements of *in-situ* oxygen transfers, initial conditions, denitrification rate and concentration of biomass (microbiology) should be the subject of future research.

Chapter 6

Conclusions and perspectives

VFCW systems are becoming popular engineered systems for wastewater management in rural areas. However, the hydraulic and biological functioning of VFCW systems is still not well known. Raw wastewater feeding the material filling the VFCW (gravel) and the large sludge deposit developed over the several functioning years (about 20 cm) are the special features of the Cemagref-type VFCW system. These typical characteristics make this kind of systems difficult to characterize. The HYDRUS/CW2D model was used to simulate both the hydraulic and biological behavior of a first stage of a two-stage VFCW.

The hydraulic calibration of the HYDRUS software was carried out through the specific assessment of the hydraulic parameters. As in the VFCW vertical heterogeneity of hydraulic properties is important, four layers composing the VFCW (a sludge layer, two layers for the mix between sludge and gravel and a gravel layer) were useful to describe its hydraulic behavior. However, this number of layer was arbitrary and we did not attempt to optimize it. We used a multi-tier approach to obtain a reliable hydraulic parameter set for these various layers. Indeed, both direct and inverse laboratory experiments and a network of TDR probes inserted within the VFCW were used for the assessment of the specific hydraulic parameters. These TDR probes usually used for the determination of soil hydraulic parameters were adapted for determining hydraulic parameters of the various layers of the VFCW, except for the sludge layer. The applied methodology with successive optimizations as well as a large range of experimental data led to a reliable hydraulic parameter set which allowed simulating water contents at different depth within the VFCW with a good accuracy. Contrarily, using data sets obtained either from laboratory experiments only or from in-situ data inversion using literature values for initialization failed. Nevertheless, to improve this methodology it might be interesting to consider confidence intervals from proposed methods into the calibration process (e.g. using a Bayesian approach). Another way to improve parameter calibration is to take into account the correlation among them. A change in one parameter can generate a variation in highly correlated parameters, with the result that none can be accurately determined. Finally, simulations should be further improved by usage of non-equilibrium models which are able to reproduce preferential flows.

Once the hydraulic calibration completed, the biological calibration of the CW2D was carried out by coupling laboratory and field measurements. On the one hand, some biological parameters were assessed for the different VFCW layers. In particular the nitrification capacity and the maximum growth rate of autotrophic biomass were determined thanks to a solid respirometry technique, developed to measure the biological activity in unsaturated porous media, i.e. samples taken from VFCW. Before measuring the maximum nitrification capacity, four injections of water with ammonium were needed in order to saturate the adsorption sites and to measure the actual nitrification. In this study an injected nitrogen mass of 100 mg N was necessary to work at the conditions of the maximum level of nitrification rate. Comparison with batch liquid experiments indicated that the solid respirometry was more appropriate due to the original medium where the bacteria were studied. With this respirometric system it was pointed out that the maximum autotrophic growth rate from activated sludge process can be directly used in the modelling of VFCW. On the other hand, an intensive monitoring was carried out within the VFCW. Different components, of the raw/treated wastewater, and within the filter were measured during a feeding period of 3.5 days long, aiming at calibrating biological parameters of the CW2D model (HYDRUS software) by adjusting the simulated values to the observed ones. Hence, with these two strategies we achieved to determine some numerical values of kinetic coefficients of biological processes, linking with nutrients diffusion and utilization (carbon, nitrogen and oxygen). The model successfully achieved to simulate COD removal and nitrification on a batch average basis, except for the first batches. It simulated the two major processes (ammonium adsorption and nitrification) occurring during the feeding period but oxygen contents within the VFCW were poorly simulated and they need improvement. The rest period was characterized by the nitrification of the nitrogen previously adsorbed and consequently high concentrations of nitrate were observed during the first next batches. Simulation results correspond to nitrogen removal observed during the feeding period and nitrogen evolutions simulated during the rest period match with trends observed on field scale. Therefore, the nitrate quantity produced during the rest period left the system during the first batches of the second simulated feeding period. But, the simulated nitrate quantity produced during the rest period was too high (nitrogen quantity previously adsorbed in the VFCW during the feeding period is reduced by 84.0 % during the rest period and transformed into nitrate) and consequently simulated nitrate concentrations were too high compared to measured data: the average relative difference reaches 67.8 % and the model over-estimate the nitrate release during the first batches. This feeding period time was the most difficult to reproduce for both the first and the second simulated feeding periods. After this nitrate release, the evolution of the simulated nitrate concentrations succeeded in reproducing measured values. Therefore, the model calibration and the CW2D model were pertinent and processes

considered in this model were adapted to the VFCW modeling (average relative differences of 27.1 % and 21.3 % between NH_4-N and NO_3-N simulated and measured concentrations, respectively.). However, due to interconnection between each process and the large number of parameter to be set up, the problem can be considered as ill-posed. Therefore, different parameter combinations could lead to a match between simulated and measured data. A protocol allowing measuring nitrogen adsorption on sludge and gravel/sludge mix could improve the nitrogen modelling. Practical knowledge of the VFCW systems remains essential to correctly calibrate the CW2D model. Contrary to the activated sludge modelling that has been deeply investigated since a long time, the CW modelling is somewhat recent and less studied. Moreover, while the activated sludge process is controlled (oxygen, nutrients, biomass contents), performed in a homogeneous medium and thus it is easier to reproduce the various media changes, the "natural", heterogeneous and less controlled characteristics of the CWs means a weaker knowledge of their behavior.

This work will participate to better define operating limits of French VFCW, particularly regarding nitrogen removal and the first stage of treatment. Improving nitrification could be carried out by increasing:

- The oxygenation. The CW2D model pointed out that during a feeding period the oxygen content within the filter is a limiting factor. An imposed aeration should increase both the oxygen content but also the cost of its building;

- The autotrophic biomass. The quantity of nitrified nitrogen as well as the autotrophic biomass expected to increase leading to the clogging of the system. We pointed out in this study the necessity of the rest periods. This parameter is not easy to modify;

- The adsorption process. The VFCW adsorption capacity could be increased by using different filtering material with higher cation exchange capacity, such as zeolite.

- The residence time of water. It can be extended if the volume of batches is smaller but their frequency is higher. However, in such case the oxygen content within the VFCW could be limiting. The residence time of water can also be extended by increasing the VFCW surface. However, because of the cost and wastewater repartition issues which could occur, this proposal is the worst for small communities.

Moreover, this present work is a step towards optimizing filter design in relation to its application specificity - i.e. wastewater characteristics, type of sewer network, geographical area, etc. - in order to anticipate rule and regulation evolutions for river quality improvement. Two applications are of special interest: sewage overflow treatment wetlands and French VFCW built in cold climate area. In both cases an adaptation of the bio-kinetic parameters may be necessary to model the adaptation of biomass to the specificity of the influent and the low temperature, respectively.

To reach these operational goals, numerical models must also be upgraded. Regarding the hydraulic modelling of the system, it was pointed out earlier that non-equilibrium models is a necessary improvement for those coarse systems, but modelling would also gain in accuracy if phenomena so far neglected are included like the evapotranspiration or the influence of reeds. Moreover, carrying out global parameter estimation should allow solving the ill-posedness problem of inverse modelling schemes and improving the hydraulic parameter assessment. A global model sensitivity analysis should allow knowing which parameter is essential to the modelling and lead to a model reduction by fixing parameters not effectively pertinent, or eliminating them from the model structure. The biological part of the model would be significantly improved if the biomass attachment/detachment phenomena and pore space occupation are taken into account. Based on the experience gained over this thesis, we suggest the introduction of a new COD fraction that would represent the very slowly biodegradable fraction. This is needed because of the very long retention time (5 to 10 years). The relative participation of adsorption to nitrogen removal process that is quite high in the studied case must now be investigated in presence of precipitation and fully developed reeds.

Appendices

Appendix I

Available models for VFCW modelling

Table I.1: Existing models for VFCW modelling

Authors/ Model	Water flow	Solute/Biomass transport	Discretization	Species considered	O_2	Processes number	Biochemical conversion	Model dim	Commentaries
Freire *et al.* (2006)	3 reactors : 2 CSTR + 1 dead zone volumes	Mass balance	-	O_2 AO7 (dye)	-	-	First-order kinetics → Froment and Bischoff (1979)	-	Industrial WW (dye) Matrix = clay+sand Considered: **ponding** and **change in porosity/ permeability** (clogging) Experimental results ≠ expected MSExcel
Mc Gechan *et al.* (2005)	Water flows through different layers, vertically, to the CW bottom	Transfers defined between tanks	Access to nitrogen concentrations in each tanks for each time step	O_2 Nitrogen cycle NH_4-N/NO_3-N/N_2 Nitrogen in the organic matter	-	Mineralization Nitrification Denitrification	Tanks Transformation equations from one tank to another = first-order exponential decomposition kinetics	-	Experiment on 1HF follows by 3VF in series Dairy farm WW Nitrogen lost in the atmosphere either by NH_3volatilization, or byN_2 No considered: microorganisms growth, biomass tanks, microbial control of nitrogen transformations Fortran program

Authors/ Model	Water flow	Solute/Biomass transport	Discretization	Species considered	O_2	Processes number	Biochemical conversion	Model dim	Commentaries
Wanko *et al.* (2006)	Richards equation + van Genuchten	- Biomass in suspension in φ_{liquid} → Taylor et Jaffé (1990) - Exchanges between biomass $\varphi_{liquid\text{-}mobile}$ and biomass $\varphi_{liquid\text{-}immobile}$ - Solute diffusion toward biofilm (interface water/biofilm) - O_2transfer $\varphi_{liquide}$ toward φ_{gas} → 6 no-linear macroscopic transport equations	Splitting operator technique (individual resolution) CONVECTION Discontinuous finite elements – explicit (time) DISPERSION "mixed-hybrides" finite elements– implicit (time) KINETICS Fourth order Runge-Kutta	O_{2gas}/O_{2liq} Organic matter	O_2 provision = $O_{2dissolved}$ + convection + molar diffusion → Dissolved/ gaseous forms Transport and uptake for the two forms	-	Monod-type kinetic equations (active biomass growing) Biomass decay = first-order kinetic Solute use by biomass in φ_{liquid}	1D	Domestic WW Matrix = sand Endogenous respiration

Authors/ Model	Water flow	Solute/Biomass transport	Discretization	Species considered	O_2	Processes number	Biochemical conversion	Model dim	Commentaries
Ojeda *et al.* (2006)	Multiphase flow (air/water) – CodeBright code	Multiphase reactive– Retraso code (Fortran) Convection, dispersion/diffusion for φ_{liquid} and φ_{gas} [Chemical reactions possible in Retraso: aqueous complexation (including redox reactions), sorption, precipitation/mineral dissolution, gas dissolution]	Finite elements for the spatial discretization DSA (Direct Substitution Approach)	$O_{2gas}/O_{2liquid}$ Organic matter (only under dissolved form) Nitrogen Sulfate Solid particles	Physical transfer O_{2atm} toward φ_{liquid}	6 processes: Hydrolysis Aerobic respiration Nitrification Denitrification Sulfate reduction Methanogenesis.	Exponential fonction for the hydrolysis Monod-type kinetic equations for the five latter processes → Van Capellen and Gaillard (1996)	2D	HF but flow model also able to simulate unsaturated VFCW Combination of flow code and reactive transport → RetrasoCodeBright Domestic WW Matrix = gravel ALL solutes are considered as readily-biodegrable <u>No considered</u>: Phosphorus, biofilm growth, O_2 from macrophytes, organic nitrogen in WW, competition for O_2 between aerobic respiration and nitrification, temperature dependence

Authors/ Model	Water flow	Solute/Biomass transport	Discretization	Species considered	O_2	Processes number	Biochemical conversion	Model dim	Commentaries
Langergraber and Simunek HYDRUS/ CW2D (1999/2001)	Richards equation + van Genuchten-Mualem + sink term (water uptake by plants) Dual-porosity possible → φ_{liquid} divided: -mobile part -immobile part	Multi-component reactive Convection-dispersion equation in φ_{liquid} Exchanges between the two parts = first-order process	Galerkin finite elements for water flow and solute transport equations [HYDRUS 1D : flow and transport = finite differences]	12 components Dissolved oxygen 3 carbon solutes 4 nitrogen solutes $Phosphorus_{inorg}$ 1 heterotrophic species (H) 2 autotrophic species (A) microorganisms present in φ_{solid} Organic matter only in φ_{liquid}	Exchange - O_2 diffusion from φ_{gas} to φ_{liquid}	9 processes with - hydrolysis (H) - organic matter mineralization (H) -nitrification (A) (**2 steps**) - denitrification (H) - bacteria lysis Adsorption for ammonium and $phosphorus_{inorg}$ (= kinetic process)	ASM2 (Monod) - pH = cst - coefficients in the rate equations = cst - stoichio. coefficients = cst **All** reactions take place in the φ_{liquid}	2D	Domestic WW Processes, diffusion coefficients and oxygen dissolved concentrations at saturation = depends on the temperature (Arrhenius) Matrix = sand Considered: ponding, dual-porosity, biofilm = homogeneous matrix, species uniformly distributed in the biofilm, heat transport Not considered: biofilm thickness, nitrogen uptake by plants, influences of particular material and biofilm growth on CW hydraulic properties

Authors/ Model	Water flow	Solute/Biomass transport	Discretization	Species considered	O_2	Processes number	Biochemical conversion	Model dim	Commentaries
Giraldi *et al.* (2010) FITOVERT	Richards equation + van Genuchten-Mualem + sink term (water uptake by plants)	<u>Dissolved compounds</u> Convective and diffusive transport: Bresler equation (1973) In φ_{liquid} = mass balance equation <u>Particular compounds</u> Iwasaki scheme (1937) developed by Ives (1969) → filtration + biomss growth	<u>Mixed form of the Richards equation</u> Space: Galerkin finite elements Time: finite differences: Picard iterative method <u>Dissolved compounds transport</u> Space: Galerkin finite elements Time: Cranck-Nicolson implicit scheme Biochemical calculations uncoupled from transport equation <u>Biochemical</u> Explicit finite differences for time <u>Particular compounds</u> Space: Petrov-Galerkin finite elements Time: finite differences	13 compounds → 7 soluble → 6 particular O_2 Organic matter Nitrogen Solid particles	O_2 transport in φ_{liquid} = same equation than for dissolved compounds Exchange between φ_{liquid} and φ_{gas} : Fick law O_2 transport in φ_{gas}: diffusion mainly = mass balance	8 equations	ASM1 Monod-type kinetic equations	1D	Tested on tertiary treatment systems Domestic WW Matrix = gravel <u>Considered</u>: **ponding**, **water loss** **Filtration** = porosity decrease → clogging + effect on simulated hydraulic conductivity <u>Not considered</u>: nutrients use by plants, O_2 transfer by plants, adsorption Matlab

Appendix II

Tables from the CW2D model

Table II.1: Stoichiometric matrix of reactions in CW2D

N	1	2	3	4	5	6	7	8	9	10	11	12	
components	O2	CR	CS	CI	XH	XANs	XANb	NH4N	NO2N	NO3N	N2N	IP	
R processes \ units	gO2	gCOD	gCOD	gCOD	gCOD	gCOD	gCOD	gN	gN	gN	gN	gP	
Heterotrophic organisms													
1 hydrolysis		$1-f_{hyd,CI}$	-1	$f_{hyd,CI}$				$\nu_{1,N}$					$\nu_{1,P}$
2 aerobic growth of heterotrophs on readily biodegradable COD	$1 - 1/Y_H$	$-1/Y_H$			1			$\nu_{2,N}$					$\nu_{2,P}$
3 NO3-growth of heterotrophs on readily biodegradable COD		$-1/Y_H$			1			$\nu_{3,N}$		$-(1-Y_H)/2.86Y_H$	$(1-Y_H)/2.86Y_H$		$\nu_{3,P}$
4 NO2-growth of heterotrophs on readily biodegradable COD		$-1/Y_H$			1			$\nu_{4,N}$	$-(1-Y_H)/1.71Y_H$		$(1-Y_H)/1.71Y_H$		$\nu_{4,P}$
5 lysis		$f_{BM,CR}$	$1-f_{BM,CR}-f_{BM,CI}$	$f_{BM,CI}$	-1			$\nu_{5,N}$					$\nu_{5,P}$
Nitrosomonas													
6 aerobic growth of N.somonas on NH4	$-(3.43-Y_{ANs})/Y_{ANs}$					1		$i_{N,BM}-1/Y_{ANs}$	$1/Y_{ANs}$				$\nu_{6,P}$
7 lysis of N.somonas		$f_{BM,CR}$	$1-f_{BM,CR}-f_{BM,CI}$	$f_{BM,CI}$		-1		$\nu_{7,N}$					$\nu_{7,P}$
Nitrobacter													
8 aerobic growth of N.bacter on NO2	$-(1.14-Y_{ANb})/Y_{ANb}$						1	$\nu_{8,N}$	$-1/Y_{ANb}$	$1/Y_{ANb}$			$\nu_{8,P}$
9 lysis of N.bacter		$f_{BM,CR}$	$1-f_{BM,CR}-f_{BM,CI}$	$f_{BM,CI}$			-1	$\nu_{9,N}$					$\nu_{9,P}$

Rate coefficients and kinetic parameters appearing in Table II.2 are defined, together with their values, in Table II.3.

Table II.2: Reaction rates in CW2D

R	Process / Reaction rate rc_j	
Heterotrophic organisms		
1	Hydrolysis	
	$rc_1 = K_h \cdot \frac{c_{CS}/c_{XH}}{K_X + c_{CS}/c_{XH}} \cdot c_{XH}$	(3.2)
2	Aerobic growth of heterotrophs on readily biodegradable COD	
	$rc_2 = \mu_H \cdot \frac{c_{O2}}{K_{Het,O2} + c_{O2}} \cdot \frac{c_{CR}}{K_{Het,CR} + c_{CR}} \cdot f_{N,Het} \cdot c_{XH}$	(3.3)
3	NO3-growth of heterotrophs on readily biodegradable COD	
	$rc_3 = \mu_{DN} \cdot \frac{K_{DN,O2}}{K_{DN,O2} + c_{O2}} \cdot \frac{c_{NO3}}{K_{DN,NO3} + c_{NO3}} \cdot \frac{K_{DN,NO2}}{K_{DN,NO2} + c_{NO2}} \cdot \frac{c_{CR}}{K_{DN,CR} + c_{CR}} \cdot f_{N,DN} \cdot c_{XH}$	(3.4)
4	NO2-growth of heterotrophs on readily biodegradable COD	
	$rc_4 = \mu_{DN} \cdot \frac{K_{DN,O2}}{K_{DN,O2} + c_{O2}} \cdot \frac{c_{NO2}}{K_{DN,NO2} + c_{NO2}} \cdot \frac{c_{CR}}{K_{DN,CR} + c_{CR}} \cdot f_{N,DN} \cdot c_{XH}$	(3.5)
5	Lysis of heterotrophs	
	$rc_5 = b_H \cdot c_{XH}$	(3.6)
Autotrophic organisms 1 – *Nitrosomonas*		
6	Aerobic growth of *Nitrosomonas* on NH4	
	$rc_6 = \mu_{ANs} \cdot \frac{c_{O2}}{K_{ANs,O2} + c_{O2}} \cdot \frac{c_{NH4}}{K_{ANs,NH4} + c_{NH4}} \cdot \frac{c_{IP}}{K_{ANs,IP} + c_{IP}} \cdot c_{XANs}$	(3.7)
7	Lysis of *Nitrosomonas*	
	$rc_7 = b_{HANs} \cdot c_{XANs}$	(3.8)
Autotrophic organisms 2 – *Nitrobacter*		
8	Aerobic growth of *Nitrobacter* on NO2	
	$rc_8 = \mu_{ANb} \cdot \frac{c_{O2}}{K_{ANb,O2} + c_{O2}} \cdot \frac{c_{NO2}}{K_{ANb,NO2} + c_{NO2}} \cdot f_{N,ANb} \cdot c_{XANb}$	(3.9)
9	Lysis of *Nitrobacter*	
	$rc_9 = b_{HANb} \cdot c_{XANb}$	(3.10)
Conversion of solid in liquid phase concentrations		
	$c_{XY} = \frac{\rho}{\theta} \cdot s_{XY}$, where $Y = H, ANs, ANb$	(3.11)
Factor for nutrients		
	$f_{N,x} = \frac{c_{NH4}}{K_{x,NH4} + c_{NH4}} \cdot \frac{c_{IP}}{K_{x,IP} + c_{IP}}$, where $x = Het, DN, ANb$	(3.12)

Table II.3: Kinetic parameters in CW2D (Henze *et al.*, 1995)

Parameter		Value
	Hydrolysis	
K_h	hydrolysis rate constant, 1 d^{-1}	3 (2)
K_X	saturation/inhibition coefficient for hydrolysis, $mg_{COD,CS}\ mg_{COD,BM}^{-1}$	0.1
	Heterotrophic microorganisms (aerobic growth)	
μ_H	maximum aerobic growth rate on CR, 1 d^{-1}	6 (3)
b_H	rate constant for lysis, 1 d^{-1}	0.4 (0.2)
$K_{het,O2}$	saturation/inhibition coefficient for O_2, $mg_{O2}\ L^{-1}$	0.2
$K_{het,CR}$	saturation/inhibition coefficient for substrate, $mg_{COD,CR}\ L^{-1}$	2
$K_{het,NH4N}$	saturation/inhibition coefficient for NH_4^+ (nutrient), $mg_{NH4N}\ L^{-1}$	0.05
$K_{het,IP}$	saturation/inhibition coefficient for P, $mg_{IP}\ L^{-1}$	0.01
	Heterotrophic microorganisms (denitrification)	
μ_{DN}	maximum denitrification rate, 1 d^{-1}	4.8 (2.4)
$K_{DN,O2}$	saturation/inhibition coefficient for O_2, $mg_{O2}\ L^{-1}$	0.2
$K_{DN,NO3N}$	saturation/inhibition coefficient for NO_3^-, $mg_{NO3N}\ L^{-1}$	0.5
$K_{DN,NO2N}$	saturation/inhibition coefficient for NO_2^-, $mg_{NO2N}\ L^{-1}$	0.5
$K_{DN,CR}$	saturation/inhibition coefficient for substrate, $mg_{COD,CR}\ L^{-1}$	4
$K_{DN,NH4N}$	saturation/inhibition coefficient for NH_4^+ (nutrient), $mg_{NH4N}\ L^{-1}$	0.05
$K_{DN,IP}$	saturation/inhibition coefficient for P, $mg_{IP}\ L^{-1}$	0.01
	Nitrification step 1 (*Nitrosomonas*)	
μ_{ANs}‡	maximum aerobic growth rate on NH_4^+, 1 d^{-1}	0.9 (0.3)
b_{ANs}‡	rate constant for lysis, 1 d^{-1}	0.15 (0.05)
$K_{ANs,O2}$‡	saturation/inhibition coefficient for O_2, $mg_{O2}\ L^{-1}$	1
$K_{ANs,NH4N}$‡	saturation/inhibition coefficient for NH_4^+, $mg_{NH4N}\ L^{-1}$	0.5
$K_{ANs,IP}$	saturation/inhibition coefficient for P, $mg_{IP}\ L^{-1}$	0.01
	Nitrification step 2 (*Nitrobacter*)	
μ_{ANb}‡	maximum aerobic growth rate on NO_2^-, 1 d^{-1}	1 (0.35)
b_{ANb}‡	rate constant for lysis, 1 d^{-1}	0.15 (0.05)
$K_{ANb,O2}$‡	saturation/inhibition coefficient for O_2, $mg_{O2}\ L^{-1}$	0.1
$K_{ANb,NO2N}$‡	saturation/inhibition coefficient for NO_2^-, $mg_{NO2N}\ L^{-1}$	0.1
$K_{ANb,NH4N}$	saturation/inhibition coefficient for NH_4^+ (nutrient), $mg_{NH4N}\ L^{-1}$	0.05
$K_{ANb,IP}$	saturation/inhibition coefficient for P, $mg_{IP}\ L^{-1}$	0.01

† Values: Henze et al. (2000), except where ‡ indicates Nowak (1996).

Appendix III

Respirometric methods for the carbon oxidation

Various methods exist for measuring the sludge biological activity. Generally, this activity results mainly in organic and inorganic carbon, nitrogenous and phosphorous compound oxidation. In the context of solid organic matter biodegradation, only the concepts concerning carbon oxidation by heterotrophic biomass were considered (Tremier *et al.*, 2005). Methods consist in measuring either the oxygen uptake, or the heat produced by these oxidations or carrying out some chemical analysis. They are validated and largely used to measure the activity of liquid materials (activated sludge), but there is a lack in literature for the measure of solid materials. To identify which methods are used to evaluate this microbial activity in a solid matrix, it is necessary to look at studies dedicated to the compost stability. These stability studies were carried out in order to efficiently control the process to avoid nuisances linked to the compost transport and conservation (smell, biogas production, pathogenic growth, etc.), themselves linked to the bacterial activity (directly or indirectly). Therefore, index or parameters directly linked to the measurement of the readily biodegradable organic matter content in the compost can be used to assess the biological stability. A low biological stability is the result of an important content of the readily biodegradable part (Adani *et al.*, 2004). Assessment methods of the biological stability can be based on physical (temperature, aeration demand, smell and color, optical density of aqueous extracts), chemical (volatile solids, C/N ratio, COD, humic substances, etc.), and biological (respiration measured either as oxygen uptake, carbon dioxide production, or heat generation, enzymatic activities, plant growth, etc.) characteristics of the compost (Barrena *et al.*, 2006). Despite the fact that a lot of methods have been proposed to determine the biological stability in solid media, there is no general consensus on the use of one common respirometric technique. Nevertheless, many research groups worked on this domain (Barrena *et al.*, 2006) and many assays have been developed under aerobic conditions (Adani *et al.*, 2004). Among all the proposed methods, respiration index based on the oxygen uptake rate or on the cumulative oxygen uptake can be successfully used to predict biological stability in heterogeneous solid waste. Therefore, respirometric tests are known to be the most reliable methods to measure the biological stability (Lasaridi *et al.*, 2000; Paletski and Young, 1995) as they are a direct measurement of the microbial activity (Adani *et al.* 2004). Anyway, as no clear trend and no net conclusion about the use of chemical parameters like COD can be made, their use is not recommended for the study of waste treatment units

including biological treatments, as reported by Lasaridi and Stentiford (1998) and Scaglia and Adani (2008).

To estimate microbial activity, various respirometric tests can be used: measurement of dissolved or gaseous oxygen concentration, change of the carbon dioxide production (Barrena *et al.*, 2006). The carbon dioxide production is directly correlated to the aerobic respiration. The most widespread measurement methods are those using alkaline traps for carbon dioxide. Some more complex methods are based on colorimetric techniques and gas chromatography. Nevertheless, respirometric methods which monitor only the carbon dioxide production underestimate the sample biodegradability. Indeed, carbon dioxide is a product resulting from aerobic and anaerobic reactions and, even if composting is a aerobic process, the development of anaerobic local zones can be observed (Haug, 1993; Epstein, 1997). Lasaridi and Stentiford (1998) declared thus that these methods can not be used to assess a respiration index of compost. Consequently, methods based on the **oxygen uptake** rate are preferred to estimate the potential biodegradability of solid organic waste (Lasaridi and Stentiford, 1998).
In addition, respirometric tests based on the oxygen uptake can be divided between static and dynamic methods in relation to the oxygen uptake measurement carried out without (static) or with (dynamic) a continuous aeration of the biomass (Scaglia *et al.*, 2000; Adani *et al.*, 2004). The choice depends also on the studied media activity: for low activity, static respirometry is recommended and dynamic ones for high activity.

- Static methods consist in oxygen uptake measurement into a closed container. Only the oxygen initially present in the container can be consumed. Air composition is measured at the beginning and at the end of the experiment (Adani *et al.*, 2004). As well as system simplicity, these methods are accurate due to the absence of entrance/exit in mass balances. However, they induce an oxygen transfer limitation through the biomass and bacterial cells which reduce or inhibit the aerobic biological processes (Paletski and Young, 1995; Adani *et al.*, 2002). Therefore, the oxygen uptake and thus the sample biodegradability can be underestimated (Giraldo and Zarate, 2001).

- These problems are not met with **dynamic** methods. They have the advantage to minimize the oxygenation limitation. In these systems, the respirometric reactor, filled with the studied sample, is continuously supplied with oxygen to ensure its diffusion within the matrix as well as aerobic conditions. In the dynamic method proposed by Adani *et al.* (2004), the dynamic respiration index (DRI, [$mgO_2.kgVS^{-1}.h^{-1}$]), is determined by measuring the difference

of the oxygen concentration between the entrance and the exit of the air flow passed through the solid sample:

$$DRI = Q \cdot \Delta O_2 \cdot Vg^{-1} \cdot 31.98 \cdot VS^{-1} \cdot \theta^{-1} \qquad \text{[Eq. III.1]}$$

with, Q: airflow [$L.h^{-1}$];

θ: acquisition time [h] ;

ΔO_2: difference in oxygen concentration in the inlet and outlet air flow of the reactor [$mL.L^{-1}$];

V_g: volume occupied by one mole of gas at inlet air temperature [$L.mol^{-1}$];

31.98: molecular weight of oxygen [$g.mol^{-1}$];

VS: total volatile solids present at the time of measurement [kg].

The biological stability degree is calculated as the mean value of the twelve indexes of instantaneous respiration (DRI_i) recorded during 24 h. In their study only one measurement was carried out every 2 hours. This value characterized by the most intense oxygen uptake ($DRI_{DiProVe}$, [$mgO_2.kgVS^{-1}.h^{-1}$]), is calculated as follows (Scaglia *et al.* 2000):

$$DRI_{DiProVe} = \sum_{t=0}^{24} \left(DRI_i(t) \right) / 12 \qquad \text{[Eq. III.2]}$$

According the assay conditions, authors point out the difference between a real dynamic respiration index (RDRI) carried out without moisture adjustment, and a potential dynamic respiration index (PDRI) carried out with moisture adjustment. According to Adani *et al.* (2001, 2003, 2004), this technique presents the following advantages: (i) continuous presence of an air flow during the measurement (dynamic condition) which does not limit the oxygen transfer through the biomass and in bacterial cells; (ii) capacity to work on large masses (up to 13 kg) saving thus the sample representativeness. Therefore, the DRI measurement represents the large-scale composting process at laboratory scale (Adani *et al.*, 2004).

The oxygen content can be measured either directly or in an aqueous solution. A method based on BOD was also suggested by Lasaridi and Stentiford (1998). The dynamic method is carried out by a continuous biomass mixing combined with an intermittent aeration Two indexes are obtained: the specific oxygen uptake rate (SOUR, [$mgO_2.gVS^{-1}.h^{-1}$]), and the oxygen demand in twenty hours (OD_{20}, [$mgO_2.gVS^{-1}$]).

- SOUR index represents the maximum rate of oxygen uptake (peak of the respirogram representing the oxygen uptake rate):

$$SOUR = \frac{60 \cdot |S|_{max} \cdot V}{m \cdot DS \cdot VS} \quad \text{[Eq. III.3]}$$

with, 60: factor change from minutes to hours;
$|S|_{max}$: absolute maximum slope [$mgO_2.L^{-1}.min^{-1}$];
V: volume of the suspension [L];
m: mass of the compost sample [g, wet weight];
DS: fraction of dry solids (from 0 to 1);
VS: fraction volatile solids (from 0 to 1).

- OD_{20} index is the cumulative oxygen demand for the first twenty hours of the test:

$$OD_{20} = \frac{60 \cdot V}{m \cdot DS \cdot VS} \cdot \int_{t=0}^{20} |S|_t \cdot dt \quad \text{[Eq. III.4]}$$

with $|S|_t$:= the rate of oxygen uptake at time t [$mgO_2.L^{-1}.min^{-1}$].

For the SOUR determination, a dissolved oxygen probe is used to measure the oxygen concentration change of a solid samples put in suspension in water under optimal conditions for the microbial activity. The OD_{20} is calculated by integrating the dissolved oxygen diminution curve from 0 h to 20 h. These two methods can be used to determine the stability of a compost sample. However, the SOUR determination is faster (Chica *et al.*, 2003) and Scaglia *et al.* (2007) showed that for a large biological stability degree, the SOUR index is less accurate than the OD_{20} index. Moreover, this method requires only a simple reading of the oxygen concentration during the experiment whereas OD_{20} method requires a graphical integration.

The dry specific oxygen uptake rate (DSOUR) for a dry solid sample is calculated by Iannotti *et al.* (1993). A comparison with the SOUR index had been carried out (Lasaridi *et al.*, 2000) to monitor the composting process. These two indexes follow the same evolution: respiration rate increase during the first decomposition steps (Iannotti *et al.*, 1993) due to the large organic molecules breaking into smaller and soluble ones, and temporarily more substrate is available. A good correlation is highlighted between these two indexes (correlation coefficient = 0.94 or0.85). But for fresh compost, DSOUR values are irregular and lower than the SOUR ones, this difference between the two indexes decreasing with composting time. Consequently, DSOUR index can not clearly represent a composting step where the bacterial activity is important (Lasaridi and Stentiford, 1998).

According to Lasaridi and Stentiford (1998), measuring the respiration rate of a compost aqueous suspension rather than a solid compost sample offers still some advantages:

- The test is not affected by changes of the sample water matrix;
- There is an immediate contact between the substrate, microorganisms and oxygen leading to maximum reaction rates;
- The liquid-gas barrier at the compost particle surface for the oxygen diffusion is not considered;
- Results obtained with liquid samples are more repeatable.

Nevertheless, methods using this kind of liquid samples move away from actual conditions and consequently the result concerning the stability level of the biodegradation kinetics does not consider the influence of the **solid matrix** characteristics (moisture, media particle size, etc.). Indeed, liquid respirometry (saturated media) is not suitable for study of unsaturated matrix because operating conditions do not reproduce processes and constraints linked to the gaseous oxygen. Moreover, under saturated conditions, predominant microorganisms can be different of those operating under unsaturated conditions. Finally, liquid respirometry is limited by the small sample quantity used for the assays (3-8 g), which is not a restrictive aspect for the solid respirometry.

In Europe, respiration activity after four days (AT_4, [$gO_2.kgDM^{-1}$]) and the DRI are recommended as parameters for the compost stability estimate (European Commission, 2001; Barrena *et al.*, 2009). AT_4 is the cumulative value of the oxygen uptake recorded during 96 h (four days). This value is obtained by numerical integration of the instantaneous DRI (DRI_i) values obtained during 96 h (European Commission, 2001).

$$AT4 = \sum_{t=0}^{96} DRI_i \qquad \text{[eq. III.5]}$$

Appendix IV

Respirometric techniques applied to studies of the compost stability, liquid sludge for composting and wastewater from VFCW

Table IV.1: Respirometric techniques applied to the compost study

Matrix type/ Process	Authors	Measurement	Procedure	Respirometric method	O_2 phase	Respirometry type	Respirometer volume /waste mass	Experiment length	T° (°C)	Water/ Moisture	Main conclusions
Organic wastes	Adani *et al.* (2004)	Biological stability	DRI Concentration difference in/out	Dynamic Continuous airflow rate	Gaseous	Solid	148 L/ 30-40 kg	96 h	-	Moisture 75%	DRI describes the biological stability in relation to the waste age DRI = useful method to measure the biological stability of organic wastes
Compost	Scaglia *et al.* (2007)	Biological stability of compost	Suspension of solid sample in an aqueous medium SOUR/OD_{20}/ OD_{12}	Dynamic (intermittent feeding) Cycles: 15 min aeration 15 min measure	Liquid	Liquid	1 kg	20 h	35	-	Confirmation that SOUR, OD_{20},OD_{12} indexes can be used as biological stability indicator OD_{20}, OD_{12} are more recommended for high degrees of biological stability
Municipal solid wastes - Mechanical-biological treatment (MBT)	Scaglia and Adani (2008)	Aerobic reactivity of waste	DRI Concentration difference in/out	Dynamic Continuous airflow rate	Gaseous	Solid	30 L/ 10-13 kg	58 h	-	Moisture 75%	-

Table IV.2: Respirometric techniques applied to the study of liquid sludge by composting

Matrix type/ Process	Authors	Measurement	Procedure	Respirometric method	O_2 phase	Respirometry type	Respirometer volume /waste mass	Experiment length	T° (°C)	Water/ Moisture	Main conclusions
Sludge compost - Composting	Lasaridi and Stentiford (1998)	Compost stability	Aqueous compost suspension. $SOUR/OD_{20}$	Dynamic (intermittent feeding) Cycles: 20 min aeration 15 min measure	Liquid	Liquid	3-8 g	30 h	30	500 mL of water	Advantages of measurements in φ_{liquid} than in φ_{solid} Identical tendencies but SOUR preferred to OD_{20} as respiration indicator: easier to calculate and relates directly to the stability degree
Sewage sludge - Composting	Tremier *et al.* (2005)	Biological reaction kinetics O_2 uptake rates OM characterisation Temperature influence on kinetics	Respirometric cell rO_2 [$mmolO_2.kgDM^{-1}.h^{-1}$]	"Static" Only recirculation of the initial gas volume	Gaseous	Solid	10 L/ 2.3 kg	10-20 days	37 - Between 19.6 and 56.9	Constant moisture 53 %	Reliable tool for the biodegradability characterisation of the solid organic matter ; biological kinetic modelling
Urban sludge-household wastes - Composting	Berthe *et al.* (2007)	Biological stability	Respirometric cell rO_2 [$mmolO_2.kgDM^{-1}.h^{-1}$]	Dynamic Continuous airflow rate (compressed)	Gaseous	Solid	10 L	700 h	40	53 % Moisture variation	Interest of the mixing during the test Respirometer: - validated in terms of T°/aeration - not validated in terms of moisture

Table IV.3: Respirometric techniques applied to the study of wastewater from VFCW

Matrix type/ Process	Authors	Measurement	Procedure	Respirometric method	O_2 phase	Respirometry type	Respirometer volume /waste mass	Experiment length	T° (°C)	Water/ Water flow	Main conclusions
Wastewater - CW VF	Giraldo and Zarate (2001)	Metabolic activities = kinetics of O_2 uptake, CO_2 production, organic matter degradation	VFCW columns (sand+ gravel) Samples in respirometer IR gas analyzer: % in O_2 and CO_2 volume	"Static" Only initial gas volume recycling When O_2content reaches a constant value → provision of fresh air provision	Gaseous	Solid	Erlenmeyer	22 h	30	-	Sorption = main mechanism for organic matter removal from the wastewater; biological oxidation bio. secondly during the rest period Degradation rate depending on O_2 content in $\varphi_{gaseous}$
Wastewater - CW VF	Andreottola *et al.* (2006)	OUR = difference between top/bottom concentrations Maximum kinetic parameters (OM oxidation = readily/slowly biodegradable COD, nitrification, endogenous respiration)	VFCW columns (sand+ gravel) A series of respirometers at the column exit	Dynamic Provision of O_2	Liquid $O_{2dissolved}$ content	Liquid	-	24-48 hours	20	3.2 L 23 $L.h^{-1}$	1) uptake of readily biodegradable COD 2) uptake of slowly biodegradable COD + nitrification 3) endogenous respiration Respirometry = valid tool to control OM oxidation + nitrification in VFCW + measure kinetic rates

Appendix V

Characteristics of the different devices available

Five respirometric devices have been identified providing an experimental volume allowing working with raw media: (1,2) the device allowing calculating the DRI, designed with two experimental cell sizes (Adani *et al.*, 2004, 2006), and (3,4,5) the respirometers developed by Gea *et al.* (2004), Tremier *et al.* (2005) and Berthe *et al.* (2007), this latter being adapted from the device developed by Tremier *et al.* (2005). Compared to others, the two latter have two main advantages. Firstly, their aeration system includes a rapid air recirculation in the cell of a part of the extracted air which ensure an oxygen diffusion more homogeneous into the biomass without any harmful behavior of the air flow (dead volume, short-circuit, etc.) than a simple forced aeration method. Therefore, oxygen is not limiting for the biodegradation (Tremier *et al.*, 2005). Secondly, in these systems the experimental cell and its immersion in a water bath allow to carry out a temperature and moisture control in order that they are homogeneous into the sample. Comparison between respirometric profiles is thus easier. Although the Tremier *et al.* (2005) respirometric device is a validated, repeatable and reproducible method for measuring oxygen uptake kinetics, respecting the solid matrix characteristics, with controlled aeration conditions, temperature and moisture, a new method presented by Berthe *et al.* (2007) improves the control of environmental parameter (Figure V.1). It couples a respirometer device with an air pycnometer. Air pycnometer provides indirect FAS measurements by relating the system's pressures and volumes using the ideal gas law. This equipment allows to observe the FAS evolution within the sample during respirometric experiments and to check that this parameter stays favorable to the sample aeration. It is designed to allow the control of operating conditions: temperature, moisture and aeration. Methane was chosen as a gas tracer after having verified that there was no significant methane production during the respirometric experiments and it was not noxious for microorganisms. It is controlled that measurements carried out with the pycnometer have no influence on respirometric measurement and repeatability of these measurements is confirmed.

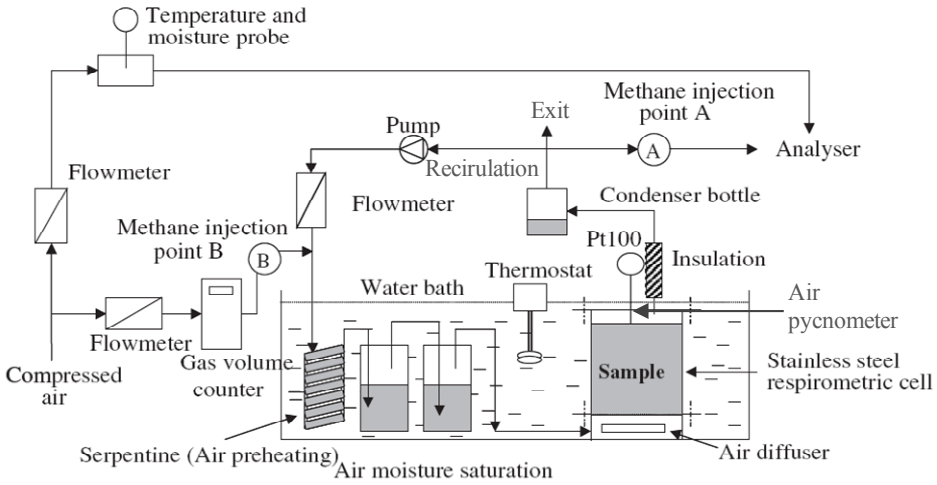


Figure V.1: Respirometric device used by Berthe *et al.* (2007) after modifications of the Tremier *et al.* (2005) device

During the Adani *et al.* (2001) respirometric tests, material mixings and water addition led to an increase of the biological activity. Authors concluded that these operations help to restore favourable conditions for the biodegradation. If a low or no oxygen uptake rate is recorded after a sample mixing, that corresponds either to a low biodegradability material, or to initial moisture content too high. Experiences carried out with the Berthe *et al.* (2007) respirometer confirmed the need to mix samples for quantifying all the biodegradable organic matter. Indeed, when the oxygen uptake rate reaches a low and stable value, in particular for sludge from wastewater treatment, material mixings stimulate again the oxygen uptake, confirming thus the presence of residual biodegradable organic. The second oxygen uptake peak can represent between 23 % and 37 % of the total consumed oxygen after a manual material mixing (Berthe *et al.*, 2007).
The presence of residual biodegradable organic matter can be explained by two biodegradation limiting factors: the moisture and the FAS of the sample (Berthe *et al.*, 2007).

- While during the respirometric experiments the material temperature is constant and homogenous, some high variations concerning the moisture content within the sample are measured between beginning and end of the test, independently of the fact that the gaseous phase is considered as completely stirred. Some areas with limiting moisture appear and lead to a new oxygen uptake after mixing.

- In the high moisture case, low FAS within the sample can be at the origin of this limiting oxygen uptake leading to oxygen diffusion problems within the sample. Indeed, after each mixings, the FAS is higher than before, confirming thus the beneficial effect of this method to get a complete biodegradation of the samples.

The main mixing effect is therefore to restore favorable environment for biodegradation (moisture and FAS within sample). This beneficial effect seems to be more important for a matrix with a high quantity of slowly biodegradable organic matter and with a low initial moisture content (Berthe *et al.*, 2007).

Despite the fact that the moisture control is not validated, the respirometer developed by Berthe *et al.* (2007), associating respirometric measurements under controlled environment and in-situ FAS measurements, is perfectly adapted for the biodegradability study of organic wastes from various origins at different evolution degrees.

References

Adani, F., Lozzi, P. and Genevini, P. (2001). Determination of biological stability by oxygen uptake on municipal solid waste and derived products. *Compost Science and Utilization*, **9**(2): 163-178.

Adani, F., Baido, D., Calcaterra, E. and Genevini, P. (2002). The influence of biomass temperature on biostabilization-biodrying of municipal solid waste. *Bioresource Technology*, **83**(3): 173-179.

Adani, F., Gigliotti, G., Valentini, F. and Laraia, R.. (2003). Respiration index determination: A comparative study of different methods. *Compost Science and Utilization*, **11**(2): 144-151.

Adani, F., Confalonieri R. and Tambone, F. (2004). Dynamic respiration index as a descriptor of the biological stability of organic wastes. *Journal of Environment Quality*, **33**(5): 1866-1876.

Adani, F., Ubbiali, C. and Generini, P. (2006). The determination of biological stability of composts using the Dynamic Respiration Index: The results of experience after two years. *Waste Management*, **26**(1): 41-48.

Aji, S., Tavolaro, S., Lantz, F. And Faraj, A. (2003). Contribution of bootstrap techniques to PLS regression: Application to the prediction model of gas-oil quality control. *Oil and Gas Science and Technology*, **58**(5): 599-608.

Altevogt, A. and Celia, M. (2004). Numerical modeling of carbon dioxide in unsaturated soils due to deep subsurface leakage. *Water Resources Research*. (40), W03509, doi:10.1029/2003WR002848.

Andreottola, G., Oliveira E., Foladori, P., Peterlini, R. and Ziglio, G. (2007). Respirometric techniques for assessment of biological kinetics in constructed wetland. *Water Science and Technology*, **56**(3): 255-261.

APHA, AWWA, WPCF. (2005). Standard methods for the examination of water and wastewater, 21th ed. Amer Public Health Assoc., *Amer. Water Works Assoc, Water Poll. Control Fed., Washington, DC.*

Archie, G. (1942). The electrical resistivity log as an aid in determining some reservoir characteristics, *Transactions America Institute Mining Metallurgical and Petroleum Engineers*, **146**: 54-62.

Asano, T. (1991) Planning and implementation of water reuse projects. *Water Science and Technology*, **24**(9): 1-10.

Barrena Gómez, R., Vázquez Lima, F. and Sánchez Ferrer, A. (2006). The use of respiration indices in the composting process: A review. *Waste Management and Research*, **24**(1): 37-47.

Barrena, R., d'Imporzano, G., Ponsá, S., Gea, T., Artola, A., Vázquez, F., Sánchez, A. and Adani, F. In search of a reliable technique for the determination of the biological stability of the organic matter in the mechanical-biological treated waste. *Journal of Hazardous Materials*, **162**(2-3): 1065-1072.

Basile, A., Ciollaro, G. and Coppola, A. (2003). Hysteresis in soil water characteristics as a key to interpreting comparisons of laboratory and field measured hydraulic properties. *Water Resources Research*, **39**(12): SBH131-SBH1312.

Berthe, L., Druilhe, C., Massiani, C., Tremier, A. and de Guardia, A. (2007). Coupling a respirometer and a pycnometer, to study the biodegradability of solid organic wastes during composting. *Biosystems Engineering*, **97**(1): 75-88.

Beven, K. and Freer, J. (2001). Equifinality, data assimilation, and uncertainty estimation in mechanistic modelling of complex environmental systems using the GLUE methodology. *Journal of Hydrology*, **249**(1-4): 11-29.

Binley, A. and Kemna, A. (2005). Dc Resistivity and Induced Polarization Methods. In: Rubin, Y. and Hubbard, S. (Ed.), Hydrogeophysics*, Springer*.

Birkinshaw, S.J. and Ewen, J. (2000). Nitrogen transformation component for SHETRAN catchment nitrate transport modelling. *Journal of Hydrology*, **230**(1-2): 1-17.

Boutin, C., Liénard, A. and Lesavre, J. (2000). Filières d'épuration pour petites collectivités: les cultures fixées sur supports fins. *Ingénieries*, **24**: 3-13.

Boutin, C., Liénard, A. and Molle, P. (2007). Les filtres plantés de roseaux, le lagunage naturel et leur association: comment ? pourquoi ? *Sinfotech* – Les fiches de synthèse.

Brix, H. (1987). Treatment of wastewater in the rhizosphere of wetland plants - the root-zone method. *Water Science and Technology*, **19**(1-2): 107-118.

Brix, H. (1997). Do macrophytes play a role in constructed treatment wetlands? *Water Science and Technology*, **35**(5): 11-17.

Brix, H. and Johansen, N.H. (2004). Guidelines for vertical flow constructed wetland systems up to 30 PE. Økologisk Byfornyelse og Spildevandsrensning No.52. *Copenhagen, Denmark: Miljøstyrelsen, Miljøministeriet.*

Burvingt, F. and Heduit, A. (1987). Cinétique de nitrification, étude bibliographique. Université Paris Val-de-Marne and Cemagref, Paris, 53 P.

Chica, A., Mohedo, J.J., Martín, M.A. and Martín, A. (2003). Determination of the stability of MSW compost using a respirometric technique. *Compost Science and Utilization*, **11**(2): 169-175.

Choubert, J.M., Marquot, A., Stricker, A.E., Gillot, S., Racault, Y., Héduit, A. (2008). Maximum growth and decay rates of autotrophic biomass to simulate nitrogen removal at 10°C with municipal activated sludge plants. *Water SA* **34**(1): 71-76.

Choubert, J.-M., Stricker, A.-E., Marquot, A., Racault, Y., Gillot, S. and Héduit, A. (2009). Updated activated sludge model no1 parameter values for improved prediction of nitrogen removal in activated sludge processes: validation at 13 full-scale plants. *Water Environment Research*, **81**(9): 858-865.

Ciollaro, G., and Romano, N. (1995). Spatial variability of the soil hydraulic properties of a volcanic soil. *Geoderma*, **65**: 263–282.

Dane, J. H. and Topp, G. C. Eds. (2002) Methods of Soil Analysis Part 4 - Physical Methods. Soil Science Society of America, Madison, WI.

Delrue, F., Choubert, J.M., Stricker, A.E., Spérandio, M., Mietton Peuchot, M. and Racault, Y. (2010). Modelling a full scale membrane bioreactor using Activated Sludge Model n°1: challenges and solutions. *Water Science and Technology*, **62**(10): 2205-2217.

DERU. 21 May 1991. La directive n° 91/271/CEE du 21 mai 1991 relative au traitement des eaux urbaines résiduaires.

Dirksen, C. and Dasberg, S. (1993). Improved calibration of time domain reflectometry soil water content measurements. *Soil Science Society of America Journal*, **57**: 660-667.

Dittmer, U., Meyer, D. and Langergraber, G. (2005). Simulation of a subsurface vertical flow constructed wetland for CSO treatment. *Water Science and Technology*, **51**(9): 225-232.

Dold, P.L., Jones, R.M. and Bye, C.M. (2005). Importance and measurement of decay rate when assessing nitrification kinetics. *Water Science and Technology*, **52**(10-11): 469-477.

Durner, W., Jansen, U. and Iden, S.C. (2008). Effective hydraulic properties of layered soils at the lysimeter scale determined by inverse modelling. *European Journal of Soil Science*, **59** (1): 114-124.

El Mossaoui, M. (2001) L'infiltration-percolation en traitement des eaux usées. Etude des performances et adaptation du procédé. *Fondation Universitaire Luxembourgeoise.*

Epstein, E. (1997). The Science of Composting. *Technomic Publishing Company, Inc., Basel, Switzerland*.

Fdz-Polanco, F.E.M., Uruena, M.A., Villaverde, S. and Garcia, P.A. (2000). Spatial distribution of heterotrophs and nitrifiers in a submerged biofilter for nitrification. *Water Research*, **34**(16): 4081–4089.

Feray, C., Volat, B., Degrange, V., Clays-Josserand, A. and Montuelle, B. (1999). Assessment of three method for detection and quantification of nitrite-oxidizing bacteria and nitrobacter in freshwater sediments (MPN-PCR, MPN-Griess, Immunofluorescence). *Microbial Ecology*, **37**: 208-217.

Ferré, P.; Knight, J.; Rudolph, D. and Kachanoski, R. (1998). The sample areas of conventional and alternative time domain reflectometry probes. *Water Resources Research*, **34**: 2971-2979.

Feyen, J., Jacques, D., Timmerman, A. and Vanderborght, J. (1998). Modelling water flow and solute transport in heterogeneous soils: A review of recent approaches. *Journal of Agricultural Engineering Research*, **70**(3): 231-256.

Ficara E. and Rozzi A. (2001). pH-stat titration to assess nitrification inhibition. *Journal of Environmental Engineering*, **127**(8): 698-704.

Flemming, H-C. (1993). Biofilms in environmental protecion. *Water Science and Technology*, **27**(7-8): 1-10.

Flint, A. L. and Flint, L. E. (2002). Porosity. In: Dane, J. and Topp, G. (Eds.), Methods of Soil Analysis. Part 4 - Physical methods. *SSSA Book Series 5, Madison, WI*, 241–254.

Forquet, N.; Wanko, A.; Molle, P.; Mosé, R. and Sadowski, A.-G. (2009a). Two-Phase flow modelling for oxygen renewal estimation in vertical flow filter: luxury or necessity? *Water Science and Technology*, **59**: 2311-2319.

Forquet, N.; Wanko, A.; Mosé, R. and Sadowski, A. (2009b). Diphasic Modelling of Vertical Flow Filter. *Ecological Engineering*, **35**(1): 47-56.

Freire, F.G., Davies, L.C., Vacas, A., Pedro, I., Novais, J.M. and Martin-Dias, S. (2006). Continuous and intermittent loading of a vertical flow constructed wetland for an azo dye treatment. *10th International Conference on Wetland Systems for Water Pollution Control,* Lisbon, Portugal, 1501-1509.

French, H. and Binley, A. (2004). Snowmelt infiltration: monitoring temporal and spatial variability using time-lapse electrical resistivity, *Journal of Hydrology*, **297**: 174-186.

Fujiyasu, Y., Pierce, C., Fan, L. and Wong, C. (2004). High dielectric insulation coating for time domain reflectometry soil moisture sensor, *Water Resources Research*, **40**: 6021-6027.

Gea, T., Barrena, R., Artola, A. and Sanchez, A. (2004). Monitoring the biological activity of the composting process: oxygen uptake rate (OUR), respirometric index (RI), and respiratory quotient (RQ). *Biotechnology Bioengineering*, **88**: 520-527.

Giraldi, D. and Iannelli, R. (2009). Measurements of water content distribution in vertical subsurface flow constructed wetlands using a capacitance probe: benefits and limitations. *Desalination*, **243**: 182-194.

Giraldi, D., Masciandaro, G., Peruzzi, E., Bianchi, V., Peruzzi, P., Ceccanti, B. and Iannelli, R. (2009). Hydraulic and biochemical analyses on full-scale sludge consolidation reed beds in Tuscany (Italy). *Water Science and Technology*, **60**(5): 1209-1216.

Giraldi, D., de Michieli Vitturi, M. and Iannelli, R. (2010). FITOVERT: A dynamic numerical model of subsurface vertical flow constructed wetlands. *Environmental Modelling and Software*, **25**(5): 633-640.

Giraldo, E., Zarate, E. (2001). Development of a conceptual model for vertical flow wetland metabolism. *Water Science and Technology*, **44**(11-12): 273-280.

Grison, C. (1999) Epuration des eaux usées par filtres plantés de macrophytes: une étude bibliographique. *Agence de l'eau Rhône-Méditerranée et Corse*.

Gregory, P.J., Poss, R., Eastham, J. and Micin, S. (1995). Use of time domain reflectometry (TDR) to measure the water content of sandy soils. *Australian Journal of Soil Research*, **33**: 265-276.

Haberl, R., Grego, S., Langergraber, G., Kadlec, R.H., Cicalini, A.-R., Dias, S.M., Novais, J.M., Aubert, S., Gerth, A., Thomas, H. and Hebner, A. (2003) Constructed wetlands for the treatment of organic pollutants. *Journal of Soils and Sediments*, **3**(2): 109-124.

Hauduc, H., Neumann, M. B., Muschalla, D., Gamerith, V., Gillot, S.and Vanrolleghem, P.A. (2011). Towards quantitative quality criteria to evaluate simulation results in wastewater treatment – A critical review. 8th IWA Symposium on Systems Analysis and Integrated Assessment. Conference Proceedings: 36-46.

Haug, R.T.. (1993). The Practical Handbook of Compost Engineering. *Lewis Publishers, Boca Raton.* p. 717.

Hayley, K., Bentley, L., Gharibi, M. and Nightingale, M. (2007). Low temperature dependence of electrical resistivity: Implications for near surface geophysical monitoring. *Geophysical Research Letters*, **34**, 5 p.

Heaton, T.H.E. (1986) Isotopic studies of nitrogen pollution in the hydrosphere and atmosphere: a review. *Chemical Geology*, **59**: 87-102.

Heimovaara, T. J. (1993). Design of triple-wire time domain reflectometry probes in practice and theory. *Soil Science Society America Journal*, **57**: 1410-1417.

Henrichs, M., Langergraber, G. and Uhl, M. (2007). Modelling of organic matter degradation in constructed wetlands for treatment of combined sewer overflow. *Science of the Total Environment*, **380**(1-3): 196-209.

Henze M., Grady C. P. L., Gujer W., Marais G.R., Matsuo T. (1987). Activated sludge model N°1, IAWQ Scientific and Technical report N°1. *London. ISSN 1010-707X,* 33 p.

Henze, M., Harremoës, P., La Cour Jansen, J. and Arvin, A. (1996). Wastewater Treatment. Biological and Chemical Processes. *Springler–Verlag: New York*.

Henze, M., Gujer, W., Mino, T., van Loosedrecht, M. (2000). Activated Sludge Models ASM1, ASM2, asm2d and ASM3. *IWA task group on mathematical modelling for design and operation of biological wastewater treatment*.

Hopmans, J.W., Simunek, J., Romano, N. and Durner, W. (2002). Simultaneous determination of water transmission and retention properties. Inverse methods. In: Dane, J., Topp, G. (Eds.), Methods of Soil Analysis. Part 4 - Physical methods. *SSSA Book Series 5, Madison, WI*, 963–1004.

Iannotti, D.A., Pang, T., Totth, B.L., Elwell, D.L., Keener, H.M. and Hoitink, H.A.J. (1993). Quantitative respirometric method for monitoring compost stability. *Compost Science and Utilization*, **1**(3): 52-65.

Jacobsen, O.H. and Schjonning, P. (1993). Laboratory calibration of time domain reflectometry for soil water measurement including effects of bulk density and texture. *Journal of Hydrology*, **151**: 147-157.

Jacques, D., Šimunek, J., Mallants, D. and Van Genuchten, M. (2005). Long term uranium migration in agricultural field soils following mineral P-fertilization. *Proceedings - 10th International Conference on Environmental Remediation and Radioactive Waste Management, ICEM'05* 2005, 934-941.

Jacques, D., Šimůnek, J., Mallants, D. and van Genuchten, M.Th. (2008). Modelling coupled water flow, solute transport and geochemical reactions affecting heavy metal migration in a podzol soil. *Geoderma*, **145**(3-4): 449-461.

Jenssen, P.D., Maehlum, T. and Krogstad, T. (1994) Adapting constructed wetlands for wastewater treatment to northern environments. *Global wetlands*, 411-420.

Jeong, J., Hidaka, T., Tsuno, H. and Oda, T. (2006). Development of biological filter as tertiary treatment for effective nitrogen removal: Biological filter for tertiary treatment. *Water Research*, **40**(6): 1127-1136.

Jiang, S., Pang, L., Buchan, G.D., Šimůnek, J., Noonan, M.J. and Close, M.E. (2010). Modelling water flow and bacterial transport in undisturbed lysimeters under irrigations of dairy shed effluent and water using HYDRUS-1D. *Water Research*, **44**(4): 1050-1061.

Kadlec, R.H., Knight, R.L. (1996). Treatment wetlands. *New York, USA: Lewis Publishers*.

Kadlec, R. H. (2000). The inadequacy of first-order treatment wetland models. *Ecological Engineering*, **15**(1-2): 105-119.

Kadlec, R., Knight, R., Vymazal, J., Brix, H.,Cooper, P. and Harberl, R. (2000). Constructed wetlands for pollution control: processes, performance, design and operation. *Portland Press LTD*.

Kadlec, R.H., Tanner, C.C., Hally, V.M. and Gibbs, M.M. (2005). Nitrogen spiraling in subsurface-flow constructed wetlands: Implications for treatment response. *Ecological Engineering*, **25**(4): 365-381.

Kadlec, R.H., (2008). The effects of wetland vegetation and morphology on nitrogen processing. *Ecological Engineering*, **33**(2): 126-141.

Kaluarachchi, J. and Parker, J. (1990) Modelling multicomponent organic chemical transport in three-fluid-phase porous media. *Journal of Contaminant Hydrology*, **5**: 349-374.

Kayser, K. and Kunst, S. (2005). Processes in vertical-flow reed beds: Nitrification, oxygen transfer and soil clogging. *Water Science and Technology*, **51**(9): 177-184.

Klute, A. and Dirksen, C. (1986). Hydraulic conductivity and diffusivity: laboratory methods. In: Klute, A. (Eds.), Methods of Soil Analysis. Part 1 – Physical and mineralogical methods. *SSSA Book Series 5, Madison, WI*, 47.

Knight, J. (1992). The Sensitivity of Time Domain Reflectometry Measurements to Lateral Variations in Soil Water Content. *Water Resources Research*, **28**: 23-45.

Knight, J. H., Ferré, P. A., Rudolph, D. L. and Kachanoski, R. G. (1997). A numerical analysis of the effects of coatings and gaps upon relative dielectric permittivity measurement with time domain reflectometry, *Water Resources Research*, **33**: 1455-1460.

Kool, J.B., Parker, J.C. and van Genuchten, M.Th. (1987). Parameter estimation for unsaturated flow and transport models - A review. *Journal of Hydrology*, **91**(3-4): 255-293.

Kumar, S., Sekhar, M., Reddy, D.V. and Mohan Kumar, M.S. (2010). Estimation of soil hydraulic properties and their uncertainty: Comparison between laboratory and field experiment. *Hydrological Processes*, **24**(23): 3426-3435.

Laber, J. (2001). Bepflantze Bodenfilter zur weitergehenden Reinigung von Oberflächenwasser und Kläranlagenabläufen, Wiener Mitteilungen, Band 167.

Lagarde, F., Tusseau-Vuillermin, M.H., Lessard, P., Héduit A., Dutrop, F. and Mouchel, J.M. (2005). Variability estimation of urban wastewater biodegradable fractions by respirometry. *Water Research,* **39**(19): 4768 - 4778.

Laloy, E., M. Weynants, C. Bielders, M. Vanclooster, and M. Javaux (2010). How efficient are one-dimensional models to reproduce the hydrodynamic behavior of structured soils subjected to multi-step outflow experiments. *Journal of Hydrology*, **393**: 37-52.

Laloy, E.; Javaux, M.; Vanclooster, M.; Roisin, C. and Bielders, C. L. (2011). Electrical Resistivity in a Loamy Soil: Identification of the Appropriate Pedo-Electrical Model. *Vadose Zone Journal*, **10**: 1023-1033.

Lambot S., F. Hupet, M. Javaux M. and M. Vanclooster (2005). Inverse modelling techniques to characterize soil transport processes. In: I. Alvarez-Benedi and R. Munoz-Carpena (eds). Soil-water-solute processes in environmental systems. Monitoring, characterization and modelling. *CRC press*. 693-709.

Lambot S., F. Hupet , M. Javaux and M. Vanclooster (2002) Inverse Estimation of Soil Hydraulic Properties from Transient Flow Experiments using Global Optimization by Multilevel Coordinate Search. *Water resources research*, **38**(11): 6.1-6.15.

Langergraber, G. (2002) Calibration of a simulation tool for subsurface flow constructed wetlands for wastewater treatment. *Developments in Water Science*, **47**: 663-670.

Langergraber, G. (2003). Simulation of subsurface flow constructed wetlands, results and further research needs. *Water Science Technology*, **48**(5): 157-166.

Langergraber, G. (2005). The role of plant uptake on the removal of organic matter and nutrients in subsurface flow constructed wetlands: A simulation study. *Water Science and Technology*, **51**(9): 213-223.

Langergraber, G. (2007). Simulation of the treatment performance of outdoor subsurface flow constructed wetlands in temperate climates. *Science of the Total Environment*, **380**(1-3): 210-219.

Langergraber, G. (2008) Modeling of processes in subsurface flow constructed wetlands: A review. *Vadose Zone Journal*, **7**(2): 830-842.

Langergraber, G. and Haberl, R. (2001). Constructed wetlands for water treatment. *Minerva Biotecnologica*, **13**(2): 123-134.

Langergraber, G., Haberl, R., Laber, J. and Pressl, A. (2003). Evaluation of substrate clogging processes in vertical flow constructed wetlands. *Water Science and Technology*, **48**(5): 25-34.

Langergraber, G. and Šimůnek, J. (2005). Modelling variably saturated water flow and multicomponent reactive transport in constructed wetlands. *Vadose Zone Journal*, **4**(4): 924-938.

Langergraber, G., Giraldi, D., Mena, J., Meyer, D., Peña, M., Toscano, A., Brovelli, A. and Korkusuz, E. A. (2009a). Recent developments in numerical modelling of subsurface flow constructed wetlands. *Science of the Total Environment*, **407**(13): 3931-3943.

Langergraber, G., Pressl, A., Leroch, K., Rohrhofer, R. and Haberl, R. (2009b) Experiences with a top layer of gravel to enhance the performance of vertical flow constructed wetlands at cold temperatures. *Water Science and Technology*, **59**(6): 1111-1116.

Lasaridi, K. E. and Stentiford, E. I. (1998). A simple respirometric technique for assessing compost stability. *Water Research*, **32**(12): 3717-3723.

Lasaridi, K.E., Stentiford, E.I. and Evans, T. (2000). Windrow composting of wastewater biosolids: Process performance and product stability assessment. *Water Science and Technology*, **42**(9): 217-226.

Lesmes, D. and Friedman, S. (2005). Relationships between the electrical and hydrogeological properties of rocks and soils. In: Rubin, Y. and Hubbard, S. (Ed.), Hydrogeophysics, *Springer*.

Liénard, A. (1987) Domestic wastewater treatment in tanks with Emergent Hydrophytes: latest results of a recent plant in France. *Water Science and Technology*, **19**(12): 373-375.

Lillo, J., Gomez, D., de Bustamante, I., Salas, J. and Martin, I. (2011). Using electrical resistivity tomography (ERT) to evaluate water flow in a vertical flow constructed wetland, *3rd International Smallwat congress, Barcelona, Spain*.

Linde, N.; Chen, J.; Kowalsky, M. B. and Hubbard, S. (2006). Hydrogeophysical parameter estimation approaches for field scale characterization. In: Vereecken, H.; Binley, A.; Cassiani, G.; Revil, A., Titov, K. (Ed.), Applied Hydrogeophysics, *Springer Netherlands*.

Loke, M. (2009). Tutorial: 2-D and 3-D electrical imaging surveys, *http://www.geoelectrical.com/downloads.php*.

Magee, P.N. (1982) Nitrogen as a potential health hazard. *Philosophical Transactions of the Royal Society of London. Series B, Biological Sciences*, **296**: 543-550

Maier, U., DeBiase, C., Baeder-Bederski, O. and Bayer, P. (2009). Calibration of hydraulic parameters for large-scale vertical flow constructed wetlands. *Journal of Hydrology*, **369**(3-4): 260-273.

Mallants, D., B. P. Mohanty, D. Jacques, and J. Feyen (1996), Spatial Variability of Hydraulic Properties in a Multi-Layered Soil Profile. *Soil Science*, **161**(3): 167-181.

Malicki, M., Plagge, R. and Roth, C. (1996). Improving the calibration of dielectric TDR soil moisture determination taking into account the solid soil. *European Journal of Soil Science*, **47**: 357-366.

Mamais, D., Jenkins, D. and Pitt, P. (1993). A rapid physical-chemical method for the determination of readily biodegradable soluble COD in municipal wastewater. *Water Research*, **27**(1): 195-197.

Marquardt, D. (1963). An algorithm for least-squares estimation of nonlinear parameters. *SIAM Journal on Applied Mathematics*, **11**: 431–441.

Marquot, A. (2006). Modelling nitrogen removal by activated sludge on full-scale plants: Calibration and evaluation of ASM1. *Université de Pau et des Pays de l'Adour*. 250 p.

Martin, J.F. and Reddy, K.R. (1997). Interaction and spatial distribution of wetland nitrogen processes. *Ecological Modelling*, **105**(1): 1-21.

Mc Bride, G.B. and Tanner, C.C. (2000). Modelling biofilm nitrogen transformations in constructed wetland mesocosms with fluctuating water levels. *Ecological Engineering*, **14**(1-2): 93-106.

McGechan, M.B., Moir, S.E., Sym, G. and Castle, K. (2005). Estimating inorganic and organic nitrogen transformation rates in a model of a constructed wetland purification system for dilute farm effluents. *Biosystems Engineering*, **91**(1): 61-75.

McNevin, D., Barford, J. and Hage, J. (1999) Adsorption and biological degradation of ammonium and sulfide on peat. *Water Research*, **33(**6): 1449–1459.

Ménoret, C. (2001) Traitement d'effluents concentrés par cultures fixées sur gravier ou pouzzolane, *Université Louis Pasteur, Strasbourg*.

Mercoiret, L., Molle, P., Forquet, N. (2010) Domestic wastewater characteristics in French rural areas: concentrations and ratios for treatment plant under 2000 population equivalent (120 kg of BOD_5 a day). *3rd International Smallwat Congress, Seville, Spain*.

Mertens, J., Madsen, H., Kristensen, M., Jacques, D. and Feyen, J. (2005). Sensitivity of soil parameters in unsaturated zone modelling and the relation between effective, laboratory and in situ estimates. *Hydrological Processes*, **19**(8): 1611-1633.

Michot, D., Benderitter, Y., Dorigny, A., Nicoullaud, B., King, D. and Tabbagh, A. (2003). Spatial and temporal monitoring of soil water content with an irrigated corn crop cover using surface electrical resistivity tomography, *Water Resources Research*, **39**: 1138-1157.

Minasny, B. and Field, D.J. (2005). Estimating soil hydraulic properties and their uncertainty: The use of stochastic simulation in the inverse modelling of the evaporation method. *Geoderma*, **126**(3-4): 277-290.

Molle, P., Liénard, A., Boutin, C.; Merlin, G. and Iwema, A. (2005). How to treat raw sewage with constructed wetlands: an overview of the french systems. *Water Science and Technology*. **51**(9): 11-21.

Molle, P. (2003) Filtres plantés de roseaux : limites hydrauliques et rétention du phosphore. *Université Montpellier II Sciences et Techniques du Languedoc.*

Molle, P., Prost-Boucle, S. and Liénard, A. (2008). Potential for total nitrogen removal by combining vertical flow and horizontal flow constructed wetlands: A full-scale experiment study. *Ecological Engineering*, **34**(1): 23-29.

Molle, P., Liénard, A., Grasmick, A. and Iwema, A. (2006). Effect of reeds and feeding operations on hydraulic behavior of vertical flow constructed wetlands under hydraulic overloads. *Water Research*, **40**(3): 606-612.

Morvannou, A., Choubert, J.-M., Vanclooster, M. and Molle, P. (2011). Solid respirometry to characterize nitrification kinetics: A better insight for modelling nitrogen conversion in vertical flow constructed wetlands. *Water Research*, **45**(16): 4995-5004.

Nowak, O., Franz, A., Svardal, K., Muller, V. and Kuhn, V. (1999). Parameter estimation for activated sludge models with the help of mass balances. *Water Science and Technology*, **39**(4): 3-120.

Morris, R., Newton, M., Knowles, P., Bencsik, M., Davies, P., Griffin, P. and McHale, G. (2011). Analysis of clogging in constructed wetlands using magnetic resonance. *Analyst*, **136**: 2283-2286.

Mualem,Y. (1976). A new model for predicting the hydraulic conductivity of unsaturated porous media. *Water Resource. Research*, **12**(3): 513-522.

Nowak, O., Schweighofer, P. and Svardal, K. (1994). Nitrification inhibition - A method for the estimation of actual maximum autotrophic growth rates in activated sludge systems. *Water Science and Technology*, **30**(6): 9-19.

Ojeda, E., Caldentey, J. and Garcia, J. (2006). 2D simulation model for evaluating biochemical pathways involved in organic matter removal in horizontal subsurface flow constructed wetlands. *10th International Conference on Wetland Systems for Water Pollution Control*, 1405-1413.

Ortigara, A.R.C., Foladori, P. and Andreottola, G. (2010). Kinetics of heterotrophic biomass and storage mechanism in wetland cores measured by respirometry. *12th IWA international conference on Constructed Wetlands, 4-9 October 2010, Venice (Italy)*.

Paletski, W.T. and Young, J.C. (1995) Stability measurement of biosolids compost by aerobic respirometry. *Compost Science & Utilization,* **3**: 16-24.

Pasztor, I., Thury, P. and Pulai, J. (2009). Chemical oxygen demand fractions of municipal wastewater for modelling of wastewater treatment. *International Journal of Environmental Science and Technology*, **6**(1): 51-56.

Petitjean, A., Wanko, A., Forquet, N., Mosé, R., Lawniczak, F. and Sadowski, A. (2011). Diphasic transfer of oxygen in vertical flow filters: A modelling approach. *Water Science and Technology*, **64**(1): 109-116.

Petitjean A., Forquet, N., Wanko, A., Laurent, J., Mosé, R. and Sadowski, A. Modelling aerobic biodegradation in vertical flow sand filters: impact of operational considerations on oxygen transfer and bacterial activity. *Submitted to Water Research*.

Radcliffe, D., and J. Šimůnek, (2010) Soil Physics with HYDRUS: Modelling and Applications. *CRC Press, Taylor and Francis Group*, 373 p.

Ramos, T.B., Gonçalves, M.C., Martins, J.C., Van Genuchten, M.Th. and Pires, F.P. (2006). Estimation of soil hydraulic properties from numerical inversion of tension disk infiltrometer data. *Vadose Zone Journal*, **5**(2): 684-696.

Reynolds, W. D. and Elrick, D. E. (2002). Constant head well permeameter (vadose zone). In: Dane, J., Topp, G. (Eds.), Methods of Soil Analysis. Part 4 - Physical methods. *SSSA Book Series 5, Madison, WI*, 844–858.

Richard, G., Sillon, J.F. and Marloie, O. (2001). Comparison of inverse and direct evaporation methods for estimating soil hydraulic properties under different tillage practices. *Soil Science Society of America Journal*, **65**(1): 215-224.

Rieger, L., Langergraber, G., Thomann, M., Fleischmann, N. and Siegrist, H. (2004). Spectral in-situ analysis of NO2, NO3, COD, DOC and TSS in the effluent of a WWTP. *Water Science and Technology*, **50**(11): 143-152.

Ritter, A., Hupet, F., Muñoz-Carpena, R., Lambot, S. and Vanclooster, M. (2003). Using inverse methods for estimating soil hydraulic properties from field data as an alternative to direct methods. *Agricultural Water Management*, **59**(2): 77-96.

Ritter A., R. Munoz-Carpena, CM. Regalado, S. Lambot and M. Vanclooster, 2004. Analysis of alternative measurement strategies for the inverse optimization of the hydraulic properties of a volcanic soil. *Journal of Hydrology*, **295**: 124-139.

Robinson, D., Jones, S., Wraith, J., Or, D. and Friedman, S. (2003a). A Review of Advances in Dielectric and Electrical Conductivity Measurement in Soils Using Time Domain Reflectrometry. *Vadose Zone Journal*, **2**: 444-475.

Robinson, D., Schaap, M., Jones, S., Friedman, S. and Gardner, C. (2003b). Considerations for Improving the Accuracy of Permittivity Measurement using Time Domain Reflectometry: Air-Water Calibration, Effects of Cable Length. *Soil Science Society America Journal*, **67**: 62-70.

Roeleveld, P.J. and Van Loosdrecht, M.C.M. (2002). Experience with guidelines for wastewater characterisation in The Netherlands. *Water Science and Technology*, **45**(6): 77-87.

Rolland, L., Molle, P., Liénard, A., Bouteldja, F. and Grasmick, A. (2009). Influence of the physical and mechanical characteristics of sands on the hydraulic and biological behaviors of sand filters. *Desalination*, **248**(1-3): 998-1007.

Romano, N. (1993). Use of an inverse method and geostatistics to estimate soil hydraulic conductivity for spatial variability analysis. *Geoderma*, **60**(1-4): 169-186.

Roth, K., Schulin, R., Flühler, H. and Attinger, W. (1990). Calibration of Time Domain Reflectometry for Water Content Measurement Using a Composite Dielectric Approach. *Water Resources Research*, **26**: 2267-2273.

Rousseau, D.P.L., Vanrolleghem, P.A. and De Pauw, N. (2004). Model-based design of horizontal subsurface flow constructed treatment wetlands: A review. *Water Research*, **38**(6): 1484-1493.

Rucker, D. (2010). Moisture estimation within a mine heap: An application of cokriging with assay data and electrical resistivity. *Geophysics*, **75**: 11-23.

Russo, D., Bresler, E., Shani, U. and Parker, J.C. (1991). Analyses of infiltration events in relation to determining soil hydraulic properties by inverse problem methodology. *Water Resources Research*, **27**(6): 1361-1373.

Santini, A., N. Romano, G. Ciollaro, and Comegna., V. (1995). Evaluation of a laboratory inverse method for determining unsaturated hydraulic properties of a soil under different tillage practices. *Soil Science*, **160**: 340–351.

Scaglia, B., Tambone, F., Genevini, P.L. and Adani, F. (2000). Respiration index determination: dynamic and static approaches. *Compost Science & Utilization,* **8**: 90-98.

Scaglia, B., Erriquens, F.G., Gigliotti, G., Taccari, M., Ciani, M., Genevini, P.L. and Adani, F. (2007). Precision determination for the specific oxygen uptake rate (SOUR) method used for biological stability evaluation of compost and biostabilized products. *Bioresource Technology*, **98**(3): 706-713.

Scaglia, B. and Adani, F. (2008). An index for quantifying the aerobic reactivity of municipal solid wastes and derived waste products. *Science of the Total Environment*, **394**(1): 183-191.

Schuh, W.M., Cline, R.L. and Sweeney, M.D. (1988) Comparison of a laboratory procedure and a textural model for predicting in situ soil water retention. *Soil Science Society of America Journal*, **52**(5): 1218-1227.

Schwager, A., Boller, M. (1997) Transport Phenomena in Intermittent Filters. *Water Science and Techonology*, **35**: 13-20.

Sikora, F.J., Tong, Z., Behrends, L.L., Steinberg, S.L. and Coonrod, H.S. (1995). Ammonium removal in constructed wetlands with recirculating subsurface flow: Removal rates and mechanisms. *Water Science and Technology*, **32**(3): 193-202.

Šimůnek, J., Šejna, M. and van Genuchten, M. Th. (1999) The HYDRUS-2D software package for simulating two-dimensional movement of water, heat, and multiple solutes in variably saturated media. Version 2.0, IGWMC - TPS - 53, *International Ground Water Modelling Center, Colorado School of Mines, Golden, Colorado*, 251 p.

Šimůnek, J., Jarvis, N.J., Van Genuchten, M.Th. and Gärdenäs, A. (2003). Review and comparison of models for describing non-equilibrium and preferential flow and transport in the vadose zone. *Journal of Hydrology*, **272**(1-4): 14-35.

Šimůnek, J., Jacques, D. van Genuchten, M. Th. and Mallants, D. (2006) Multicomponent geochemical transport modelling using the HYDRUS computer software packages. *Journal America Water Resources Association*, **42**(6): 1537-1547.

Spanjers, H. and Vanrolleghem, P. (1995). Respirometry as a tool for rapid characterization of wastewater and activated sludge. *Water Science and Technology*, **31**(2): 105-114.

Stackman, W.P., Valk, G.A. and Horst, G.G. (1969). Determination of soil moisture retention. Sand box apparatus, range pF0 - pF2.7. *ICW, Wageningen.*

Stolte, J., J.L. Freijer, W. Bouten, C. Dirksen, J.M. Halbertsma, J.C., Van Dam, J.A. Van Den Berg, G.J. Veerman, and J.H.M.Wosten. (1994). Comparison of six methods to determine unsaturated soil hydraulic conductivity. *Soil Science Society America Journal*, **58**: 1596–1603.

Stricker, A.E. (2000). Application de la modélisation à l'étude du traitement de l'azote par boues activées en aération prolongée : comparaison des performances en temps sec et en temps de pluie. *Université Strasbourg 1 – Louis Pasteur*.

Stricker, A.E., Lessard, P., Heduit, A. and Chatellier, P. (2003). Observed and simulated effect of rain events on the behavior of an activated sludge plant removing nitrogen. *Journal of environmental Engineering and Science,* **2**(6): 429-440.

Surmacz-Gorska J., Demuynck C., Vanrolleghem and Verstraete W. (1995) Nitrification process control in activated sludge using oxygen uptake rate measurements. *Environmental Technology,* **16**: 569 - 577.

Thurston, R.V., Russo, R.C. and Vinogradov, G.A. (1981) Ammonia toxicity to fishes. The effect of pH on the toxicity of the un-ionized ammonia species. *Environmental Science and Technology*, **15**: 837-840.

Tietz, A., Hornek, R., Langergraber, G.,Kreuzinger, N. and Haberi, R. (2007). Diversity of ammonia oxidising bacteria in a vertical flow constructed wetland. *Water Science and Technology*, **56**(3): 241-247.

Topp, G., Davis, J. and Annan, A. (1980). Electromagnetic Determination of Soil Water Content: Measurement in Coaxial Transmission Lines. *Water Resources Research*, **16**: 574.

Toscano, A., Langergraber, G., Consoli, S. and Cirelli, G.L. (2009). Modelling pollutant removal in a pilot-scale two-stage subsurface flow constructed wetlands. *Ecological Engineering*, **35**(2): 281-289.

Tremier, A., de Guardia A., Massiani, C., Paul, E. and Martel, J. L. (2005). A respirometric method for characterising the organic composition and biodegradation kinetics and the temperature influence on the biodegradation kinetics, for a mixture of sludge and bulking agent to be co-composted. *Bioresource Technology*, **96**(2): 169-180.

Troesch, S., Liénard, A., Molle, P., Merlin, G. and Esser, D. (2009). Treatment of septage in sludge drying reed beds: A case study on pilot-scale beds. *Water Science and Technology*, **60**(3): 643-653.

Tschui, M., Boller, M., Gujer, W.,Eugster, J., Mader, C. and Stengel, C. (1994). Tertiary nitrification in aerated pilot biofilters. *Water Science and Technology*, **29**(10-11): 53-60

Tyroller, L., Rousseau, D.P.L., Santa, S. and García, J. (2010). Application of the gas tracer method for measuring oxygen transfer rates in subsurface flow constructed wetlands. *Water Research*, **44**(14): 4217-4225.

van Genuchten, M.Th. (1980). A closed-form equation for predicting the hydraulic conductivity of unsaturated soils. *Soil Science Society of America* Journal, **44**: 892-898.

van Genuchten, M. Th., F. J. Leij, and S. R. Yates. (1991) .The RETC Code for Quantifying the Hydraulic Functions of Unsaturated Soils, Version 1.0. EPA Report 600/2-91/065, *U.S. Salinity Laboratory, USDA, ARS, Riverside, California.*

Verbist, K., Cornelis, W.M., Gabriels, D., Alaerts, K. and Soto, G. (2009). Using an inverse modelling approach to evaluate the water retention in a simple water harvesting technique. *Hydrology and Earth System Sciences*, **13**(10): 1979-1992.

Vigne, E., Choubert, J.-M., Canler, J.-P., Héduit, A., Sorensen, K. and Lessard, P. (2010). A biofiltration model for tertiary nitrification of municipal wastewaters. *Water Research*, **44**(15): 4399-4410.

Vigne, E., Choubert, J.M., Canler, J.P., Héduit, A., Sorensen, K. and Lessard, P. (2011). The role of loading rate, backwashing, water and air velocities in an up-flow nitrifying tertiary filter. *Bioressource Technology*, **102**(2): 904–912.

Vincent, J., Molle, P., Wisniewski, C. and Liénard, A. (2011). Sludge drying reed beds for septage treatment: Towards design and operation recommendations. *Bioresource Technology*, **102**(17): 8327-8330.

Vrugt, J.A., Gupta, H.V., Bastidas, L.A., Bouten, W. and Sorooshian, S. (2003). Effective and efficient algorithm for multiobjective optimization of hydrologic models. *Water Resources Research*, **39**(8): SWC51-SWC519.

Wanko, A., Mose, R., Carrayrou, J. and Sadowski, A.G. (2006). Simulation of biodegradation in infiltration seepage - Model development and hydrodynamic calibration. *Water, Air, and Soil Pollution*, **177**(1-4): 19-43.

Water Environment Research Foundation [WERF] (2003). Methods for Wastewater. Characterization in Activated Sludge Modelling, Report 99-WWF-3, *Alexandria, Virginia.*

Wessolek, G., Plagge, R., Leij, F.J. and van Genuchten, M.Th. (1994). Analysing problems in describing field and laboratory measured soil hydraulic properties. *Geoderma*, **64**(1-2): 93-110.

Wind, G.P. (1968). Capillary conductivity data estimated by a simple method. In: Rijtema, P.E., Wassink, H. (Eds.), Water in the Unsaturated Zone, vol. 1. Proceedings of the Wageningen Symposium, 19–23 June 1966. *Int. Assoc. Sci. Hydrol. Publ. (IASH), Gentbrugge, The Netherlands and UNESCO, Paris*.

WPCF (1983). Nutrient Control, Manual of Practice. Publication number FD-7, Water Pollution Control Federation, Washington, DC.

Yamaguchi, T., Moldrup, P., Rolston, D.E., Ito, S. and Teranishi, S. (1996). Nitrification in porous media during rapid, unsaturated water flow. *Water Research*, **30**(3): 531-540.

Yeh, T., Liu, S., Glass, R., Baker, K., Brainard, J., Alumbaugh, D. and LaBrecque, D. (2002). A geostatistically based inverse model for electrical resistivity surveys and its applications to vadose hydrology. *Water Resources Research*, **38**: 141-141.

Zhang, K., Burns, I.G., Greenwood, D.J., Hammond, J.P. and White, P.J. (2010). Developing a reliable strategy to infer the effective soil hydraulic properties from field evaporation experiments for agro-hydrological models. *Agricultural Water Management*, **97**(3): 399-409.

Zou, Z.-Y., Young, M.H., Li, Z. and Wierenga, P.J. (2001). Estimation of depth averaged unsaturated soil hydraulic properties from infiltration experiments. *Journal of Hydrology*, **242**(1-2): 26-42.

Publications and Conferences

Publications in international journals

- Morvannou, A., Choubert, J-M., Vanclooster M. and Molle P. 2011. Solid respirometry to characterize nitrification kinetics: A better insight for modelling nitrogen conversion in vertical flow constructed wetlands. *Water Research*, **45**(16): 4995-5004.

- Morvannou, A., Forquet, N., Vanclooster, M. and Molle, P. (in preparation). On the characterization of the hydraulic properties of the filtering material of a Vertical Flow Constructed Wetland (VFCW).

- Forquet, N., Morvannou, A., Molle, P. and Vanclooster, M. (in preparation). Imaging of Vertical Flow Constructed Wetland using Electrical Resistivity Tomography and Time Domain Reflectometry.

- Morvannou, A., Choubert, J-M., Vanclooster, M. and Molle, P. (in preparation). Nitrogen removal modelling in first stage of a French vertical flow constructed wetlands.

Conferences

Oral presentations

- Morvannou, A., Choubert, J-M., Vanclooster M. and Molle P. Solid respirometry to characterize biodegradation kinetics in VFCW. *12th International Conference on Wetland Systems for Water Pollution Control*. 4-8 October 2010, Venice.

- Morvannou, A., Forquet, N., Vanclooster M. and Molle P. Hydraulic properties characterization of the filtering material of a VFCW. *Joint meeting of Society of Wetland Scientists, Wetpol and Wetland Biogeochemistry Symposium* - 3-8 July 2011, Prague.